Atlas of new and revised high-resolution spectroscopy of six CO isotopologues in the 101–115 nm range

Jean-Louis Lemaire, A. Heays, M. Eidelsberg, Lisseth Gavilan, G. Stark, S. Federman, J. Lyons, N. de Oliveira

A&A 614, A114 (2018)
https://doi.org/10.1051/0004-6361/201732114

Astronomy & Astrophysics

Atlas of new and revised high-resolution spectroscopy of six CO isotopologues in the 101–115 nm range

Transition energies of the $v' = 0$, 1, 2, and 3 to $v'' = 0$ bands of the $B^1\Sigma^+$, $C^1\Sigma^+$, and $E^1\Pi$ to $X^1\Sigma^+$ states, related term values, and molecular constants

J. L. Lemaire[1,⋆], A. N. Heays[2], M. Eidelsberg[2], L. Gavilan[3], G. Stark[4], S. R. Federman[5], J. R. Lyons[6], and N. de Oliveira[7]

[1] Institut des Sciences Moléculaires d'Orsay (ISMO), CNRS – Université Paris-Sud (UMR 8214), 91405 Orsay, France
e-mail: jean-louis.lemaire@u-psud.fr
[2] Observatoire de Paris, LERMA, UMR 8112 du CNRS, Meudon, France
[3] Université Versailles St-Quentin, Sorbonne Universités, UPMC Paris 06, CNRS/INSU, LATMOS-IPSL, 78280 Guyancourt, France
[4] Department of Physics, Wellesley College, Wellesley, MA 02481, USA
[5] Department of Physics and Astronomy, University of Toledo, Toledo, OH 43606, USA
[6] School of Earth and Space Exploration, Arizona State University, Tempe, AZ 85281, USA
[7] DESIRS Beam Line, Synchrotron SOLEIL, Saint Aubin, France

Received 17 October 2017 / Accepted 15 November 2017

ABSTRACT

Our knowledge of astronomical environments containing CO depends on accurate molecular data to reproduce and interpret observed spectra. The recent and future improvements of ultraviolet space instrumentation, both in sensitivity and resolution, require increasingly detailed laboratory molecular spectroscopy as a reference. As part of a long-term experimental campaign at the SOLEIL Synchrotron facility, we have acquired gas-phase absorption spectra of six CO isotopologues in the vacuum ultraviolet. These spectra are recorded using the Fourier-transform spectrometer installed on the DESIRS beamline, providing a unique resolving power up to 10^6 in the 8–13 eV range. We have used resolutions in the 300 000–450 000 range for this campaign, which enable the analysis of individual line positions. We report new measurements on neighboring Rydberg states in the 101–115 nm range that could also be used as f-value calibrators, namely $B^1\Sigma^+$, $C^1\Sigma^+$, and $E^1\Pi$, for six CO isotopologues. This range encompasses the absorption transitions $B(v' = 0$, 1, and 2), $C(v' = 0$, 1, 2, and 3), and $E(v' = 0$, 1, 2, and 3) from $X^1\Sigma^+(v'' = 0)$. Higher resolution laser-based measurements of CO isotopologues from the literature are used to improve the absolute calibration and accuracy of our data. The overall uncertainty of the great majority of the line positions presented in this atlas is estimated to be 0.01 cm^{-1}. In addition, some of the data derived from transition energies measurements, such as term values and molecular constants, are obtained for the first time, and others are improvements on previous sparser or lower spectral resolution datasets.

Key words. molecular data – methods: laboratory: molecular – techniques: spectroscopic – techniques: interferometric

1. Introduction

This work is part of a larger effort to catalog, interpret, and model the photoabsorption spectrum of CO in the 90–155 nm wavelength region. These measurements are performed at the third-generation SOLEIL synchrotron facility in Saint-Aubin, France. We employ the Fourier-transform spectrometer (FTS) installed on the DESIRS beam line, a unique instrument that combines high spectral resolution and a high signal-to-noise ratio (S/N) in the vacuum ultraviolet (VUV) wavelength range.

In the course of our earlier work (2008–2015) on CO photoabsorption spectroscopy in the 90–155 nm region, we were mainly interested in oscillator strengths and perturbations for several CO isotopologues. A large part of this work concerned the Rydberg W–X bands and Rydberg complexes in the 92.5–97.5 nm range: Eidelsberg et al. (2012, 2014, 2017) for $^{12}C^{16}O$, $^{13}C^{16}O$, $^{12}C^{18}O$, and $^{13}C^{18}O$, respectively, and perturbations in the W–X bands (Heays et al. 2014) and the f-value measurements of the lowest VUV states (Stark et al. 2014), while another part dealt with the A–X bands for $^{13}C^{16}O$ (Gavilan et al. 2013) and $^{13}C^{18}O$ (Lemaire et al. 2016). The common goal of these studies was the accurate determination of oscillator strengths, with an absolute calibration made by reference to the unperturbed $B^1\Sigma^+(v' = 0)$–$X^1\Sigma^+(v'' = 0)$ band that was previously well characterized by high-resolution (0.14 cm^{-1}) laser-based measurements (Stark et al. 1999) and by synchrotron-based measurements (Federman et al. 2001). The $B^1\Sigma^+$–$X^1\Sigma^+$ bands were already extensively investigated for four isotopologues ($^{12}C^{16}O$, $^{13}C^{16}O$, $^{12}C^{18}O$, and $^{13}C^{18}O$) in both absorption and emission (Eidelsberg et al. 1987) using the Observatoire de Paris (Meudon, France) 10 m VUV grating spectrograph. In that work, term values were derived for the B00, B10, and B20 absorption bands. The uncertainty on the absolute wavenumbers was estimated to be ±0.1 cm^{-1}.

Throughout this paper, the notation is simplified as follows: states are designed by their symmetry (e.g., $X^1\Sigma^+$ or $E^1\Pi$), while a band is denoted $E^1\Pi(v')$–$X^1\Sigma^+(v'')$ or for brevity $EXv'v''$, for

⋆ Previously at Observatoire de Paris (LERMA), France.

example, EX20 for $v' = 2$ and $v'' = 0$, or shorter: E20. The notation indicating the isotopologues is also simplified in tables and figures, where we write, for example, 1216 for $^{12}C^{16}O$, etc.

The current investigation describes our high-resolution measurements of the $B^1\Sigma^+$, $C^1\Sigma^+$, and $E^1\Pi$ states for six CO isotopologues in the 101–115 nm range. This range encompasses the following absorption transitions: $B(v' = 0, 1$ and 2), $C(v' = 0, 1, 2$ and 3), and $E(v' = 0, 1, 2$ and 3) from the fundamental electronic state $X(v'' = 0)$.

This work revisits and completes, 25 yr later, part of the CO atlas of transition frequencies started by the Paris-Meudon Observatory team (Eidelsberg et al. 1991; Le Floch 1992), and initiated by the work of Letzelter et al. (1987) and Viala et al. (1988) on the photoabsorption and photodissociation cross sections, either measured or calculated for the four isotopologues $^{12}C^{16}O$, $^{12}C^{18}O$, $^{13}C^{16}O$, and $^{13}C^{18}O$. It improves and completes calculations derived from the combination of earlier low-resolution measurements of term values and molecular constants of B00 and B10 for $^{12}C^{16}O$ (Le Floch & Amiot 1985), of C00 and E00 for $^{12}C^{16}O$ (Le Floch 1992), and of B00, B10, C00 and E00 for $^{12}C^{18}O$ and $^{13}C^{18}O$ (Haridass et al. 1994). Line positions of B20 for $^{12}C^{16}O$ have been studied by Baker & Launay (1994).

This work also revisits and completes earlier experimental work at low resolution on E00 and E10 (Baker et al. 1993, 1994). Higher resolution work (Cacciani et al. 1995, 2001; Cacciani & Ubachs 2004; Drabbels et al. 1993a,b; Ubachs et al. 1995, 2000) is discussed in detail in Sect. 2.1 as these data are used in this work for the absolute calibration of our data.

It is also worth mentioning the extensive work of Morton & Noreau (1994), which provides a compilation of electronic transitions (including BX00 to BX20, CX00 to CX30, and EX00 to EX20) in the CO molecule ($^{12}C^{16}O$, $^{12}C^{18}O$, $^{13}C^{16}O$, and $^{13}C^{18}O$). Line positions are limited in this work to $J'' \leq 6$. This paper includes all experimental data published up to 1994.

A first detailed model of CO photodissociation, based on laboratory data, including depth-dependent attenuation and isotope-selective self-shielding of photodissociation rates, was developed by van Dishoeck & Black (1988) to model in detail, coupled with a chemical network, the structure and chemistry of a variety of interstellar clouds. This work, updated by measurements produced in the subsequent 20 yr, was revisited by Visser et al. (2009), including self- and mutual-shielding of all isotopologues (in particular, for the first time, $^{12}C^{17}O$ and $^{13}C^{17}O$) as well as shielding by atomic and molecular hydrogen.

All term values are referenced to the $X^1\Sigma^+(v'' = 0,\ J'' = 0)$ ground state of the respective isotopologues, according to the ground-state energy levels determined by Guelachvili et al. (1983) and Farrenq et al. (1991).

This work only reports and is based on lines that are observed and clearly identified in spectra, with the exception of the extremely congested Q-branches of the E state (at low J) for which we report in our tables literature values obtained at very high resolution (for E00 and E10) or estimated (for E20) for the sake of completeness.

This article is organized as follows. Section 2 briefly describes the experimental setup and the analysis procedure. Section 3 presents our results: line assignments, term values, and molecular constants for each state (B, C, and E) and bands observed. The last section presents our concluding remarks.

2. Experimental setup and data analysis

CO spectra are recorded at high resolution using the vacuum-ultraviolet Fourier-transform spectrometer (VUV-FTS) available on beamline DESIRS (Dichroïsme Et Spectroscopie par Interaction avec le Rayonnement Synchrotron) of the SOLEIL synchrotron. The beamline and spectrometer have been described in detail in previous publications (de Oliveira et al. 2009, 2011, 2016; Nahon et al. 2012, 2013).

Four bottles of isotopically purified gases, namely $^{12}C^{16}O$ (Alphagaz, 99.997%), $^{12}C^{18}O$ (ICON Isotopes, ^{18}O 99%), $^{13}C^{16}O$ (Messer, ^{13}C 99.1%; ^{16}O 99.95%), $^{13}C^{18}O$ (Cambridge Isotopes, ^{13}C 99%, ^{18}O 95%), and one bottle containing a $^{12}C^{16}O/^{12}C^{17}O/^{12}C^{18}O$ mixture (ICON Isotopes, 41.5%, 48.5%, and 9.9% respectively), are used to obtain data for five isotopologues. The presence of a sixth isotopologue, the rarely studied $^{13}C^{17}O$, is detected as an impurity in the $^{13}C^{16}O$ and $^{13}C^{18}O$ bottles, and serves to complete this analysis, which provides a consistent dataset on six natural isotopologues.

Sample gases continuously flow through a 10 cm long windowless absorption cell that is open on both sides through capillary tubes. Most spectra are recorded at room temperature (295 K), but a few are obtained with the central part of the cell cooled by liquid nitrogen; this results in a gas temperature of 90 ± 5 K. In some cases, these cooled spectra are useful for improved line assignations by reducing the number of lines in a spectrum and their Doppler broadening.

A total of 69 spectra, recorded at different pressures and spectral resolutions, were analyzed for this work (amounting to 3327 individual lines). The analysis was performed line by line, determining the line positions by modeling them as Gaussian or Voigt functions (for ~97% of the cases), and at times extracting them from simulations of the spectra of blended lines. In order to improve the accuracy, the present results rely on up to four different records for a given band and a given isotopologue. The bands observed in this work are reported in Table 1.

A key element of this work is the need for absolute wavelength calibration. The first step in the calibration procedure is provided by the FTS team. In summary, the raw FTS interferogram data based on the accurate measurement of the mirror displacement are first phase-corrected and then Fourier-transformed into a frequency spectrum. The resulting spectra are frequency-calibrated using atomic lines from different origins that appear in the spectra (de Oliveira et al. 2011, 2016). The accuracy of individual rovibrational lines is not only dependent on the accuracy of the absolute frequency calibration atomic lines, but also on the spectral resolution and on the strength and blendedness of each measured line. The parameters involved are the number, N, of independent scanning steps for a given line, which depends itself on the width, W, (mainly Doppler) of the measured line, and on the S/N compared to the background continuum signal. The final accuracy of line positions, σ in wavenumbers, reported by de Oliveira et al. (2011), is based on the empirical expression $\Delta(\sigma) \sim W/(S/N \times \sqrt{N})$ (see also their reference 20).

Lemaire et al. (2016) reported line positions determined from VUV-FTS spectra with a relative accuracy better than $\sim \pm 0.008\,cm^{-1}$ at $87\,000\,cm^{-1}$ (or $\sim \pm 0.01$ pm at 115 nm). A comparison of wavenumber measurements of common sets of lines from multiple independent spectra is consistent with this estimated accuracy.

Two methods were used to place all spectra on a unique wavelength scale. First, more than 30 atomic lines (mainly Xe I, Kr I, and sometimes O I) present in the studied range were

Table 1. Summary of bands measured at high resolution.

State	$X^1\Sigma^+$	$B^1\Sigma^+$			$C^1\Sigma^+$				$E^1\Pi$			
Band	X	BX			CX				EX			
v'–v''	$v=0$	00	10	20	00	10	20	30	00	10	20	30
Isotopologue												
$^{12}C^{16}O$	*	✓	✓	✓	✓	✓	✓	✓	✓	✓	✓	✓
$^{12}C^{17}O$	*	✓	✓	no	✓	✓	no	✓	✓	✓	✓	✓
$^{12}C^{18}O$	*	✓	✓	✓	✓	✓	✓	✓	✓	✓	✓	✓
$^{13}C^{16}O$	*	✓	✓	✓	✓	✓	✓	✓	✓	✓	✓	✓
$^{13}C^{17}O$	*	✓	✓	no	✓	✓	no	no	✓	✓	no	no
$^{13}C^{18}O$	*	✓	✓	✓	✓	✓	✓	✓	✓	✓	✓	✓

Notes. ✓: observed, no: not observed. * are data calculated from Farrenq et al. (1991).

Table 2. References to the high-resolution calibration band or lines used (reference labels sorted by publication dates are given at the bottom of the table).

State	$B^1\Sigma^+$			$C^1\Sigma^+$				$E^1\Pi$			
Band	BX			CX				EX			
$v'v''$	00	10	20	00	10	20	30	00	10	20	30
Isotopologue											
$^{12}C^{16}O$	$b_{l\bullet}$, $c_{l\bullet}$, $\mathbf{j}_l$	$c_{l\bullet}$	$a_{b\bullet}$	$b_{l\bullet}$, $e_\bullet$, $\mathbf{j}_l$	$e_\bullet$, $g_{b\bullet}$			$d_{l\bullet}$, $h_{b\bullet}$, $\mathbf{j}_l$	$a_\bullet$, $d_{l\bullet}$, f_b		
$^{12}C^{17}O$				$e_{l\bullet}$	g_l			$d_\bullet$	f_b		
$^{12}C^{18}O$	$c_{l\bullet}$			$e_\bullet$	$e_\bullet$, $g_{b\bullet}$			$a_\bullet$, $d_\bullet$	$a_\bullet$, $d_\bullet$, f_b		
$^{13}C^{16}O$	$c_{l\bullet}$, $k_\bullet$			$e_\bullet$	$e_\bullet$, $g_{b\bullet}$			$a_\bullet$, $d_\bullet$, $h_{b\bullet}$	$a_\bullet$, $d_\bullet$, f_b		
$^{13}C^{17}O$					g_l				f_b		
$^{13}C^{18}O$					$g_{b\bullet}$			$a_\bullet$, $h_{l\bullet}$	$a_\bullet$, f_b		

Notes. References providing data for bands with fewer than about ten lines are indexed with l and for more than ten lines with b. References providing term values and/or molecular constants are indexed with a filled blue dot.
References. a: Baker et al. (1993, 1994); Baker (1994). b: Drabbels et al. (1993a). c: Drabbels et al. (1993b). d: Cacciani et al. (1995). e: Ubachs et al. (1995). f: Ubachs et al. (2000). g: Cacciani et al. (2001). h: Cacciani & Ubachs (2004). j: Daprà et al. (2016). k: Niu et al. (2016).

used with reference frequencies taken from the NIST atomic lines database[1]. The presence of these gases is due to unintentional minor contamination or to a column of rare gas introduced on the beamline intended to filter out high-frequency harmonics generated in the undulator. Most of these lines have been measured with an accuracy of 10^{-3} nm and some with an accuracy of up to 10^{-6} nm. These latter are O I: 115.21512 nm (Kaufman & Edlén 1974), Xe I: 106.125564 nm, 105.612829 nm, 104.383497 nm (Yoshino & Freeman 1985; Brandi et al. 2001), and Kr I: 100.1060639 nm (Brandi et al. 2002). The positions of these lines are shown in Fig. 1.

Second, the random error associated with calibrating the wavenumber scale via a small number of atomic transitions can sometimes be improved upon by including reference data for molecular lines. For this aim, high-resolution laser measurements of some CO lines (and isotopologues) available in the literature were employed (Cacciani et al. 1995, 2001; Cacciani & Ubachs 2004; Drabbels et al. 1993a,b; Ivanov et al. 2008; Philip et al. 2004; Ubachs et al. 1994, 1995, 2000, and recently Daprà et al. 2016). Most of these measurements, obtained by narrow-band laser spectroscopy in one- or two-photon experiments, rely on the I_2- or Te_2-saturation spectrum as primary absolute calibrators, associated with the marks of an actively stabilized Fabry-Pérot étalon. They are summarized in the next subsection (in alphabetical order) and are cited in the corresponding sections.

[1] http://physics.nist.gov/PhysRefData/ASD/lines_form.html

To overcome the lack of calibration data for some bands, we considered the overlapping regions of contiguous scans. A given setting of the undulator delivers a quasi-Gaussian beam profile of width ~5 nm at $1/e$ of the peak signal. An absorption scan encompasses about 3–5 bands, as can be seen in Fig. 1. With the right choice of undulator settings, we were able to measure at least three bands in a single scan. In this way, a band with no calibration reference can be surrounded by two bands subject to accurate calibration, for instance, the B20 band surrounded by the B10 and C00 bands.

The final accuracy of our measurements also relied upon isotopologue cross calibrations. These were obtained through mixed isotopologue samples (as is the case for the available $^{12}C^{16}O$–$^{12}C^{17}O$ bottle, which contains some small amount of $^{12}C^{18}O$, and as in the case of $^{13}C^{17}O$, which was present as an impurity in $^{13}C^{16}O$ and $^{13}C^{18}O$ bottles). Even with pure gas samples, isotopologue impurities may show up in spectra that were recorded at high pressures. We also prepared and used on purpose mixed isotopologue samples allowing for such cross calibrations.

It is worth noting that more data were collected for this work than are included in papers dedicated to oscillator strength measurements. Those are restricted in pressure range and consequently in number of lines observed, in order to keep optical depths <1.5, or absorption lower than 78%, for the accurate determination of oscillator strengths. For this study we used higher pressures in order to observe high J' levels and isotopologues present in small amounts. As described above, we also use cooled gases to remove possible ambiguities.

2.1. Laser calibration benchmarks and associated data

An absolute calibration of lines requires the availability of accurately determined standards, either atomic or molecular, as close as possible to the lines under study. There are many reported laser-based measurements of CO VUV transitions with accurate absolute calibrations based on primary standards. Some previous work has been limited to a few lines of each vibrational band, while others offer almost complete bands for use as comparisons for calibration purposes. Data like this exist for most CO isotopologues. They are summarized in detail in this section.

Reports of laser-based measurements that were used to accurately calibrate our spectra often also presented an analysis of the rotational structure of the bands under study, providing associated data such as term values, reduced term values, and molecular constants. These results are also mentioned in detail in this section as they are compared later to our own results.

Depending on the data available, laser calibrated benchmarks could in some cases be derived from transitions other than the one-photon P, R, and Q transitions of this study. When two-photon O, S, or Q transitions were available, the corresponding one-photon transitions for the R- and P-branches were recalculated by way of term values, taking into account that common-J' term values (TVs) of the excited state calculated from various one- and two-photon transition frequencies, that is, $\mathrm{TV}(O_{J'=i\leftarrow J''=i+2})$, $\mathrm{TV}(P_{J'=i\leftarrow J''=i+1})$, $\mathrm{TV}(Q_{J'=i\leftarrow J''=i})$, $\mathrm{TV}(R_{J'=i\leftarrow J''=i-1})$, and $\mathrm{TV}(S_{J'=i\leftarrow J''=i-2})$, have to be equal.

We summarize below all references providing laser calibration benchmarks that were used for this work, as well as the associated data mentioned above. They are sorted by alphabetical order of authors. With the exception of the first laser high-resolution measurements (Baker et al. at Paris-Meudon Observatory and Drabbels et al. at Nijmegen University), the majority of CO molecular calibration lines used here were measured using ultra-high resolution lasers at VU University Amsterdam (Cacciani et al., Daprà et al., Ivanov et al., Niu et al., and Ubachs et al.).

Baker (1994)
This paper reports some perturbations observed in the B20 state of $^{12}C^{16}O$ that are due to the interaction with the $^3\Pi$(F1) spin-orbit component of the $k^3\Pi(0)$–$X^1\Sigma^+(0)$ band. Line positions and term values are given for B20 and kX00.

Baker & Launay (1994)
This paper analyzes the $k^3\Pi(v'=2,\ 3$ and $5)$–$X^1\Sigma^+(0)$ bands, the first one perturbing the E00 band, and the last one the E10 band. Line positions and term values are given for kX20, kX30, and kX50.

Baker et al. (1993, 1994)
These papers provide a study of the E00 and E10 bands for four isotopologues, $^{12}C^{16}O$, $^{13}C^{16}O$, $^{12}C^{18}O$, and $^{13}C^{18}O$. Spectra were recorded using 2 + 1 resonantly enhanced multiphoton excitation showing the five rotational branches O, P, Q, R, and S at a resolution of ~0.1 cm^{-1}. Spectra were acquired either separately for each isotopologue or with mixtures of several, and were then separated by time of flight mass spectrometry, in order to obtain an accurate relative calibration between isotopologues. Perturbations of E10 were analyzed. Term values (for three isotopologues of E00 and four of E10) and molecular constants (for E10) are also given for the four isotopologues.

Cacciani & Ubachs (2004)
This paper gives Q-branch transition frequencies of E00 [Q: $J'=1$–8] for $^{12}C^{16}O$ and [Q: $J'=1$–7] for $^{13}C^{16}O$ and $^{13}C^{18}O$. Measured and calculated transition frequencies for E00 of $^{12}C^{16}O$ [up to $J'=34$ with gaps] and $^{13}C^{16}O$ [up to $J'=42$ with gaps], obtained by three different experimental methods, are accessible as supplementary data.

Cacciani et al. (1995)
This paper provides a few term values for $^{12}C^{16}O$ (the E00 band [$J'=31$, 41, and 44] and E10 band [$J'=5$–13]), focused in both cases around perturbations. Molecular constants are also determined for $^{12}C^{16}O$ (E00 and E10), $^{13}C^{16}O$ (E00 and E10), $^{12}C^{18}O$ (E00 and E10), and $^{12}C^{17}O$ (E00). Transition frequencies were tabulated in a later paper (Cacciani & Ubachs 2004).

Cacciani et al. (2001)
This paper provides transition frequencies for R- and P-branch lines of the C10 band for $^{12}C^{16}O$ [R: $J'=0$–27; P: $J'=1$–31], $^{12}C^{18}O$ [R: $J'=0$–13; P: $J'=1$–8, 10], $^{13}C^{16}O$ [R: $J'=0$–15; P: $J'=1$–5, 9–20], $^{13}C^{18}O$ [$R=J'=0$–5, 8–12; P: $J'=1, 3, 5$–8], and a few for $^{12}C^{17}O$ [R: $J'=0$–2; P: $J'=1$] and $^{13}C^{17}O$ [R: $J'=0$–1, 3–5; P: $J'=1$–3]. Molecular constants are also calculated for the six isotopologues, although at lower accuracy for $^{12}C^{17}O$ and $^{13}C^{17}O$.

Daprà et al. (2016)
This paper is mainly based on data for $^{12}C^{16}O$ published by the Amsterdam team over several years and gives measured wavelengths (Tables 6–8; called molecular parameters) for the R and P (and Q for E00) $J'=0$–5 transitions of the B00, C00, and E00 bands. Their results are expressed with an accuracy of up to the sixth digit (in nanometers) and an error bar of between 3 and 13 in units of this digit. The restriction to the lowest rotational states ($J'\leq 5$) is due to the fact that this paper is aimed at the comparison with quasar observations. These data are the most accurate to date. They result from measurements and not from calculations, as can be deduced from the fact that term values for a given level, determined through the R- and P-branches, are not strictly equal.

Drabbels et al. (1993a)
This paper reports observed transition frequencies for $^{12}C^{16}O$ of the Q- and S-branch lines of B00 [$J'=0$–14 for Q and 0–1 for S] and of C00 [$J'=0$–6 for Q and 0–1 for S]. Corresponding molecular constants are also calculated from these data.

Drabbels et al. (1993b) This paper completes the previous paper with additional measurements of Q lines for B10 [$J'=0$–2], for $^{13}C^{16}O$ B00 [$J'=0$–2], and for $^{12}C^{18}O$ B00 [$J'=0$–1]. There is also a slight revision of $^{12}C^{16}O$ B00 [$J'=0$–4 for Q and 0–1 for S], but as this paper was submitted earlier than the previous paper, it is not clear which should be considered as the more accurate.
Molecular constants are calculated for these four bands.

Ivanov et al. (2008)
This paper reports "extreme-ultraviolet laser metrology of O I transitions" (about 20 lines in the 94.86–102.82 nm range) that are used for absolute calibration purposes, when oxygen is present, for E20 and higher energy states.

Niu et al. (2016)
While focused on the spectroscopy and perturbation analysis of the $A^1\Pi(v=0)$ state of $^{13}C^{16}O$, this paper provides deperturbed molecular constants for B00.

Ubachs et al. (1994)
This paper summarizes the work performed in the 91.2–115 nm range by the Amsterdam and Nijmegen teams over several years, reporting molecular constants for many states of four isotopologues and, of relevance to the present work, for $^{12}C^{16}O$ (B00, B10, C00), $^{13}C^{16}O$ (B00), and $^{12}C^{18}O$ (B00).

Ubachs et al. (1995)
This is a laser spectroscopic study of $^{12}C^{17}O$ (observed here for the first time) R- and P-branch lines of C00 [$J'=10$–17 for R and 10–15 for P] and derived molecular constants. The latter are also

given for C00 and C10 for $^{12}C^{16}O$, $^{13}C^{16}O$, and $^{12}C^{18}O$, but no transition frequencies are available.

Ubachs et al. (2000)

This paper reports the transition frequencies of E10 for six isotopologues. For $^{12}C^{16}O$ [R: $J'=0$–26 with three gaps; Q: $J'=8$–21 with two gaps; P: $J'=5$–28 with three gaps], $^{12}C^{18}O$ [R: $J'=0$–11; Q: $J'=8$–13 with one gap; P: $J'=2$–13 with three gaps], $^{13}C^{16}O$ [R: $J'=0$–20 with five gaps; Q: $J'=7$–23; P: $J'=2$–20], $^{13}C^{18}O$ [R: $J'=0$–20 with two gaps; Q: $J'=1$,18; no P], a few for $^{12}C^{17}O$ [R: $J'=0$–1; Q: $J'=1$–2; no P] and for $^{13}C^{17}O$ [R: $J'=0$–12 with six gaps; Q: $J'=1$–12; P: $J'=3$]. The very high resolution (up to $\sim 3\times10^6$) achieved by a narrow-band laser source allowed assigning the Q-branch lines with an absolute accuracy of 0.003 cm^{-1} for all six natural CO isotopologues. Molecular constants are also derived for the ground-state $X(v''=0)$, E10 and the perturbing k60 bands.

References to the available absolute high-resolution calibration band or lines we used are summarized in Table 2 for each band and for each isotopologue. The availability of term values and/or molecular constants derived from the laser-based measurements is also noted in the table.

We also mention the mainly theoretical work of Lefèbvre-Brion & Eidelsberg (2012), which presents molecular constants (T_v and B_v) for E00, E10, E20, and E30 derived from our VUV-FTS high-resolution CO datasets, extracted before the absolute wavelength calibration of this work.

2.2. Data analysis

2.2.1. Atlas of measured wavelengths and wavenumbers

In order to place the atlas on an absolute wavelength scale, we compared our measured data with the entire set of calibration references from Table 2 (including all isotopologues when available). The average of their differences provides the value of a shift that was applied to correct the raw experimental wavelengths. As proof of the accuracy of the data delivered by the VUV-FTS team, this correction was usually very small ($<3.4\times10^{-5}$ nm or 0.03 cm^{-1}). Two sets of measured transition energies (including calibration shift corrections from the wavelength standards), R_{ms} and P_{ms}, corresponding to the R- and P-branches (and additionally Q_{ms} for $^1\Pi$ states), were the result from this procedure.

In order to check the quality of our transition energy determinations, we compared for each J' the values of

$A = R_{(J'=i+1\leftarrow J''=i)} - P_{(J'=i+1\leftarrow J''=i+2)}$ to those of

$B = X_{J''=i+2} - X_{J''=i}$,

according to the method of combination differences (Herzberg et al. 1950). For each band and for each J', we calculated the difference A–B between these two quantities, which we defined as $2\times\delta_P$.

These differences lead to uncertainties in the term values TV_R and TV_P. Some publications interested in precise term values shared equally for each J' the difference between TV_R and TV_P (or between R and P, in order to calculate corrected transition energies $R_{corr}=(R_{ms}-\delta_P)$ and $P_{corr}=(P_{ms}+\delta_P)$, which produces a single best-term value based on both lines. We did not follow this procedure here, but kept the measured values.

2.2.2. Atlas of term values and molecular constants

For each measured band, we used the line positions of R- and P-branch lines that terminate on the same upper rotational levels to calculate common upper-level term values with uncertainties.

The agreement of the term values calculated from independently measured P- and R-branch transitions with a common upper J-level, TV_R, and TV_P, is never perfect because of experimental noise and in some cases line broadening. However, as we described above, the excellent reproducibility of the measurements obtained with the VUV-FTS for a given band and a given isotopologue from spectra recorded at different times suggests that when the discrepancy is larger than the random fitting errors, it reveals the possible presence of a local perturbation that modifies the shape of one of the lines involved. For each $J'=i+1$ level, the final term value was obtained by averaging the term values $TV_R=R_{J'=i+1\leftarrow J''=i}+X_{J''=i}$ and $TV_P=P_{J'=i+1\leftarrow J''=i+2}+X_{J''=i+2}$ that were calculated from measured line positions of each rotational branch, R_{ms} and P_{ms}. The relative difference is again $2\times\delta_P$. As a final result, R_{ms}, P_{ms} and δ_P values are tabulated for each band and isotopologue. Both R_{ms} and P_{ms} are given in wavelengths and wavenumbers (and δ_P in wavenumbers), and are presented in separate tables for ^{12}C- and ^{13}C-bearing CO species.

Term values of the upper levels for all six isotopologues were derived from these two independent measurements. They are presented in separate tables for each band. while reduced term values are shown with graphs for better visualization. We must be careful for high J' term values in two specific cases: (a) a high value of δ_P (we adopted in this work a limit of 0.125 cm^{-1}) might mean that one of the lines is less well identified than the other (or does not belong to the studied band), even if the two R and P lines are both clearly observed, and (b) no δ_P value indicates that only one transition is present, either R or P. In the first case, we kept the TV derived from a single level, while in the second case, erratic TV values had to be rejected. All these tables and graphs are introduced for each state in the following sections.

For each band and isotopologue, the statistical uncertainty on term values was obtained by calculating over all J', when both R and P levels were measured, the average and standard deviation (at 2σ) of $2\times\delta_P/2$. The division by a factor of two takes into account that each term value results from two independent measurements (R_{ms} and P_{ms}) and that at least two different records (up to four in some cases, as described above) provide the same line position results. Each average is displayed in statistical tables, alongside its standard deviation (at 2σ), showing the dispersion in our measurements. An average closer to zero means that the δ_P values are randomly distributed, ensuring no bias in our measurements. A standard deviation closer to zero signifies a high probability of the absence of perturbation(s).

The molecular constants T_v, B_v, and D_v were least-squares fitted to the experimental term values using a second-order polynomial. Following the above remarks, only a subset of term values was considered at times, particularly for high J' term values. Reduced term values were finally calculated for each vibrational level by subtracting a model defined by

$$TV(J) = T_v + B_v \times J(J+1) - D_v \times J^2(J+1)^2$$

for the e-parity levels of the $B^1\Sigma^+$ and $C^1\Sigma^+$ sates and the f-parity levels of the $E^1\Pi$ state, while for the e-parity levels of $E^1\Pi$, the additional term

$$q \times J(J+1) - q_D \times J^2(J+1)^2$$

takes the Λ-doubling of this state into account (so that $q=B_e-B_f$ and $q_D=D_e-D_f$, where the e and f subscripts refer to the parity of the considered levels). For the $E^1\Pi$ state, the Λ-doubling

components can be either calculated by subtracting the molecular constants deduced from the e- and f-parity levels, or they can be directly obtained by fitting the TV_e–TV_f differences for each level to a second-order polynomial. The results of both methods are presented in Sect. 3.5. Their values were graphically compared according to their oxygen isotopic content to check for anomalies that are due to perturbations. In almost every case, our molecular constants were generated by much larger datasets than those referenced in Sect. 2.1 (see also Table 2).

It is worth noting that the lines in the R- and P-branches are in general not observed up to the same J'. It is also possible, in the case of high-pressure spectra, that some lines observed at high J' values belong to a weak unidentified underlying band. As a consequence, some reduced term value graphs could present a break or jump for the last higher J' values. This break, however, could correspond in some cases to a real perturbation.

3. Results and discussion

The results presented here constitute the first part of an atlas of the Rydberg states at wavelengths below 115 nm for six isotopologues of CO. They update and complete the previous CO atlas at the higher resolution provided by the VUV-FTS coupled to the SOLEIL synchrotron (Eidelsberg et al. 1991; for revised band origin wavenumbers, see Eidelsberg et al. 1992). They also fill some gaps and provide higher J' lines that were previously not observed with high-resolution laser methods.

In addition to the atlas of absolute wavelengths and wavenumbers for the B, C, and E states of the six CO isotopologues, we provide for the derived term value atlas for each observed band. As a further step, we calculate reduced term values and molecular parameters. The latter are compared according to their oxygen isotopic content, and when possible, with previous determinations.

Figure 1 shows the bandhead wavelengths of the states and bands studied in this work. Table 1 summarizes the measured bands for each isotopologue. Some isotopologue bands are not recorded because of the combination of low oscillator strengths and low available pressures or partial pressures. Low partial pressure is particularly a problem in the case of $^{13}C^{17}O$, which is observed as a minor contaminant in high-pressure spectra of both $^{13}C^{16}O$ and $^{13}C^{18}O$.

For all ^{12}C (or ^{13}C)-bearing isotopologues, the isotope shift spacing between bandheads increases almost linearly with v' vibrational number, allowing for an easier differentiation of the lines pertaining to a given isotopologue for increasing v' and J'.

3.1. Specific cases of $^{12}C^{17}O$ and $^{13}C^{17}O$

3.1.1. $^{12}C^{17}O$

As $^{12}C^{17}O$ is mixed in almost equal proportions with $^{12}C^{16}O$ in our sample, the absolute calibration of $^{12}C^{17}O$ transitions benefits from the absolute calibration of $^{12}C^{16}O$ (as well as $^{12}C^{18}O$, which is also present in a small amount).

3.1.2. $^{13}C^{17}O$

The case of $^{13}C^{17}O$ is specific because it is observed in the high-pressure spectra of either $^{13}C^{16}O$ or $^{13}C^{18}O$. The occurrence of the $^{13}C^{17}O$ bands is due to isotopic contamination of the $^{13}C^{16}O$ and $^{13}C^{18}O$ bottles. Based on the relative strengths of identical absorption features, the ratio of the isotopologues

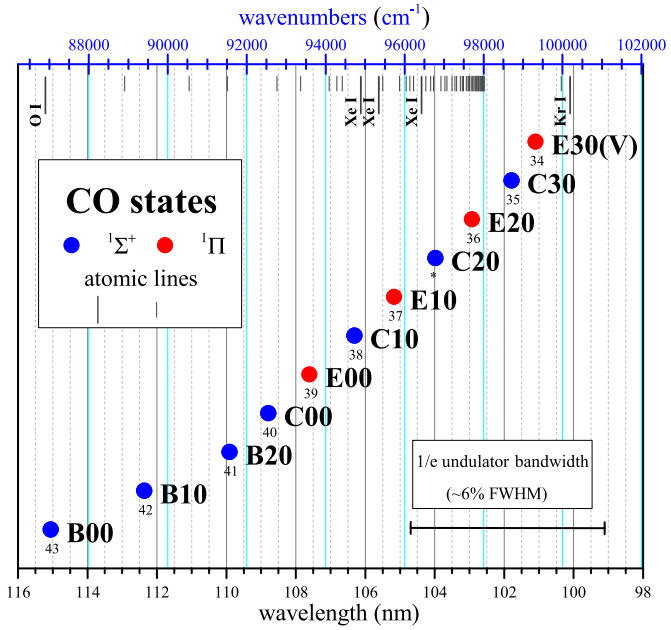

Fig. 1. Bandhead wavelengths of $^{12}C^{16}O$ states and bands studied in this work. We also include the previously used numerical index notation (34–43) (Letzelter et al. 1987; Eidelsberg & Rostas 1990, etc.). Atomic line calibrators are indicated with | : for primary lines at high accuracy (1 fm or better) and with | : for secondary lines at medium accuracy (0.1 pm) (for the latter, mostly Xe I and a few Ar I and Kr I, see the NIST atomic line tables for identification), and the 1/e undulator bandwidth are shown as well.

in the $^{13}C^{16}O$ gas sample, sorted by concentration, is found to be $^{13}C^{16}O$:$^{13}C^{18}O$:$^{13}C^{17}O$:$^{12}C^{16}O$ = 1:0.041:0.073:0:0045. The high CO pressure needed to observe the minor $^{13}C^{17}O$ species leads to strong absorption and saturation of the main species spectrum. Combined with the fact that the isotopic shifts of $v' = 0$ bands are very small ($\leq$1 cm^{-1} for B00 and C00 and $\leq$3 cm^{-1} for E00), $^{13}C^{17}O$ lines for low J' are difficult to extract because of blending with saturated (broadened) lines. This effect is weaker for increasing J' because of the difference between molecular constants of the different isotopologues. $^{13}C^{17}O$ lines of B00 with $J' > 2$ are measured nearly as accurately (~0.04 cm^{-1}) as for the main isotopologue (either $^{13}C^{16}O$ or $^{13}C^{18}O$), similarly for C00 lines with $J' > 6$. The search for low J' line positions is facilitated by considering the values extrapolated from the clearly observed high J' line levels (up to $J' = 23$ for B00, $J' = 21$ for B10, $J' = 39$ for C10, and $J' = 26$ for E00), which leads to an accuracy better than 0.08 cm^{-1} for the low J'. This effect is less noticeable for $v' \geq 1$ as the spacing of spectra bandheads of the different isotopologues increases with v'.

All this concerns R- and P-branches, but there is an additional difficulty for Q-branches that we consider in the E-state subsection.

3.2. $X^1\Sigma^+$ state

In order to calculate the term values of all the bands presented here, high-accuracy data provided by Guelachvili et al. (1983) and Farrenq et al. (1991) were used. From their set of Dunham coefficients, rotational levels of the $v'' = 0$ $X^1\Sigma^+$ ground state were calculated up to $J'' = 48$ with an uncertainty of 10^{-3} cm^{-1}, which is at least as good as our own high-resolution measurements. Table 9 lists the ground-state rotational levels of the six

Table 3. References to table and figure numbers for the $B^1\Sigma^+$ state.

Band	Transition wavelengths			Term values	Reduced TV
	Tables		Figure	Table	Figure
	^{12}C	^{13}C			
B00	A.1	A.2	2	A.3	4
B10	A.4	A.5	3	A.6	5
B20	A.7	A.7	A.1	A.8	A.2

isotopologues studied here, $^{12}C^{16}O$, $^{12}C^{17}O$, $^{12}C^{18}O$, $^{13}C^{16}O$, $^{13}C^{17}O$, and $^{13}C^{18}O$. For each isotopologue, these J'' levels are adjusted to a ninth-order polynomial to obtain their molecular constants. They are reported in Table A.31.

For the sake of consistency between all isotopologues, we did not use the data on the $^{12}C^{16}O$ ground state by Varberg & Evenson (February 1992), which were published a few months after Farrenq et al. (October 1991). The latter provide data for six isotopologues, and a check on $^{12}C^{16}O$ B00 revealed a better agreement at high J' between the term values TV_R and TV_P derived for the R- and P-branches.

3.3. $B^1\Sigma^+$ state

The B00 and B10 bands were observed for all isotopologues, while B20 was observed for all bands except for $^{12}C^{17}O$ and $^{13}C^{17}O$. The lack of the B20 band in the $^{12}C^{17}O$ spectra is explained by the low pressure used in scans of this isotopologue. For $^{13}C^{17}O$, the absence is due to the combination of a very low partial pressure and the decreasing oscillator strength with v'.

A total of 19 CO laser-calibrated lines (14 for $^{12}C^{16}O$, 2 for $^{12}C^{18}O$, and 3 for $^{13}C^{16}O$) were used to determine a shift correction of -7.5×10^{-6} nm ($0.006\,cm^{-1}$) for B00 and 3 lines for B10, resulting in a shift correction of -1.2×10^{-5} nm ($0.0095\,cm^{-1}$). These low values attest to the accuracy of our measurements. These corrections were applied to all isotopologues as their spectra are placed, as mentioned above, on a unique scale. Our term values are consistent within the uncertainty with those calculated by Le Floch & Amiot (1985) and Haridass et al. (1994), the latter resulting from the combination of B–A data with high-resolution A–X data obtained with the former Ottawa 10.6 m vacuum-grating spectrograph. For $^{12}C^{16}O$ B00, the average difference between our values and the Daprà et al. (2016) values is 5.0×10^{-6} nm.

For $^{12}C^{17}O$, the present results complete a preliminary version of our B00 data that was incorporated in Hakalla et al. (2016) in order to perform the deperturbation analysis of the $A^1\Pi$ state of $^{12}C^{17}O$, for which earlier optical measurements of B–A and C–A transitions were combined with our vacuum ultraviolet B–X results. Similarly, for $^{13}C^{17}O$, our results of B00 and B10 were used in Hakalla et al. (2017) to perform the deperturbation analysis of the $A^1\Pi$ state of $^{13}C^{17}O$.

The data for $^{13}C^{18}O$ are slightly better calibrated than in our recent paper (Lemaire et al. 2016) for B00 and B10. In addition, they are extended to higher J' levels for B10.

As indicated above, the B20 band was calibrated using the surrounding B10 and C00 bands, leading to a common shift correction of $+1.0\times10^{-5}$ nm ($-0.0083\,cm^{-1}$) that was applied to all isotopologues. Figure A.3 illustrates for the four observed isotopologues the perturbations observed in B20 (also studied in $^{12}C^{16}O$ and $^{13}C^{16}O$ by Baker 1994).

Table 4. Statistical uncertainty on the measured term values: δ_P average and std. dev. (at 2σ) (see Sect. 2.2.2) for the $B^1\Sigma^+$ state.

Band	Species	N	$\overline{\delta_P}$ (cm^{-1})	Std. dev. (cm^{-1})
B00	1216	62	0.000	0.007
	1217	44	0.007	0.023
	1218	60	0.003	0.022
	1316	60	0.011	0.026
	1317	36	0.001	0.026
	1318	54	0.002	0.006
B10	1216	60	0.00	0.02
	1217	30	−0.010	0.033
	1218	52	−0.001	0.009
	1316	54	−0.001	0.013
	1317	40	−0.011	0.027
	1318	38	0.007	0.010
B20	1216	22	−0.003	0.034
	1217			
	1218	22	0.019	0.038
	1316	30	−0.006	0.021
	1317			
	1318	30	−0.005	0.032

Notes. N: number of rotational transitions (R and P) involved in the statistics.

For $^{12}C^{16}O$, $^{12}C^{18}O$, $^{13}C^{16}O$, and $^{13}C^{18}O$, our absolutely calibrated data provide transition frequencies and term values for B00, B10, and B20 that are consistent at slightly higher accuracy with those measured by Eidelsberg et al. (1987), which were obtained with the Observatoire de Paris (Meudon, France) 10 m VUV grating spectrograph. The same remark applies to the line positions obtained by Baker (1994) for B20 of $^{12}C^{16}O$ with the same instrument.

Table 3 lists table and figure numbers associated with the BX bands. Table 4 gives the statistical uncertainty on the term values for the BX bands (see text in Sect. 2.2.2).

3.4. $C^1\Sigma^+$ state

C00, C10, C20, and C30 were observed for $^{12}C^{16}O$, $^{12}C^{18}O$, $^{13}C^{16}O$, and $^{13}C^{18}O$. For $^{12}C^{17}O$, all bands were observed except for C20, for the same reason as for B20. For $^{13}C^{17}O$, only C00 and C10 were observed; C20 and C30 are not observed for the same reason as for B20.

It is worth noting that for $^{12}C^{18}O$, the C30 band does not appear in the same room-temperature spectra obtained at pressures where C20 is observed. It is only observed in a low-temperature spectrum recorded at 90 ± 5 K, showing a limited number of J' levels.

Sixteen CO laser-calibrated lines were used to determine a shift correction of 1.3×10^{-5} nm ($-0.011\,cm^{-1}$) for C00. Seventy-two laser-calibrated lines were considered (not including $^{12}C^{17}O$ and $^{13}C^{17}O$, for which the number of lines in Cacciani et al. 2001 is limited) to determine the shift correction of 3.4×10^{-5} nm ($-0.031\,cm^{-1}$) for C10.

Our term values are consistent with those calculated by Haridass et al. (1994), which were obtained from the combination of C–A data with high-resolution A–X data obtained with the former Ottawa spectrograph. For $^{12}C^{16}O$ C00, the average difference between our values and the values of Daprà et al. (2016) is 4.4×10^{-5} nm ($-0.037\,cm^{-1}$).

For C00, the present results complete a preliminary version of our $^{12}C^{17}O$ data (as for B00) and provide new data on $^{13}C^{17}O$.

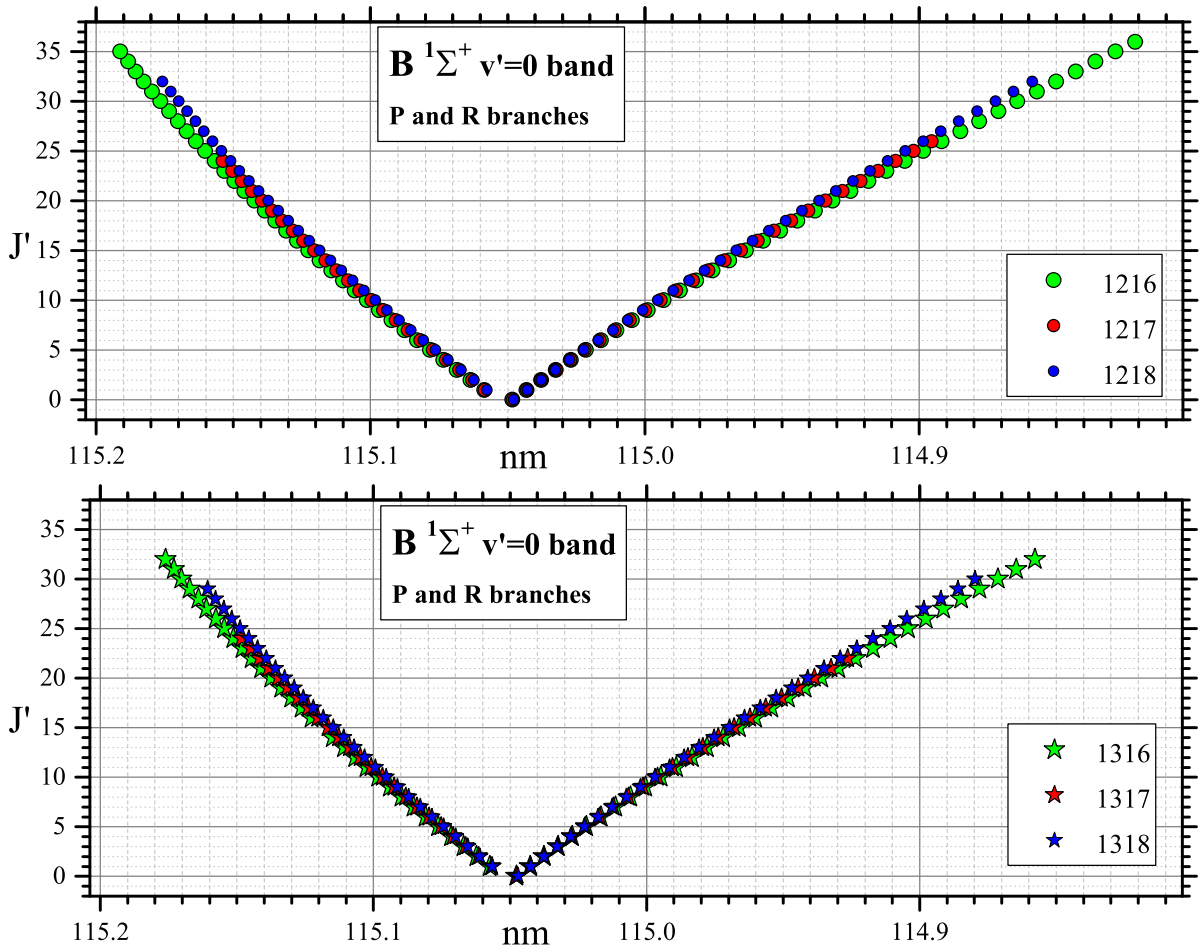

Fig. 2. Transition wavelengths of the $B^1\Sigma^+(v'=0)$–$X^1\Sigma^+(v''=0)$ band for six CO isotopologues.

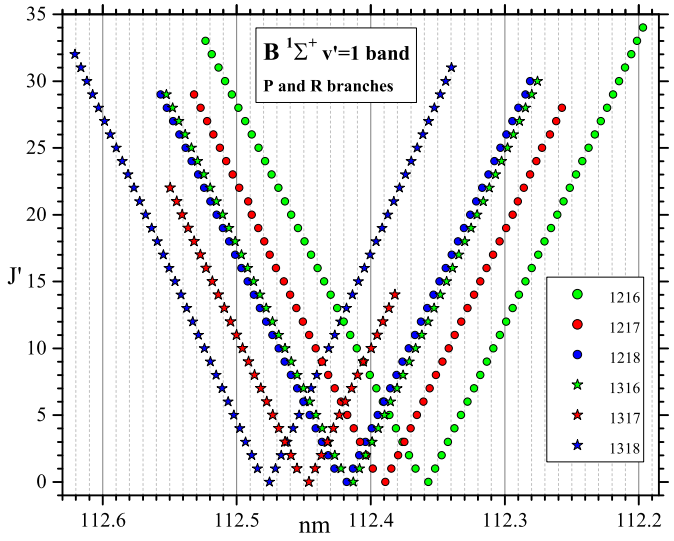

Fig. 3. Transition wavelengths of the $B^1\Sigma^+(v'=1)$–$X^1\Sigma^+(v''=0)$ band for six CO isotopologues.

Both were used in order to perform the deperturbation analysis of the $A^1\Pi$ state of $^{12}C^{17}O$ (Hakalla et al. 2016) and of $^{13}C^{17}O$ (Hakalla et al. 2017).

As for B00 and B10, the present data for $^{13}C^{18}O$ are slightly better calibrated and extend to higher J' levels than in our recent paper (Lemaire et al. 2016) for C00.

Table 5. References to table and figure numbers for the $C^1\Sigma^+$ state.

Band	Transition wavelengths			Term values	Reduced TV
	Tables		Figure	Table	Figure
	^{12}C	^{13}C			
C00	A.9	A.10	A.4	A.11	A.6
C10	A.12	A.13	A.5	A.14	A.7
C20	A.15	A.15	A.8	A.16	A.9
C30	A.17	A.17	A.10	A.18	A.11

The absolute calibration for C20 and C30 was obtained using the two surrounding primary atomic standards as calibrators (the Xe I line at 104.383497 nm for C20, and the Kr I line at 100.1060639 nm for C30, see Fig. 1) and checking that the numerous secondary standards (in the case of C20) are in agreement with each other (at an accuracy higher than 0.01 pm) for the five isotopologues.

Table 5 lists table and figure numbers associated with the CX bands. Table 6 gives the statistical uncertainty on the term values for the CX bands (see text in Sect. 2.2.2).

3.5. $E^1\Pi$ state

E00, E10, E20, and E30 [the latter formerly labeled as the **V** ($\mathbf{A}^2\Pi$) $^3\Pi$ state by Eidelsberg & Rostas (1990), with the present assignment confirmed by Lefèbvre-Brion & Eidelsberg (2012)] were observed for all isotopologues, with the exception

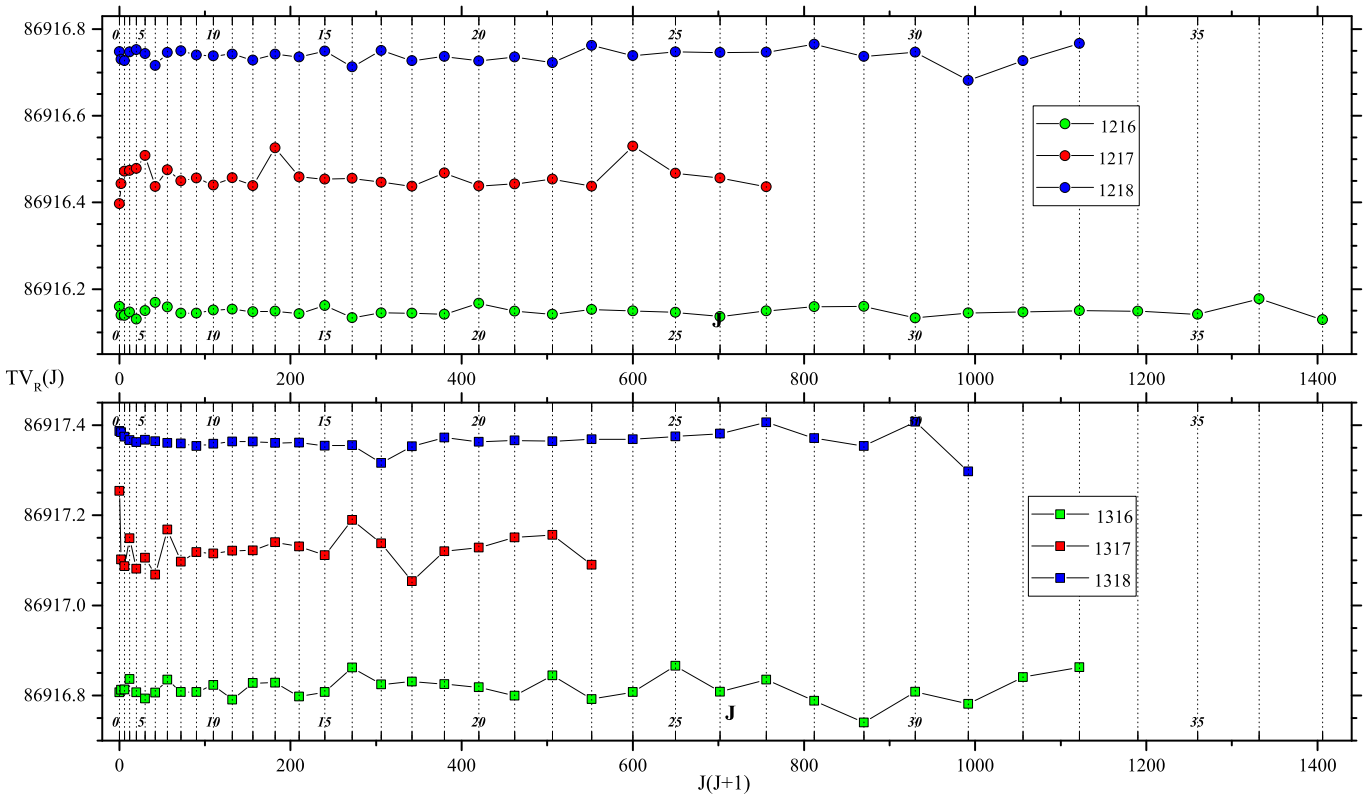

Fig. 4. Reduced term values (cm^{-1}) of the $B^1\Sigma^+(v'=0)$ levels for six CO isotopologues.

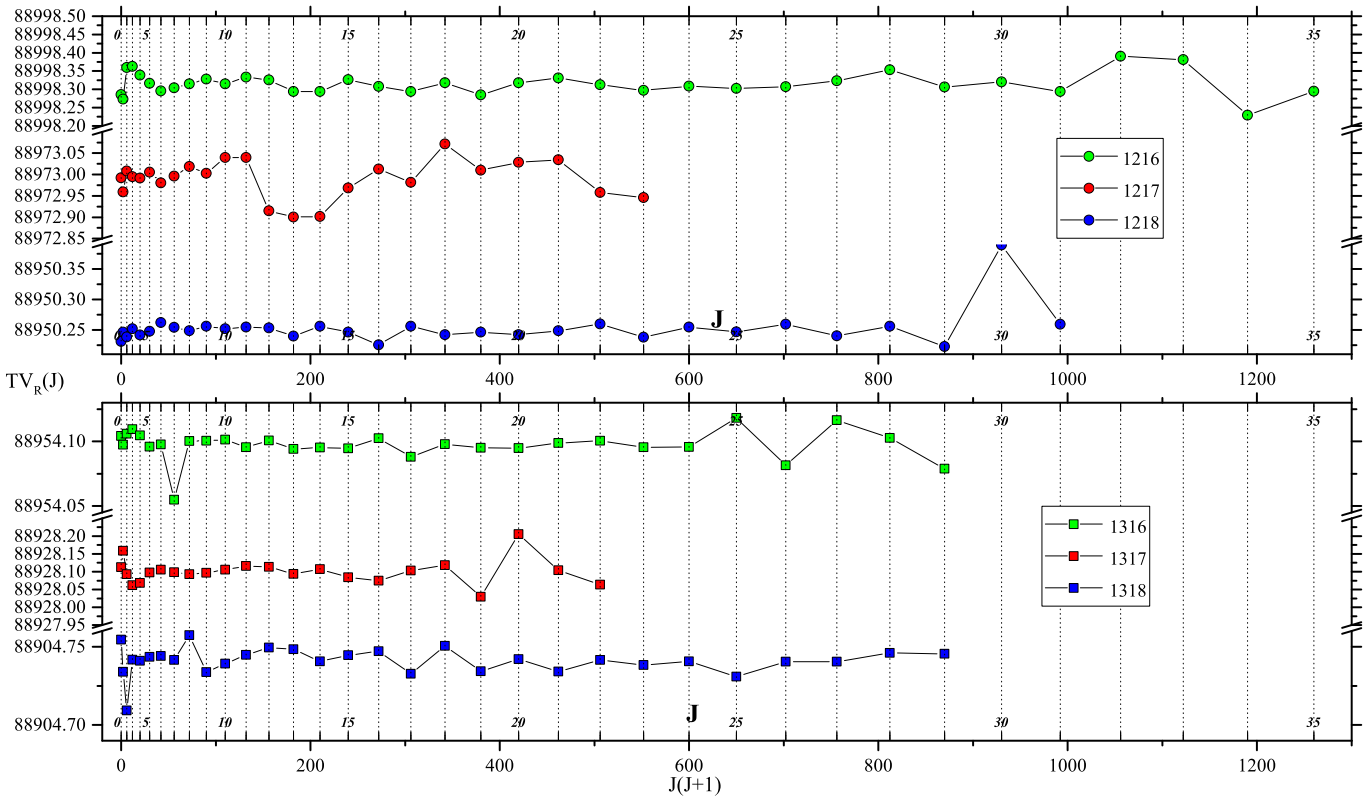

Fig. 5. Reduced term values (cm^{-1}) of the $B^1\Sigma^+(v'=1)$ levels for six CO isotopologues.

of E20 and E30 for $^{13}C^{17}O$ (as for B20 because of the combination of a very low partial pressure and decreasing oscillator strength with v').

For E20 and E30 of $^{12}C^{18}O$, the same remark holds as for C30. These two bands do not appear in spectra taken at room-temperature at pressures where E10 is observed. It is only observed in low-temperature spectra recorded at 90 ± 5 K, showing a limited number of J'.

For all isotopologues, the rotational spacing is extremely small for the Q-branch of E00, E10, and E20, giving rise to congested spectra that require better resolution than available with the VUV-FTS and smaller Doppler broadening. This is particularly noticeable for the Q-branch of E10, where the lines are very slightly blueshifted with J' compared to the Q-branch of E00, which is slightly blueshifted, and the Q-branch of E20, which is slightly redshifted. Only with the use of a very narrow-band laser were Cacciani & Ubachs (2004) able to separate the Q-branch of E00, and Ubachs et al. (2000) did this in combination with a deperturbation analysis for E10. The Q-branch of E30 has a very different aspect (similar to A–X transitions) with a redshifted Q-branch and a returning limb for the R-branch with increasing J' (see for comparison Figs. A.12, A.17, and A.25 vs. A.28, and also Figs. A.15, A.16, A.24, and A.27 vs. Figs. A.30–A.36).

A careful analysis is required to distinguish the lines in the E00 bands of the different isotopologues. Spectra recorded at different pressures were used for this purpose. Figure A.16 illustrates the difficulty of this task for E00 with three spectra for $^{13}C^{18}O$ and 2 for $^{13}C^{16}O$. Figure A.27 shows the easier example of E20 for $^{13}C^{16}O$ and $^{13}C^{18}O$, and Figs. A.30–A.36 show the example of E30 for $^{13}C^{18}O$.

There is very good agreement for the R- and P-branch line positions between our present results and other high-resolution measurements (Cacciani et al. 1995; Cacciani & Ubachs 2004 for E00 and Ubachs et al. 2000 for E10).

E00 was calibrated using a few levels observed by Cacciani et al. (1995) for $^{12}C^{16}O$ [3 lines] and a large set of R and P levels (Cacciani & Ubachs 2004) for $^{12}C^{16}O$ [60 lines] and $^{13}C^{16}O$ [32 lines] obtained by their methods labeled 1 and 0 (these data have to be calculated from the supplementary data, but no data are available for $^{13}C^{18}O$). The resulting shift correction is estimated as 2.3×10^{-5} nm (-0.020 cm^{-1}). Comparison to Daprà et al. (2016) shows an average difference of 3.8×10^{-5} nm for E00. For $^{12}C^{18}O$ and $^{13}C^{18}O$, our term values for E00 (e- and f-parity) match those calculated by Haridass et al. (1994) well, which were obtained from the combination of E–A data with high-resolution A–X data collected with the former Ottawa spectrograph. For the Q-branch of $^{12}C^{16}O$, $^{13}C^{16}O$, and $^{13}C^{18}O$, which we cannot separate, we report the Cacciani & Ubachs (2004) observed transition frequencies (see their Table 1). We merged the Cacciani et al. data with our higher-J' measurements. For the other isotopologues, $^{12}C^{17}O$ and $^{12}C^{18}O$, the Q bandhead up to $J' \approx 9$ was simulated to reproduce the observed spectra. These calculated data were merged with our measured data at higher J'. For the last isotopologue, $^{13}C^{17}O$, the Q-branch was simulated by interpolation of the $^{13}C^{16}O$ and $^{13}C^{18}O$ transitions (but these data are not reported in the table) in order to assign the few observed high J' Q-lines.

E10 was calibrated by a few lines observed by Cacciani et al. (1995) for $^{12}C^{16}O$ [9 lines] and a large set by Ubachs et al. (2000) of R and P lines for $^{12}C^{16}O$ [42 R and P lines], for $^{12}C^{17}O$ [2 R lines], $^{12}C^{18}O$ [24 P and R lines], $^{13}C^{16}O$ [25 P and R lines], and $^{13}C^{18}O$ [18 R lines]. The absolute calibration for E10 obtained with the R and P levels is also confirmed by the presence of closely surrounding Xe I atomic lines (see Fig. 1).

Table 6. Statistical uncertainty on the measured term values: δ_P average and std. dev. (at 2σ) (see Sect. 2.2.2) for the $C^1\Sigma^+$ state.

Band	Species	N	$\overline{\delta_P}$ (cm^{-1})	Std. dev. (cm^{-1})
C00	1216	72	0.010	0.027
	1217	66	−0.011	0.034
	1218	70	0.000	0.010
	1316	72	0.000	0.013
	1317	70	0.004	0.021
	1318	78	−0.001	0.007
C10	1216	62	0.001	0.013
	1217	42	0.001	0.010
	1218	52	−0.008	0.022
	1316	54	0.008	0.045
	1317	44	0.006	0.043
	1318	56	−0.003	0.017
C20	1216	28	0.003	0.012
	1217			
	1218	14	0.007	0.044
	1316	16	0.004	0.043
	1317			
	1318	14	−0.015	0.019
C30	1216	32	0.025	0.038
	1217	6	−0.007	0.048
	1218	16	−0.002	0.053
	1316	16	−0.004	0.056
	1317			
	1318	26	0.016	0.044

Notes. N: number of rotational transitions (R and P) involved in the statistics.

The resulting shift correction is estimated to be 5.0×10^{-6} nm. As it is not possible to distinguish the Q-branch of E10 for all isotopologues, we report in the tables the values obtained by Ubachs et al. (2000), merged with our measured data at higher J'. Our dataset for R- and P-branches extends those of Ubachs et al. (2000) to high J' values. Sample spectra are shown for $^{12}C^{16}O$ in Fig. A.20, $^{12}C^{17}O$ in Fig. A.21, $^{12}C^{18}O$ in Fig. A.22, $^{13}C^{16}O$ in Fig. A.23, and $^{13}C^{18}O$ in Fig. A.24. All of them show additional lines, and among them, lines that belong to the perturbing state $k^3\Pi(v' = 5$ and 6)–$X^1\Sigma^+(v' = 0)$ (Baker & Launay 1994; Ubachs et al. 2000). The lower panel of Fig. A.21 shows the simulated absorption spectrum of $^{12}C^{17}O$ at room temperature.

For E20 and E30, only low-resolution spectra without absolute calibration are available (Ogawa & Ogawa 1974 for $^{12}C^{16}O$ E20) and the Eidelsberg et al. (1991) atlas for $^{12}C^{16}O$, $^{12}C^{18}O$, $^{13}C^{16}O$, and $^{13}C^{18}O$ for both E20 and E30, with either measured or extrapolated or calculated line positions. Consequently, the absolute calibration of E20 and E30, for which there are no previous high-resolution measurements, was obtained in the same way as for C20 and C30, using the two surrounding primary atomic standards as calibrators and checking that the numerous secondary standards (in the case of E20) are in agreement with each other (at an accuracy higher than 0.01 pm) for five isotopologues (with the exception of $^{13}C^{17}O$). For E20, the Q-branch up to $J' = 6$ or 7 was obtained in the same way as for E10 by simulating our recorded spectra and merging them with the higher measurable J', up to ∼10–20, depending on the isotopologue. Figure A.27 shows the simulated absorption spectra of $^{12}C^{16}O$ at 90 K and at room temperature. Finally, as indicated above, all branches of E30 have well-resolved transitions for all observed

Table 7. References to table and figure numbers for the $E^1\Pi$ state.

Band	Transition wavelengths			Term values	Reduced TV	
	Tables		Figure	Table	Figure	
	^{12}C	^{13}C			e-par.	f-par.
E00	A.19	A.20	A.12	A.21	A.13	A.14
E10	A.22	A.23	A.17	A.24	A.18	A.19
E20	A.25	A.26	A.25	A.29	A.26	
E30	A.27	A.28	A.28	A.30	A.29	

isotopologues. Figures A.30–A.36 show spectra for all five isotopologues; in some cases, the results obtained at 293 K and 90 K are compared, which are useful to separate the R-branch lines.

In order to verify the quality of our frequency determinations for the Q-branch, we use a method similar to the combination differences. We compared the values of the Λ-type doubling of the upper state obtained through the R- and P-branches, $\Lambda_R(J)$ and $\Lambda_P(J)$ (for $J \geq 1$) with

$$\Lambda_R(J) = [R(J-1) + X(J-1)] - [Q(J) + X(J)] \text{ and}$$
$$\Lambda_P(J) = [P(J+1) + X(J+1)] - [Q(J) + X(J)].$$

For all isotopologues and all bands (E00, E01, E02, and E03), the results are consistent with the value of Λ_d provided in the term value tables. The Λ doubling of the upper state is graphically represented for all isotopologues in each band, E00, E10, E20, and E30, in Fig. A.37 together with polynomial fits (linear in most cases).

Table 7 lists table and figure numbers associated with the EX bands. Table 8 gives the statistical uncertainty on the e-parity term values of the EX bands (see text in Sect. 2.2.2).

4. Concluding remarks

Our work presents a comprehensive and homogeneous set of absolutely calibrated line positions from which term values and molecular constants are derived. In most cases, these were obtained from larger sets of data than earlier determinations. Our data complete previous determinations and fill many gaps, particularly concerning the B20, C20, C30, E20, and E30 bands of all isotopologues. We also provide new data, particularly for the $^{12}C^{17}O$ and $^{13}C^{17}O$ isotopologues.

A final verification of the absolute accuracy of our whole set of results is provided by comparison with the data reported by Daprà et al. (2016). These datasets were not considered as calibrators because they were derived from others cited in Sect. 2.1, but we verified that they are in good agreement (at least for the six J' levels included therein) with our own results on B00, C00, and E00 for $^{12}C^{16}O$.

In conclusion, the overall uncertainty of our data is a combination of the relative fitting accuracy in line positions (for a well-resolved typical line ~0.008 cm^{-1}) and of the accuracy in the calibrators and in the ground state (up to ~0.003 cm^{-1}). Most of the line positions are thus determined to an accuracy of ~0.009 cm^{-1}. For some weak (mainly at high J') or a few blended lines, the fitting errors are estimated to be as large as 0.10–0.15 cm^{-1}. Uncertainties on term value data are reflected in the δ_P values presented in the term value tables.

Molecular constants are compiled in Table A.31 for all states and bands. In this table the E state e- and f-parity are treated independently, and we calculate in Table A.32 $T_v(1)$ (average of T_v for e- and f-parity), $q_v = B_e - B_f$, and $q_{Dv} = D_e - D_f$. These molecular constants are also obtained by a quadratic fit of the Λ-doubling data shown in Fig. A.37 and reported in Table A.33.

Table 8. Statistical uncertainty on the measured term values: δ_P average and std. dev. (at 2σ) (see Sect. 2.2.2) for the e-parity levels (R and P) for the $E^1\Pi$ state.

Band	Species	N	$\overline{\delta_P}$ (cm^{-1})	Std. dev. (cm^{-1})
E00	1216	58	0.002	0.014
	1217	48	0.003	0.015
	1218	64	0.001	0.014
	1316	74	0.009	0.018
	1317	30	−0.008	0.018
	1318	68	0.018	0.032
E10	1216	50	0.004	0.031
	1217	38	0.009	0.024
	1218	44	0.004	0.021
	1316	54	0.000	0.018
	1317	36	−0.001	0.002
	1318	62	0.009	0.026
E20	1216	36	0.003	0.015
	1217	18	−0.004	0.026
	1218	20	0.008	0.015
	1316	36	0.001	0.014
	1317			
	1318	48	−0.003	0.027
E30	1216	30	−0.001	0.046
	1217	16	−0.002	0.037
	1218	18	−0.005	0.030
	1316	18	0.003	0.019
	1317			
	1318	22	0.000	0.010

Notes. N: number of rotational transitions (R and P) involved in the statistics.

In order to check the consistency of our term values, we compare their trends for the six CO isotopologues in Fig. A.38. The term value differences between ^{16}O and ^{18}O bearing isotopologues are compared both for ^{12}C and ^{13}C versus the B, C, and E states. Term values are also compared as a function of v' for each states, and a linear fit is drawn through all isotopologues present in each (T_V, v') data point. Both comparisons show a similar behavior.

The statistical table for the term values (see Tables 4, 6, and 8) can reveal the possible presence of perturbations when there is a large spread in the standard deviation (>0.043 cm^{-1}, namely for $^{12}C^{16}O$ (E30), for $^{12}C^{17}O$ (C30), for $^{12}C^{18}O$ (C20 and C30), for $^{13}C^{16}O$ (C10, C20 and C30), for $^{13}C^{17}O$ (C10), and for $^{13}C^{18}O$ (C30). Anomalies in the molecular constants also reveal evidence of perturbations, as shown in Fig. A.39, which illustrates this point more clearly than Table A.31. While T_v mainly depends on the absolute calibration, B_v and especially D_v are very sensitive to perturbations, as shown in Fig. A.39.

Perturbations will be discussed in detail in a subsequent paper. Another forthcoming development of this work will be a comprehensive atlas of oscillator strengths and cross sections for the states, bands, and isotopologues presented here.

Acknowledgements. We acknowledge SOLEIL for providing the synchrotron radiation facilities. All the data have been obtained on beamline DESIRS using the VUV-FTS spectrometer during proposals 20140051, 20120715, 20110121, 20100018, 20090021, and 20080025. We acknowledge assistance from the SOLEIL beamline staff (L. Nahon beamline manager), NdO (VUV-FTS manager and coauthor), and D. Joyeux (designer and builder of the VUV-FTS). This

Table 9. Rotational energy levels (cm^{-1}) of the $X^1\Sigma^+$ ground state for six CO isotopologues (calculated from the Farrenq et al. 1991 Dunham coefficients).

J''	$^{12}C^{16}O$	$^{12}C^{17}O$	$^{12}C^{18}O$	$^{13}C^{16}O$	$^{13}C^{17}O$	$^{13}C^{18}O$
0	0	0	0	0	0	0
1	3.845	3.748	3.662	3.676	3.579	3.493
2	11.535	11.244	10.986	11.028	10.736	10.478
3	23.069	22.487	21.971	22.055	21.472	20.956
4	38.448	37.477	36.617	36.757	35.786	34.926
5	57.670	56.214	54.924	55.134	53.677	52.388
6	80.735	78.696	76.891	77.185	75.145	73.340
7	107.642	104.924	102.518	102.909	100.190	97.783
8	138.390	134.895	131.802	132.305	128.809	125.715
9	172.978	168.610	164.743	165.372	161.003	157.136
10	211.404	206.066	201.341	202.109	196.770	192.044
11	253.667	247.262	241.593	242.515	236.108	230.438
12	299.766	292.197	285.498	286.588	279.017	272.317
13	349.698	340.869	333.055	334.326	325.495	317.679
14	403.461	393.276	384.261	385.727	375.540	366.523
15	461.054	449.416	439.116	440.791	429.150	418.847
16	522.475	509.288	497.616	499.515	486.324	474.650
17	587.721	572.888	559.761	561.896	547.059	533.928
18	656.789	640.215	625.546	627.932	611.354	596.681
19	729.677	711.266	694.971	697.622	679.206	662.906
20	806.383	786.039	768.033	770.962	750.612	732.601
21	886.902	864.530	844.729	847.950	825.571	805.763
22	971.233	946.737	925.056	928.582	904.079	882.391
23	1059.372	1032.657	1009.011	1012.857	986.133	962.480
24	1151.315	1122.285	1096.591	1100.771	1071.731	1046.028
25	1247.059	1215.620	1187.794	1192.320	1160.870	1133.034
26	1346.601	1312.658	1282.615	1287.502	1253.546	1223.492
27	1449.936	1413.395	1381.051	1386.312	1349.757	1317.401
28	1557.061	1517.827	1483.099	1488.748	1449.498	1414.757
29	1667.971	1625.950	1588.755	1594.805	1552.767	1515.557
30	1782.662	1737.760	1698.015	1704.480	1659.559	1619.797
31	1901.131	1853.254	1810.876	1817.769	1769.870	1727.473
32	2023.371	1972.426	1927.332	1934.667	1883.698	1838.582
33	2149.380	2095.273	2047.380	2055.170	2001.037	1953.120
34	2279.151	2221.790	2171.015	2179.274	2121.884	2071.084
35	2412.680	2351.972	2298.233	2306.975	2246.234	2192.468
36	2549.962	2485.814	2429.030	2438.267	2374.083	2317.268
37	2690.991	2623.311	2563.400	2573.145	2505.427	2445.482
38	2835.763	2764.459	2701.339	2711.606	2640.260	2577.102
39	2984.271	2909.251	2842.841	2853.643	2778.577	2712.127
40	3136.509	3057.682	2987.901	2999.252	2920.375	2850.549
41	3292.473	3209.748	3136.515	3148.427	3065.647	2992.366
42	3452.156	3365.442	3288.676	3301.163	3214.389	3137.572
43	3615.552	3524.758	3444.380	3457.454	3366.596	3286.161
44	3782.655	3687.690	3603.619	3617.295	3522.261	3438.129
45	3953.457	3854.233	3766.390	3780.679	3681.380	3593.470
46	4127.954	4024.380	3932.685	3947.601	3843.946	3752.179
47	4306.137	4198.125	4102.499	4118.054	4009.954	3914.251
48	4488.001	4375.461	4275.825	4292.033	4179.399	4079.679

research was supported by NASA (grants NNG 06-GG70G and NNX10AD80G to the Univ. of Toledo and NNX09AC5GG to Wellesley College). J. R. L. and G. S. thank the NASA Origins of Solar System program (Grant NNX14AD49G) for funding. A. H., while in the Amsterdam team, acknowledges support from the Dutch astrochemistry network (DAN) from the Netherlands Organisation for Scientific Research (NWO) under grant 648.000.002 and the research fellowship program of PSL Research University Paris. J. L. L. thanks the ISMO-CNRS (Institut des Sciences Moléculaires d'Orsay at Université Paris-Sud) for hosting him as visiting researcher.

References

Baker, J. J. 1994, J. Mol. Spec., 167, 323
Baker, J., & Launay, F. 1994, J. Mol. Spec., 165, 75
Baker, J., Lemaire, J. L., Couris, S., et al. 1993, Chem. Phys., 178, 569
Baker, J., Lemaire, J. L., Couris, S., et al. 1994, AIP Conf. Proc., 312, 355
Brandi, F., Velchev, I., Hogervorst, W., & Ubachs, W. 2001, Phys. Rev. A, 64, 032505
Brandi, F., Hogervorst, W., & Ubachs, W. 2002, J. Phys. B, 35, 1071

Cacciani, P., & Ubachs, W. 2004, J. Mol. Spectr., 225, 62
Cacciani, P., Hogervorst, W., & Ubachs, W. 1995, J. Chem. Phys, 102, 8308
Cacciani, P., Brandi, F., Velchev, I., et al. 2001, Eur. Phys. J. D, 15, 47
Daprà, M., Niu, M. L., Salumbides, E. J., Murphy, T., & Ubachs, W. 2016, ApJ, 826, 192
de Oliveira, N., Joyeux, D., Phalippou, D., et al. 2009, Rev. Sci. Instrum., 80, 043101
de Oliveira, N., Roudjane, M., Joyeux, D., et al. 2011, Nat. Photon., 5, 149
de Oliveira, N., Joyeux, D., Roudjane, M., et al. 2016, J. Synchrotron Radiat, 23, 887
Drabbels, M., Meerts, W. L., & ter Meulen, J. J. 1993a, J. Chem. Phys., 99, 2352
Drabbels, M., Heinze, J., ter Meulen, J. J., & Meerts, W. L. 1993b, J. Chem. Phys., 99, 5701
Eidelsberg, M., & Rostas, F. 1990, A&A, 235, 472
Eidelsberg, M., Roncin, J.-Y., Le Floch, A., et al. 1987, J. Mol. Spectr., 121, 309
Eidelsberg, M., Benayoun, J. J., Viala, Y. P., & Rostas, F. 1991, A&AS, 90, 231
Eidelsberg, M., Benayoun, J. J., Viala, Y. P., et al. 1992, A&A, 265, 839
Eidelsberg, M., Lemaire, J. L., Federman, S., et al. 2012, A&A, 543, A69
Eidelsberg, M., Lemaire, J. L., Federman, S. R., et al. 2014, A&A, 566, A96
Eidelsberg, M., Lemaire, J. L., Federman, S. R., et al. 2017, A&A, 602, A76
Farrenq, R., Guelachvili, G., Sauval, A. J., Grevesse, N., & Farmer, C. B. 1991, J. Mol. Spectr., 149, 375
Federman, S. R., Fritts, M., Cheng, S., Menningen, K. M., Knauth, D. C., & Fulk, K. 2001, ApJS, 134, 133
Gavilan, L., Lemaire, J. L., Eidelsberg, M., et al. 2013, J. Phys. Chem. A, 117, 9644
Guelachvili, G., de Villeneuve, D., Farrenq, R., Urban, W., & Verges, J. 1983, J. Mol. Spectr., 98, 64
Hakalla, R., Niu, M. L., Field, R. W., et al. 2016, RSC Adv., 6, 31588
Hakalla, R., Niu, M. L., Field, R. W., et al. 2017, J. Quant. Spectr. Rad. Transf., 189, 312
Haridass, C., Paddy Teddy, S., & Le Floch, A. C. 1994, J. Mol. Spectr., 168, 429
Heays, A. N., Eidelsberg, M., Stark, G., et al. 2014, J. Chem. Phys., 141, 144311
Herzberg, G. 1950, in Spectra of Diatomic Molecules, Molecular Spectra and Molecular Structure, 2nd ed. (New York: Van Nostrand Reinhold), 1
Ivanov, T. I., Salumbides, E. J., Vieitez, M. O., et al. 2008, MNRAS, 389, 4
Kaufman, V., & Edlén, B. 1974, J. Phys. Chem. Ref. Data, 3, 825
Lefèbvre-Brion, H., & Eidelsberg, M. 2012, J. Mol. Spectr., 271, 59
Le Floch, A. 1992, J. Mol. Spectr. 155, 177
Le Floch, A., & Amiot, C. 1985, Chem. Phys., 97, 379
Lemaire, J. L., Eidelsberg, M., Heays, A. N., et al. 2016, J. Phys. B, 49, 4001
Letzelter, C., Eidelsberg, M., Rostas, F., Breton, J., & Thieblemont, B. 1987, Chem. Phys., 114, 273
Morton, D. C., & Noreau, L. 1994, ApJS, 95, 301
Nahon, L., de Oliveira, N., Garcia, G., et al. 2012, J. Synchrotron Radiat., 19, 508
Nahon, L., de Oliveira, N., Garcia, G. A., et al. 2013, J. Phys. Conf. Ser., 425, 122004
Niu, M. L., Hakalla, R., Madhu Trivikram, T., et al. 2016, Mol. Phys., 114, 2857
Ogawa, S., & Ogawa, M. 1974, J. Mol. Spectr., 49, 4540
Philip, J., Sprengers, J. P., Cacciani, P., de Lange, C. A., & Ubachs, W. 2004, Appl. Phys. B, 78, 737
Stark, G., Lewis, B. R., Gibson, S. T., & England, J. P. 1999, ApJ, 520, 732
Stark, G., Heays, A. N., Lyons, J. R., et al. 2014, ApJ, 788, 67
Ubachs, W., Eikema, K. S. E., Levelt, P. F., et al. 1994, ApJ, 427, L55
Ubachs, W., Hinnen, P. C., Hansen, P., et al. 1995, J. Mol. Spectr., 174, 388
Ubachs, W., Velchev, I., & Cacciani, P. 2000, J. Chem. Phys., 113, 547
van Dishoeck, E. F., & Black, J. H. 1988, ApJ, 334, 771
Viala, Y. P., Letzelter, C., Eidelsberg, M., & Rostas, F. 1988, A&A, 193, 265
Visser, R., van Dishoeck, E. F., & Black, J. H. 2009, A&A, 503, 323
Yoshino, K., & Freeman, D. E. 1985, J. Opt. Soc. Am. B, 2, 1268

Appendix A: Additional figures and tables

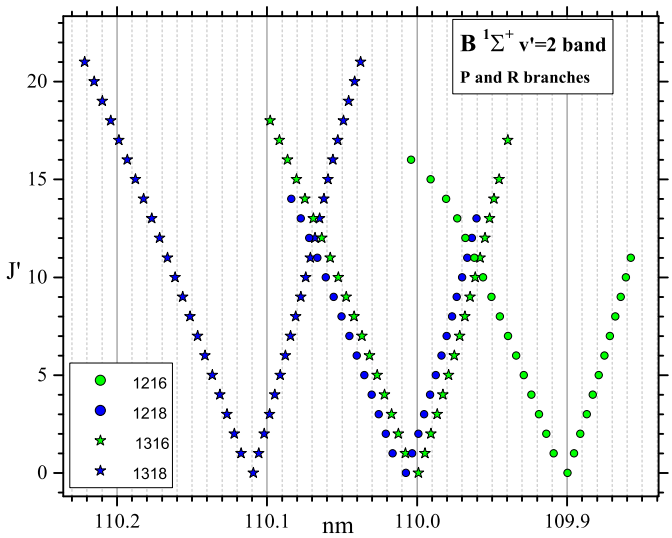

Fig. A.1. Transition wavelengths of the $B^1\Sigma^+(v'=2)$–$X^1\Sigma^+(v''=0)$ band for the four observed CO isotopologues.

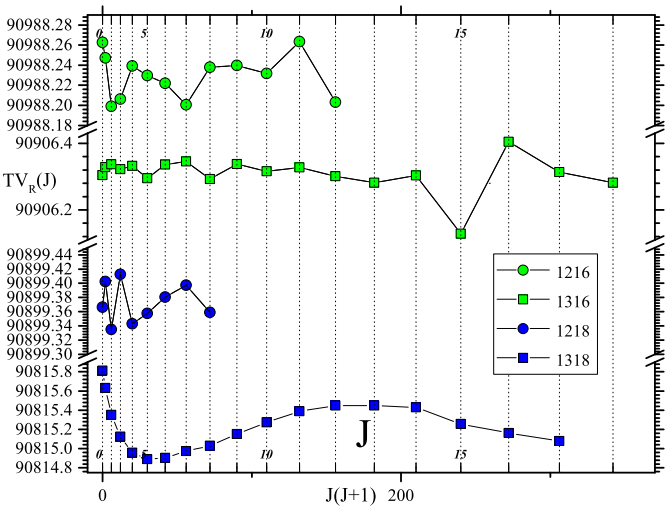

Fig. A.2. Reduced term values (cm^{-1}) of the $B^1\Sigma^+(v'=2)$ levels for the four observed CO isotopologues.

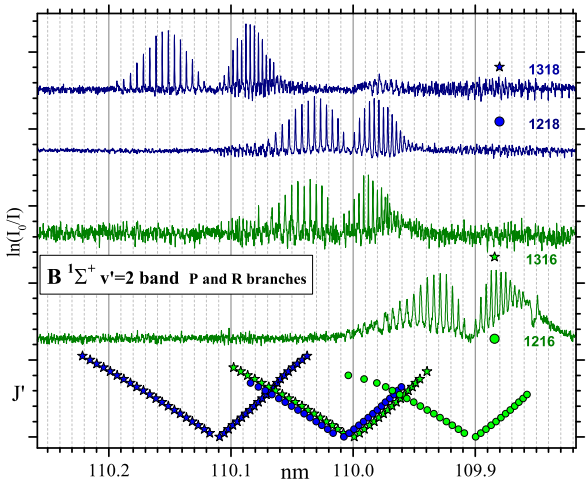

Fig. A.3. Sample of B20 spectra for the four observed isotopologues, in some cases showing perturbations.

Table A.1. Measured transition wavelengths and wavenumbers of the $B^1\Sigma^+(v'=0)$–$X^1\Sigma^+(v''=0)$ band for $^{12}C^{16}O$, $^{12}C^{17}O$, and $^{12}C^{18}O$.

$B^1\Sigma^+(v'=0)$–$X^1\Sigma^+(v''=0)$															
	$^{12}C^{16}O$					$^{12}C^{17}O$					$^{12}C^{18}O$				
J''	R_{ms} (nm)	P_{ms} (nm)	R_{ms} (cm^{-1})	P_{ms} (cm^{-1})	δ_P	R_{ms} (nm)	P_{ms} (nm)	R_{ms} (cm^{-1})	P_{ms} (cm^{-1})	δ_P	R_{ms} (nm)	P_{ms} (nm)	R_{ms} (cm^{-1})	P_{ms} (cm^{-1})	δ_P
0	115.04826		86920.042			115.04802		86920.225			115.04772		86920.452		
1	115.04305	115.05849	86923.984	86912.315	6	115.04289	115.05805	86924.101	86912.649	−17	115.04274	115.05747	86924.214	86913.086	10
2	115.03774	115.06355	86927.998	86908.496	1	115.03770	115.06286	86928.023	86909.015	−17	115.03766	115.06229	86928.053	86909.445	16
3	115.03240	115.06850	86932.031	86904.758	9	115.03245	115.06765	86931.990	86905.397	5	115.03258	115.06702	86931.892	86905.873	26
4	115.02696	115.07339	86936.140	86901.066	9	115.02708	115.07244	86936.048	86901.779	20	115.02741	115.07166	86935.799	86902.368	3
5	115.02144	115.07823	86940.314	86897.411	0	115.02189	115.07715	86939.971	86898.222	51	115.02224	115.07621	86939.706	86898.932	14
6	115.01590	115.08294	86944.501	86893.853	6	115.01641	115.08178	86944.113	86894.726	0	115.01689	115.08076	86943.750	86895.497	−4
7	115.01030	115.08760	86948.737	86890.331	3	115.01098	115.08637	86948.218	86891.261	9	115.01156	115.08523	86947.780	86892.121	9
8	115.00463	115.09223	86953.021	86886.840	4	115.00540	115.09083	86952.437	86887.897	−5	115.00615	115.08960	86951.870	86888.822	−15
9	114.99887	115.09679	86957.379	86883.393	−12	114.99982	115.09527	86956.656	86884.542	16	115.00067	115.09389	86956.013	86885.583	−11
10	114.99304	115.10125	86961.787	86880.030	−8	114.99412	115.09965	86960.966	86881.235	11	114.99514	115.09817	86960.195	86882.353	−9
11	114.98716	115.10565	86966.228	86876.707	2	114.98844	115.10396	86965.262	86877.982	17	114.98953	115.10237	86964.437	86879.182	−21
12	114.98121	115.11000	86970.730	86873.423	3	114.98244	115.10818	86969.800	86874.802	−5	114.98382	115.10648	86968.756	86876.080	−1
13	114.97524	115.11428	86975.249	86870.193	9	114.97678	115.11233	86974.081	86871.665	63	114.97812	115.11059	86973.067	86872.978	20
14	114.96914	115.11849	86979.863	86867.016	−8	114.97085	115.11640	86978.566	86868.594	−17	114.97233	115.11460	86977.447	86869.952	10
15	114.96304	115.12261	86984.475	86863.908	−2	114.96487	115.12041	86983.090	86865.568	−2	114.96654	115.11853	86981.828	86866.986	2
16	114.95686	115.12666	86989.151	86860.854	1	114.95884	115.12440	86987.654	86862.558	−1	114.96062	115.12237	86986.307	86864.089	−1
17	114.95060	115.13070	86993.892	86857.806	−17	114.95278	115.12830	86992.241	86859.620	6	114.95465	115.12622	86990.824	86861.184	−23
18	114.94430	115.13459	86998.662	86854.872	−7	114.94661	115.13215	86996.913	86856.714	−9	114.94864	115.12988	86995.373	86858.423	10
19	114.93787	115.13846	87003.527	86851.949	−10	114.94040	115.13590	87001.608	86853.881	−23	114.94258	115.13363	86999.959	86855.594	−4
20	114.93149	115.14226	87008.359	86849.088	9	114.93414	115.13954	87006.349	86851.136	2	114.93644	115.13721	87004.607	86852.893	−3
21	114.92501	115.14597	87013.265	86846.284	−8	114.92781	115.14325	87011.143	86848.341	−5	114.93027	115.14077	87009.278	86850.208	−3
22	114.91843	115.14963	87018.241	86843.524	−7	114.92137	115.14680	87016.015	86845.662	−8	114.92399	115.14424	87014.032	86847.590	0
23	114.91184	115.15323	87023.231	86840.809	3	114.91489	115.15028	87020.926	86843.033	51	114.91774	115.14768	87018.765	86844.996	−9
24	114.90519	115.15676	87028.271	86838.153	−3	114.90849	115.15382	87025.775	86840.364		114.91137	115.15097	87023.589	86842.514	−18
25	114.89849	115.16021	87033.342	86835.550	−2	114.90196		87030.716			114.90494	115.15428	87028.458	86840.018	−9
26	114.89170	115.16360	87038.490	86832.989	−6	114.89540		87035.688			114.89851	115.15751	87033.329	86837.583	16
27	114.88486	115.16694	87043.673	86830.477	2						114.89198	115.16071	87038.275	86835.170	−1
28	114.87798	115.17019	87048.886	86828.026	6						114.88544	115.16379	87043.230	86832.847	1
29	114.87110	115.17337	87054.100	86825.627	9						114.87886	115.16681	87048.216	86830.570	18
30	114.86409	115.17650	87059.409	86823.267	−1						114.87215	115.16985	87053.300	86828.278	−10
31	114.85707	115.17958	87064.733	86820.943	6						114.86552	115.17272	87058.325	86826.115	99
32	114.84998	115.18257	87070.105	86818.688	0						114.85872	115.17581	87063.479	86823.785	
33	114.84285	115.18550	87075.509	86816.485											
34	114.83569		87080.944												
35	114.82841		87086.459												
36	114.82121		87091.926												

Notes. Column description (refer also to Sect. 2.2) for each isotopologue. Col. 1: J''. Cols. 2 and 3: R_c and P_c calibrated wavelengths. Cols. 4 and 5: R_c and P_c calibrated wavenumbers. Col. 6: δ_P wavenumber corrections applied to TV_P in units of the least significant digit ($-\delta_P$ is applied to TV_R). No value indicates the absence of one of the branches, either R or P. An asterisk indicates when both R- and P-branches are present at high J', either the potential presence of a perturbing state or that one of the lines shows a larger uncertainty than the other.

Table A.2. Measured transition wavelengths and wavenumbers of the $B^1\Sigma^+(v'=0)$–$X^1\Sigma^+(v''=0)$ band for $^{13}C^{16}O$, $^{13}C^{17}O$, and $^{13}C^{18}O$ (same column description as for Table A.1).

$B^1\Sigma^+(v'=0)$–$X^1\Sigma^+(v''=0)$															
	$^{13}C^{16}O$					$^{13}C^{17}O$					$^{13}C^{18}O$				
J''	R_{ms} (nm)	P_{ms} (nm)	R_{ms} (cm^{-1})	P_{ms} (cm^{-1})	δ_P	R_{ms} (nm)	P_{ms} (nm)	R_{ms} (cm^{-1})	P_{ms} (cm^{-1})	δ_P	R_{ms} (nm)	P_{ms} (nm)	R_{ms} (cm^{-1})	P_{ms} (cm^{-1})	δ_P
0	115.04759		86920.550			115.04746		86920.648			115.04708		86920.935		
1	115.04260	115.05741	86924.320	86913.131	12	115.04250	115.05669	86924.396	86913.675	−80	115.04236	115.05640	86924.501	86913.894	11
2	115.03751	115.06222	86928.166	86909.498	8	115.03741	115.06146	86928.242	86910.072	9	115.03756	115.06098	86928.128	86910.435	1
3	115.03243	115.06695	86932.005	86905.925	8	115.03261	115.06621	86931.869	86906.484	72	115.03269	115.06548	86931.809	86907.036	3
4	115.02726	115.07159	86935.912	86902.421	4	115.02753	115.07076	86935.708	86903.048	0	115.02777	115.06993	86935.527	86903.675	9
5	115.02199	115.07623	86939.895	86898.917	5	115.02247	115.07524	86939.533	86899.665	−1	115.02278	115.07432	86939.298	86900.360	−4
6	115.01664	115.08079	86943.939	86895.474	7	115.01717	115.07963	86943.539	86896.350	0	115.01773	115.07861	86943.115	86897.120	0
7	115.01130	115.08525	86947.976	86892.106	6	115.01206	115.08404	86947.402	86893.020	−2	115.01262	115.08287	86946.978	86893.903	4
8	115.00586	115.08962	86952.089	86888.807	6	115.00669	115.08820	86951.462	86889.879	−22	115.00746	115.08707	86950.879	86890.732	6
9	115.00033	115.09400	86956.270	86885.500	8	115.00136	115.09250	86955.491	86886.633	16	115.00224	115.09120	86954.826	86887.614	5
10	114.99480	115.09828	86960.452	86882.269	14	114.99597	115.09669	86959.567	86883.470	2	114.99694	115.09527	86958.834	86884.542	−7
11	114.98919	115.10248	86964.695	86879.099	22	114.99049	115.10078	86963.711	86880.382	−22	114.99160	115.09925	86962.872	86881.537	−1
12	114.98340	115.10668	86969.074	86875.929	−25	114.98491	115.10478	86967.932	86877.363	−17	114.98619	115.10319	86966.963	86878.563	−6
13	114.97778	115.11065	86973.325	86872.933	55	114.97932	115.10876	86972.160	86874.359	0	114.98074	115.10706	86971.086	86875.642	3
14	114.97190	115.11477	86977.773	86869.824	−9	114.97368	115.11267	86976.426	86871.409	8	114.97520	115.11089	86975.276	86872.752	−6
15	114.96607	115.11868	86982.183	86866.876	39	114.96798	115.11654	86980.738	86868.488	18	114.96964	115.11463	86979.482	86869.929	18
16	114.96015	115.12261	86986.663	86863.908	−41	114.96218	115.12036	86985.127	86865.606	−68	114.96406	115.11836	86983.704	86867.115	5
17	114.95415	115.12625	86991.203	86861.161	−6	114.95640	115.12386	86989.500	86862.965	7	114.95832	115.12197	86988.047	86864.391	7
18	114.94813	115.13010	86995.759	86858.257	2	114.95050	115.12768	86993.965	86860.082	54	114.95255	115.12559	86992.414	86861.659	10
19	114.94202	115.13379	87000.383	86855.473	−6	114.94454	115.13144	86998.476	86857.246	−2	114.94678	115.12905	86996.780	86859.049	13
20	114.93588	115.13741	87005.031	86852.742	11	114.93845	115.13480	87003.085	86854.711	1	114.94092	115.13247	87001.216	86856.469	2
21	114.92967	115.14100	87009.732	86850.034	19	114.93244	115.13825	87007.635	86852.108	45	114.93503	115.13585	87005.674	86853.919	6
22	114.92345	115.14453	87014.441	86847.372	−25	114.92641	115.14167	87012.200	86849.529	1	114.92907	115.13917	87010.186	86851.415	−3
23	114.91707	115.14784	87019.272	86844.875	−6		115.14493		86847.070	2	114.92305	115.14242	87014.744	86848.963	−4
24	114.91069	115.15130	87024.104	86842.266	24		115.14828		86844.543		114.91699	115.14561	87019.333	86846.557	5
25	114.90421	115.15462	87029.011	86839.762	−30						114.91087	115.14876	87023.967	86844.181	−2
26	114.89776	115.15771	87033.897	86837.432	68						114.90468	115.15182	87028.655	86841.873	−2
27	114.89128	115.16109	87038.806	86834.883	18						114.89849	115.15483	87033.344	86839.604	−6
28	114.88477	115.16410	87043.738	86832.613	26						114.89227	115.15775	87038.056	86837.402	13
29	114.87802	115.16722	87048.852	86830.261	18						114.88589	115.16072	87042.889	86835.162	
30	114.87132	115.17026	87053.929	86827.969	38						114.87968		87047.594		
31	114.86461	115.17312	87059.015	86825.813	77										
32	114.85780	115.17607	87064.177	86823.589											

Table A.3. Term values (cm^{-1}) of the $B^1\Sigma^+(v'=0)$ levels for six CO isotopologues.

	$B^1\Sigma^+(v'=0)$					
J'	$^{12}C^{16}O$	$^{12}C^{17}O$	$^{12}C^{18}O$	$^{13}C^{16}O$	$^{13}C^{17}O$	$^{13}C^{18}O$
0	86916.160	86916.397	86916.748	86916.807	86917.254	86917.387
1	86920.036 (6)	86920.242 (−17)	86920.441 (10)	86920.538 (12)	86920.728 (−80)	86920.924 (11)
2	86927.828 (1)	86927.866 (−17)	86927.860 (16)	86927.988 (8)	86927.965 (9)	86927.993 (1)
3	86939.524 (9)	86939.261 (5)	86939.012 (26)	86939.186 (8)	86938.906 (72)	86938.604 (3)
4	86955.091 (9)	86954.456 (20)	86953.860 (3)	86954.056 (4)	86953.341 (0)	86952.756 (9)
5	86974.588 (0)	86973.474 (51)	86972.402 (14)	86972.664 (5)	86971.495 (−1)	86970.457 (−4)
6	86997.979 (6)	86996.185 (0)	86994.635 (−4)	86995.022 (7)	86993.210 (0)	86991.686 (0)
7	87025.233 (3)	87022.801 (9)	87020.633 (9)	87021.118 (6)	87018.686 (−2)	87016.452 (4)
8	87056.375 (4)	87053.147 (−5)	87050.312 (−15)	87050.879 (6)	87047.613 (−22)	87044.756 (6)
9	87091.422 (−12)	87087.316 (16)	87083.682 (−11)	87084.386 (8)	87080.255 (16)	87076.590 (5)
10	87130.365 (−8)	87125.255 (11)	87120.766 (−9)	87121.628 (14)	87116.492 (2)	87111.969 (−7)
11	87173.190 (2)	87167.015 (17)	87161.557 (−21)	87162.539 (22)	87156.359 (−22)	87150.879 (−1)
12	87219.893 (3)	87212.529 (−5)	87206.032 (−1)	87207.234 (−25)	87199.837 (−17)	87193.316 (−6)
13	87270.486 (9)	87261.933 (63)	87254.234 (20)	87255.606 (55)	87246.948 (0)	87239.278 (3)
14	87324.954 (−8)	87314.967 (−17)	87306.112 (10)	87307.659 (−9)	87297.646 (8)	87288.771 (−6)
15	87383.326 (−2)	87371.844 (−2)	87361.707 (2)	87363.461 (39)	87351.948 (18)	87341.782 (18)
16	87445.528 (1)	87432.507 (−1)	87420.944 (−1)	87423.016 (−41)	87409.956 (−68)	87398.324 (5)
17	87511.644 (−17)	87496.935 (6)	87483.946 (−23)	87486.183 (−6)	87471.444 (7)	87458.347 (7)
18	87581.619 (−7)	87565.139 (−9)	87550.575 (10)	87553.097 (2)	87536.506 (54)	87521.965 (10)
19	87655.461 (−10)	87637.152 (−23)	87620.923 (−4)	87623.698 (−6)	87605.321 (−2)	87589.082 (13)
20	87733.196 (9)	87712.873 (2)	87694.934 (−3)	87697.994 (11)	87677.680 (1)	87659.685 (2)
21	87814.750 (−8)	87792.393 (−5)	87772.643 (−3)	87775.973 (19)	87753.653 (45)	87733.811 (6)
22	87900.174 (−7)	87875.682 (−8)	87854.007 (0)	87857.707 (−25)	87833.204 (1)	87811.440 (−3)
23	87989.471 (3)	87962.700 (51)	87939.097 (−9)	87943.030 (−6)	87916.277 (2)	87892.581 (−4)
24	88082.606 (−3)	88053.582	88027.794 (−18)	88032.105 (24)		87977.219 (5)
25	88179.588 (−2)	88148.060	88120.189 (−9)	88124.904 (−30)		88065.363 (−2)
26	88280.407 (−6)	88246.337	88216.236 (16)	88221.263 (68)		88157.003 (−2)
27	88385.089 (2)	88348.346	88315.945 (−1)	88321.380 (18)		88252.153 (-6)
28	88493.603 (6)		88419.326 (1)	88425.092 (26)		88350.732 (13)
29	88605.938 (9)		88526.311 (18)	88532.467 (18)		88452.813
30	88722.072 (−1)		88636.981 (−10)	88643.620 (38)		88558.446
31	88842.065 (6)		88751.216 (99)	88758.333 (77)		88667.391
32	88965.864 (0)		88869.201	88876.784		
33	89093.476		88990.811	88998.843		
34	89224.889					
35	89360.095					
36	89499.139					
37	89641.888					

Notes. The δ_P value in parentheses (in units of the least significant digit) corresponds to the wavenumber correction applied to TV_P and TV_R. There is no value when the term value is derived from a single transition, either R or P. An asterisk indicates when both R- and P-branches are present at high J', either the potential presence of a perturbing state or that one of the lines shows a larger uncertainty than the other (see also Sect. 2.2.2).

Table A.4. Transition wavelengths and wavenumbers of the $B^1\Sigma^+(v'=1)$–$X^1\Sigma^+(v''=0)$ band for $^{12}C^{16}O$, $^{12}C^{17}O$, and $^{12}C^{18}O$ (same column description as for Table A.1).

$B^1\Sigma^+(v'=1)$–$X^1\Sigma^+(v''=0)$															
	$^{12}C^{16}O$					$^{12}C^{17}O$					$^{12}C^{18}O$				
J''	R_{ms} (nm)	P_{ms} (nm)	R_{ms} (cm^{-1})	P_{ms} (cm^{-1})	δ_P	R_{ms} (nm)	P_{ms} (nm)	R_{ms} (cm^{-1})	P_{ms} (cm^{-1})	δ_P	R_{ms} (nm)	P_{ms} (nm)	R_{ms} (cm^{-1})	P_{ms} (cm^{-1})	δ_P
0	112.35693		89002.078			112.38895		88976.717			112.41779		88953.892		
1	112.35196	112.36657	89006.010	88994.440	−39	112.38419	112.39839	88980.487	88969.244	12	112.41315	112.42705	88957.565	88946.569	−17
2	112.34707	112.37139	89009.885	88990.621	−36	112.37947	112.40319	88984.226	88965.451	−13	112.40851	112.43163	88961.238	88942.939	2
3	112.34225	112.37614	89013.704	88986.858	−5	112.37475	112.40783	88987.965	88961.774	−4	112.40389	112.43630	88964.891	88939.252	−1
4	112.33743	112.38104	89017.523	88982.983	−2	112.36999	112.41260	88991.734	88958.002	−5	112.39925	112.44090	88968.564	88935.609	−1
5	112.33261	112.38593	89021.342	88979.108	2	112.36530	112.41734	88995.443	88954.249	9	112.39461	112.44554	88972.240	88931.939	5
6	112.32779	112.39083	89025.162	88975.232	7	112.36054	112.42208	88999.214	88950.496	4	112.39000	112.45017	88975.886	88928.281	4
7	112.32290	112.39572	89029.037	88971.357	−16	112.35582	112.42685	89002.959	88946.726	21	112.38538	112.45477	88979.547	88924.639	−3
8	112.31809	112.40055	89032.856	88967.538	19	112.35113	112.43159	89006.668	88942.973	7	112.38075	112.45940	88983.209	88920.982	4
9	112.31327	112.40544	89036.675	88963.663	−1	112.34637	112.43629	89010.440	88939.259	−3	112.37615	112.46404	88986.856	88917.313	0
10	112.30845	112.41027	89040.494	88959.843	9	112.34165	112.44103	89014.181	88935.505	−3		112.46865		88913.669	−5
11	112.30363	112.41517	89044.313	88955.968	−8	112.33723	112.44573	89017.688	88931.794	5	112.36692	112.47327	88994.166	88910.015	
12	112.29889	112.41999	89048.076	88952.149	5	112.33246	112.45047	89021.460	88928.041	−96	112.36232	112.47789	88997.804	88906.360	0
13	112.29407	112.42489	89051.895	88948.274	−9	112.32778	112.45523	89025.172	88924.274	−41	112.35772	112.48252	89001.453	88902.705	3
14	112.28926	112.42979	89055.714	88944.399	8	112.32291	112.46005	89029.034	88920.464	−63	112.35309	112.48716	89005.116	88899.035	−9
15	112.28451	112.43469	89059.477	88940.523	−2	112.31811	112.46475	89032.839	88916.751	0	112.34856	112.49175	89008.710	88895.409	24
16	112.27977	112.43952	89063.240	88936.704	−9	112.31335	112.46947	89036.613	88913.022	28	112.34397	112.49643	89012.345	88891.714	2
17	112.27495	112.44442	89067.059	88932.829	−14	112.30844	112.47416	89040.502	88909.310	100	112.33938	112.50105	89015.982	88888.060	−24
18	112.27021	112.44932	89070.822	88928.954	9	112.30364	112.47900	89044.308	88905.485	*	112.33479	112.50560	89019.617	88884.462	2
19	112.26547	112.45421	89074.585	88925.086	41	112.29881	112.48367	89048.141	88901.793	*	112.33025	112.51028	89023.214	88880.767	15
20	112.26080	112.45919	89078.292	88921.147	16	112.29409	112.48861	89051.886	88897.890	*	112.32572	112.51492	89026.808	88877.101	4
21	112.25605	112.46402	89082.055	88917.328	−33	112.28929	112.49337	89055.692	88894.129	*	112.32116	112.51955	89030.416	88873.449	−12
22	112.25138	112.46885	89085.762	88913.509	16	112.28449	112.49804	89059.499	88890.442	*	112.31664	112.52415	89033.999	88869.811	−12
23	112.24671	112.47385	89089.469	88909.555	17		112.50297		88886.540	*	112.31213	112.52878	89037.580	88866.158	5
24	112.24204	112.47880	89093.175	88905.646	5		112.50773		88882.780		112.30764	112.53347	89041.137	88862.453	−8
25	112.23744	112.48370	89096.826	88901.770	25						112.30314	112.53808	89044.704	88858.814	−11
26	112.23277	112.48867	89100.533	88897.839	−7						112.29867	112.54274	89048.246	88855.135	−13
27	112.22818	112.49358	89104.183	88893.964	20						112.29421	112.54738	89051.787	88851.472	5
28	112.22365	112.49855	89107.778	88890.032	−4						112.28981	112.55209	89055.274	88847.753	−2
29	112.21912	112.50346	89111.372	88886.157	9							112.55673		88844.088	
30	112.21467	112.50852	89114.911	88882.158	−19						112.28095		89062.303		
31	112.21014	112.51347	89118.505	88878.251	−44										
32	112.20554	112.51848	89122.156	88874.289	*										
33	112.20130	112.52330	89125.526	88870.484											
34	112.19682		89129.089												

Table A.5. Transition wavelengths and wavenumbers of the $B^1\Sigma^+(v'=1)$–$X^1\Sigma^+(v''=0)$ band for $^{13}C^{16}O$, $^{13}C^{17}O$, and $^{13}C^{18}O$ (same column description as for Table A.1).

$B^1\Sigma^+(v'=1)$–$X^1\Sigma^+(v''=0)$															
	$^{13}C^{16}O$					$^{13}C^{17}O$					$^{13}C^{18}O$				
J''	R_{ms} (nm)	P_{ms} (nm)	R_{ms} (cm^{-1})	P_{ms} (cm^{-1})	δ_P	R_{ms} (nm)	P_{ms} (nm)	R_{ms} (cm^{-1})	P_{ms} (cm^{-1})	δ_P	R_{ms} (nm)	P_{ms} (nm)	R_{ms} (cm^{-1})	P_{ms} (cm^{-1})	δ_P
0	112.41288		88957.775			112.44578		88931.752			112.47553		88908.224		
1	112.40823	112.42217	88961.460	88950.428	2	112.44134	112.45491	88935.259	88924.534	14	112.47108	112.48434	88911.748	88901.262	−4
2	112.40358	112.42682	88965.140	88946.745	1	112.43684	112.45939	88938.822	88920.988	7	112.46667	112.48878	88915.235	88897.755	47
3	112.39895	112.43146	88968.803	88943.079	1	112.43232	112.46399	88942.395	88917.351	21	112.46224	112.49329	88918.736	88894.190	4
4	112.39430	112.43610	88972.484	88939.408	−8	112.42778	112.46857	88945.987	88913.731	8	112.45781	112.49761	88922.237	88890.780	6
5	112.38966	112.44074	88976.160	88935.739	6	112.42326	112.47307	88949.566	88910.174	−10	112.45339	112.50202	88925.731	88887.293	4
6	112.38508	112.44541	88979.784	88932.044	4	112.41872	112.47753	88953.154	88906.648	−19	112.44896	112.50642	88929.232	88883.815	−5
7	112.38038	112.45005	88983.506	88928.376	−3	112.41420	112.48203	88956.732	88903.091	−3	112.44452	112.51081	88932.750	88880.345	−4
8	112.37574	112.45473	88987.179	88924.670	0	112.40967	112.48657	88960.317	88899.498	0	112.44011	112.51522	88936.232	88876.865	−5
9	112.37111	112.45932	88990.843	88921.043	2	112.40515	112.49110	88963.898	88895.920	2	112.43566	112.51960	88939.751	88873.407	−2
10	112.36648	112.46396	88994.512	88917.372	−5	112.40061	112.49562	88967.491	88892.353	−4	112.43124	112.52403	88943.255	88869.908	9
11	112.36184	112.46859	88998.185	88913.710	3	112.39606	112.50011	88971.089	88888.802	0	112.42680	112.52843	88946.766	88866.432	4
12	112.35724	112.47325	89001.833	88910.028	6	112.39159	112.50461	88974.629	88885.244	23	112.42239	112.53281	88950.256	88862.974	9
13	112.35261	112.47789	89005.499	88906.362	0	112.38708	112.50915	88978.199	88881.657	6	112.41797	112.53720	88953.752	88859.508	−1
14	112.34802	112.48253	89009.138	88902.694	7	112.38259	112.51366	88981.753	88878.094	−13	112.41355	112.54158	88957.250	88856.052	4
15	112.34340	112.48718	89012.793	88899.019	−6	112.37807	112.51813	88985.332	88874.569	−10	112.40912	112.54598	88960.754	88852.576	1
16	112.33882	112.49181	89016.428	88895.363	−7	112.37356	112.52266	88988.903	88870.989	4	112.40472	112.55035	88964.233	88849.121	9
17	112.33422	112.49644	89020.070	88891.703	−1	112.36910	112.52719	88992.439	88867.414	−25	112.40031	112.55474	88967.723	88845.655	11
18	112.32964	112.50111	89023.699	88888.012	−6	112.36466	112.53161	88995.953	88863.923	−75	112.39593	112.55915	88971.194	88842.179	−4
19	112.32506	112.50574	89027.330	88884.355	−3	112.36016	112.53601	88999.520	88860.443	−42	112.39152	112.56349	88974.684	88838.754	−1
20	112.32050	112.51040	89030.942	88880.676	5	112.35553	112.54065	89003.189	88856.779		112.38714	112.56790	88978.149	88835.276	3
21	112.31595	112.51506	89034.552	88876.993	−2	112.35116		89006.647		−16	112.38275	112.57227	88981.624	88831.822	2
22	112.31141	112.51970	89038.146	88873.325	0		112.54955		88849.754	−82	112.37839	112.57666	88985.082	88828.356	2
23	112.30689	112.52436	89041.731	88869.645	2		112.55399		88846.247		112.37402	112.58104	88988.542	88824.905	1
24	112.30237	112.52904	89045.313	88865.954	0						112.36968	112.58543	88991.979	88821.442	4
25	112.29790	112.53370	89048.863	88862.268	−16						112.36533	112.58982	88995.424	88817.981	3
26	112.29334	112.53833	89052.475	88858.615	7						112.36099	112.59422	88998.859	88814.508	0
27	112.28900	112.54309	89055.917	88854.858	31						112.35668	112.59859	89002.272	88811.056	6
28	112.28453	112.54776	89059.467	88851.165	−51						112.35240	112.60300	89005.666	88807.582	−6
29	112.27983	112.55238	89063.191	88847.525							112.34810	112.60738	89009.072	88804.129	−21
30											112.34386	112.61177	89012.434	88800.668	−45
31											112.33968	112.61611	89015.745	88797.245	−26
32												112.62060		88793.700	

Table A.6. Term values (cm^{-1}) of the $B^1\Sigma^+(v' = 1)$ levels for six CO isotopologues.

	$B^1\Sigma^+(v' = 1)$					
J'	$^{12}C^{16}O$	$^{12}C^{17}O$	$^{12}C^{18}O$	$^{13}C^{16}O$	$^{13}C^{17}O$	$^{13}C^{18}O$
0	88998.285	88972.992	88950.231	88954.104	88928.113	88904.754
1	89002.117 (−39)	88976.706 (12)	88953.908 (−17)	88957.774 (2)	88931.738 (14)	88908.229 (−4)
2	89009.891 (−36)	88984.248 (−13)	88961.225 (2)	88965.135 (1)	88938.830 (7)	88915.193 (47)
3	89021.425 (−5)	88995.474 (−4)	88972.225 (−1)	88976.167 (1)	88949.538 (21)	88925.709 (4)
4	89036.776 (−2)	89010.457 (−5)	88986.863 (−1)	88990.866 (−8)	88963.859 (8)	88939.686 (6)
5	89055.970 (2)	89029.202 (9)	89005.177 (5)	89009.235 (6)	88981.783 (−10)	88957.159 (4)
6	89079.006 (7)	89051.653 (4)	89027.160 (4)	89031.290 (4)	89003.262 (−19)	88978.124 (−5)
7	89105.913 (−16)	89077.889 (21)	89052.781 (−3)	89056.972 (−3)	89028.303 (−3)	89002.576 (−4)
8	89136.660 (19)	89107.875 (7)	89082.060 (4)	89086.415 (0)	89056.922 (0)	89030.538 (−5)
9	89171.247 (−1)	89141.567 (−3)	89115.010 (0)	89119.482 (2)	89089.125 (2)	89061.950 (−2)
10	89209.644 (9)	89179.052 (−3)	89151.604 (−5)	89156.220 (−5)	89124.906 (−4)	89096.879 (9)
11	89251.906 (−8)	89220.242 (5)	89191.858	89196.619 (3)	89164.261 (0)	89135.295 (4)
12	89297.976 (5)	89265.046 (−96)	89235.759 (0)	89240.694 (6)	89207.174 (23)	89177.195 (9)
13	89347.851 (−9)	89313.698 (−41)	89283.299 (3)	89288.421 (0)	89253.640 (6)	89222.574 (−1)
14	89401.585 (8)	89366.104 (−63)	89334.517 (−9)	89339.818 (7)	89303.706 (−13)	89271.427 (4)
15	89459.177 (−2)	89422.310 (0)	89389.354 (24)	89394.872 (−6)	89357.303 (−10)	89323.772 (1)
16	89520.541 (−9)	89482.227 (28)	89447.823 (2)	89453.591 (−7)	89414.478 (4)	89379.593 (9)
17	89585.729 (−14)	89545.800 (100)	89509.985 (−24)	89515.943 (−1)	89475.252 (−25)	89438.872 (11)
18	89654.772 (9)	89613.225 (*)	89575.740 (2)	89581.971 (−6)	89539.574 (−75)	89501.656 (−4)
19	89727.571 (41)	89684.226 (*)	89645.149 (15)	89651.635 (−3)	89607.349 (−42)	89567.876 (−1)
20	89804.246 (16)	89759.033 (*)	89718.182 (4)	89724.947 (5)	89678.726	89637.588 (3)
21	89884.708 (−33)	89837.552 (*)	89794.854 (−12)	89801.906 (−2)	89753.817 (−16)	89710.749 (2)
22	89968.942 (16)	89919.709 (*)	89875.157 (−12)	89882.502 (0)	89832.299 (−82)	89787.386 (2)
23	90056.978 (17)	90005.651 (*)	89959.050 (5)	89966.726 (2)		89867.472 (1)
24	90148.835 (5)		90046.599 (−8)	90054.588 (0)		89951.018 (4)
25	90244.465 (25)		90137.739 (−11)	90146.100 (−16)		90038.004 (3)
26	90343.893 (−7)		90232.510 (−13)	90241.177 (7)		90128.457 (0)
27	90447.113 (20)		90330.857 (5)	90339.945 (31)		90222.345 (6)
28	90554.124 (−4)		90432.841 (−2)	90442.280 (−51)		90319.679 (−6)
29	90664.829 (9)		90538.373	90548.215		90420.444 (−21)
30	90779.363 (−19)			90657.996		90524.674 (−45)
31	90897.617 (−44)		90760.318			90632.256 (−26)
32	91019.750 (114)					90743.218
33	91145.527					
34	91274.905					
35	91408.240					

Notes. See note to Table A.3.

Table A.7. Transition wavelengths and wavenumbers of the $B^1\Sigma^+(v'=2)$–$X^1\Sigma^+(v''=0)$ band for $^{12}C^{16}O$, $^{12}C^{18}O$, $^{13}C^{16}O$, and $^{13}C^{18}O$ (same column description as for Table A.1).

$B^1\Sigma^+(v'=2)$–$X^1\Sigma^+(v''=0)$															
	$^{12}C^{16}O$					$^{12}C^{17}O$					$^{12}C^{18}O$				
J''	R_{ms} (nm)	P_{ms} (nm)	R_{ms} (cm^{-1})	P_{ms} (cm^{-1})	δ_P	R_{ms} (nm)	P_{ms} (nm)	R_{ms} (cm^{-1})	P_{ms} (cm^{-1})	δ_P	R_{ms} (nm)	P_{ms} (nm)	R_{ms} (cm^{-1})	P_{ms} (cm^{-1})	δ_P
0	109.89971		90992.051								110.00738		90902.992		
1	109.89540	109.90893	90995.619	90984.418	56						110.00327	110.01622	90906.389	90895.688	39
2	109.89111	109.91378	90999.172	90980.403	24						109.99911	110.02077	90909.826	90891.929	29
3	109.88689	109.91868	91002.666	90976.347	17						109.99518	110.02550	90913.075	90888.021	7
4	109.88291	109.92366	91005.963	90972.226	22						109.99130	110.03015	90916.282	90884.180	31
5	109.87893	109.92874	91009.259	90968.022	−34						109.98750	110.03514	90919.423	90880.059	14
6	109.87509	109.93391	91012.440	90963.744	2						109.98375	110.04008	90922.523	90875.979	2
7	109.87134	109.93930	91015.546	90959.284	26						109.98016	110.04511	90925.491	90871.825	28
8	109.86773	109.94480	91018.537	90954.734	5						109.97668	110.05028	90928.368	90867.556	42
9	109.86416	109.95028	91021.494	90950.200	−10						109.97346	110.05558	90931.030	90863.180	−13
10	109.86082	109.95591	91024.261	90945.544	33						109.96986	110.06082	90934.007	90858.854	−63
11	109.85751	109.96172	91027.004	90940.738	−75						109.96646	110.06633	90936.818	90854.306	46
12		109.96739		90936.049	−41						109.96346	110.07184	90939.299	90849.758	90
13		109.97343		90931.055							109.96039	110.07739	90941.838	90845.177	*
14												110.08381		90839.879	
15		109.98507		90921.431											
16		109.99080		90916.695											
17		109.99628		90912.165											

	$^{13}C^{16}O$					$^{13}C^{17}O$					$^{13}C^{18}O$				
J''	R_{ms} (nm)	P_{ms} (nm)	R_{ms} (cm^{-1})	P_{ms} (cm^{-1})	δ_P	$R_{ms}R_{ms}$ (nm)	P_{ms} (nm)	R_{ms} (cm^{-1})	P_{ms} (cm^{-1})	δ_P	R_{ms} (nm)	P_{ms} (nm)	R_{ms} (cm^{-1})	P_{ms} (cm^{-1})	δ_P
%0	109.99898		90909.934								110.10911		90819.007		
1	109.99477	110.00782	90913.413	90902.629	19						110.10544	110.11722	90822.034	90812.318	−15
2	109.99069	110.01237	90916.786	90898.869	−9						110.10190	110.12178	90824.954	90808.558	2
3	109.98662	110.01699	90920.150	90895.052	−32						110.09829	110.12662	90827.932	90804.567	−39
4	109.98274	110.02175	90923.358	90891.119	0						110.09475	110.13145	90830.853	90800.584	11
5	109.97887	110.02665	90926.557	90887.071	7						110.09121	110.13643	90833.773	90796.479	0
6	109.97513	110.03168	90929.649	90882.917	10						110.08767	110.14133	90836.694	90792.439	−7
7	109.97160	110.03671	90932.568	90878.762	18						110.08427	110.14624	90839.500	90788.392	12
8	109.96807	110.04188	90935.487	90874.493	−6						110.08086	110.15121	90842.314	90784.296	2
9	109.96460	110.04718	90938.357	90870.116	−53						110.07753	110.15625	90845.062	90780.142	2
10	109.96121	110.05242	90941.160	90865.789	−13						110.07426	110.16130	90847.760	90775.980	−5
11	109.95794	110.05793	90943.865	90861.240	−5						110.07106	110.16641	90850.402	90771.770	−7
12	109.95471	110.06344	90946.536	90856.691	4						110.06807	110.17159	90852.870	90767.502	21
13	109.95157	110.06907	90949.133	90852.046	30						110.06501	110.17691	90855.395	90763.119	−37
14	109.94868	110.07477	90951.524	90847.337	−9						110.06230	110.18223	90857.632	90758.737	−10
15	109.94531	110.08041	90954.312	90842.685	−11						110.05929	110.18768	90860.117	90754.248	*
16		110.08638		90837.758	−29						110.05610	110.19314	90862.751	90749.751	−84
17	109.93942	110.09183	90959.185	90833.264							110.05283	110.19866	90865.451	90745.205	59
18		110.09781		90828.328							110.04901	110.20425	90868.605	90740.602	*
19											110.04562	110.20978	90871.404	90736.049	*
20											110.04167	110.21522	90874.666	90731.570	*
21											110.03767	110.22149	90877.969	90726.409	

Table A.8. Term values (cm^{-1}) of the $B^1\Sigma^+(v'=2)$ levels for $^{12}C^{16}O$, $^{12}C^{18}O$, $^{13}C^{16}O$, and $^{13}C^{18}O$.

	$B^1\Sigma^+(v'=2)$					
J'	$^{12}C^{16}O$	$^{12}C^{17}O$	$^{12}C^{18}O$	$^{13}C^{16}O$	$^{13}C^{17}O$	$^{13}C^{18}O$
0	90988.263		90899.350	90906.304		90815.811
1	90991.994 (56)		90902.953 (39)	90909.915 (19)		90819.021 (−15)
2	90999.441 (24)		90910.021 (29)	90917.098 (−9)		90825.525 (2)
3	91010.690 (17)		90920.805 (7)	90927.845 (−32)		90835.471 (−39)
4	91025.714 (22)		90935.014 (31)	90942.205 (0)		90848.877 (11)
5	91044.445 (−34)		90952.885 (14)	90960.108 (7)		90865.779 (0)
6	91066.928 (2)		90974.345 (2)	90981.681 (10)		90886.168 (−7)
7	91093.150 (26)		90999.386 (28)	91006.816 (18)		90910.023 (12)
8	91123.183 (5)		91027.966 (42)	91035.483 (−6)		90937.280 (2)
9	91156.937 (−10)		91060.182 (−13)	91067.845 (−53)		90968.026 (2)
10	91194.439 (33)		91095.836 (−63)	91103.742 (−13)		91002.203 (−5)
11	91235.740 (−75)		91135.302 (46)	91143.274 (−5)		91039.811 (−7)
12	91280.712 (−41)		91178.322 (90)	91186.375 (4)		91080.819 (21)
13			91224.469 (*)	91233.094 (30)		91125.223 (−37)
14	91382.486		91274.893	91283.468 (−9)		91173.085 (−10)
15	91439.170			91337.262 (−11)		91224.278 (122)
16	91499.886			91395.131 (−29)		91279.049 (−84)
17				91456.260		91337.342 (59)
18				91521.080		91399.167 (*)
19						91464.729 (*)
20						91533.242 (*)
21						91607.267
22						91683.733

Notes. See note to Table A.3.

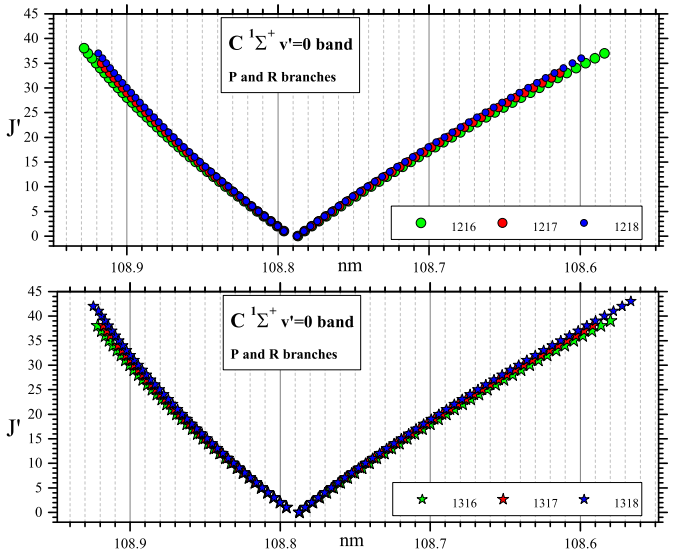

Fig. A.4. Transition wavelengths of the $C^1\Sigma^+(v' = 0)$–$X^1\Sigma^+(v'' = 0)$ band for six CO isotopologues.

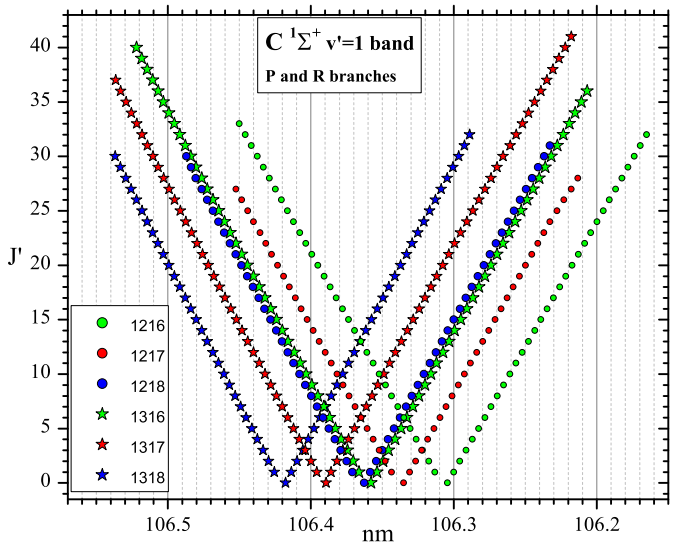

Fig. A.5. Transition wavelengths of the $C^1\Sigma^+(v' = 1)$–$X^1\Sigma^+(v'' = 0)$ band for six CO isotopologues.

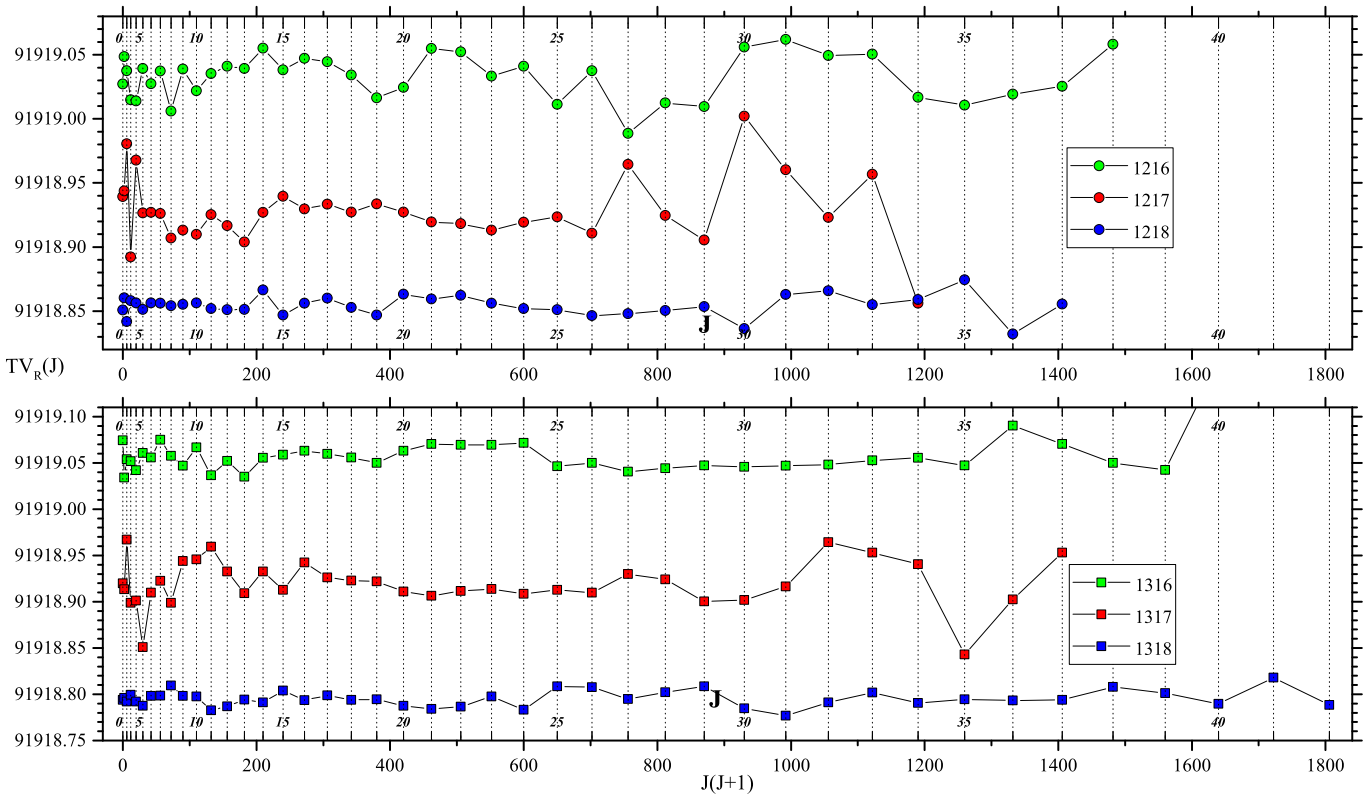

Fig. A.6. Reduced term values (cm^{-1}) of the $C^1\Sigma^+(v'=0)$ levels for six CO isotopologues.

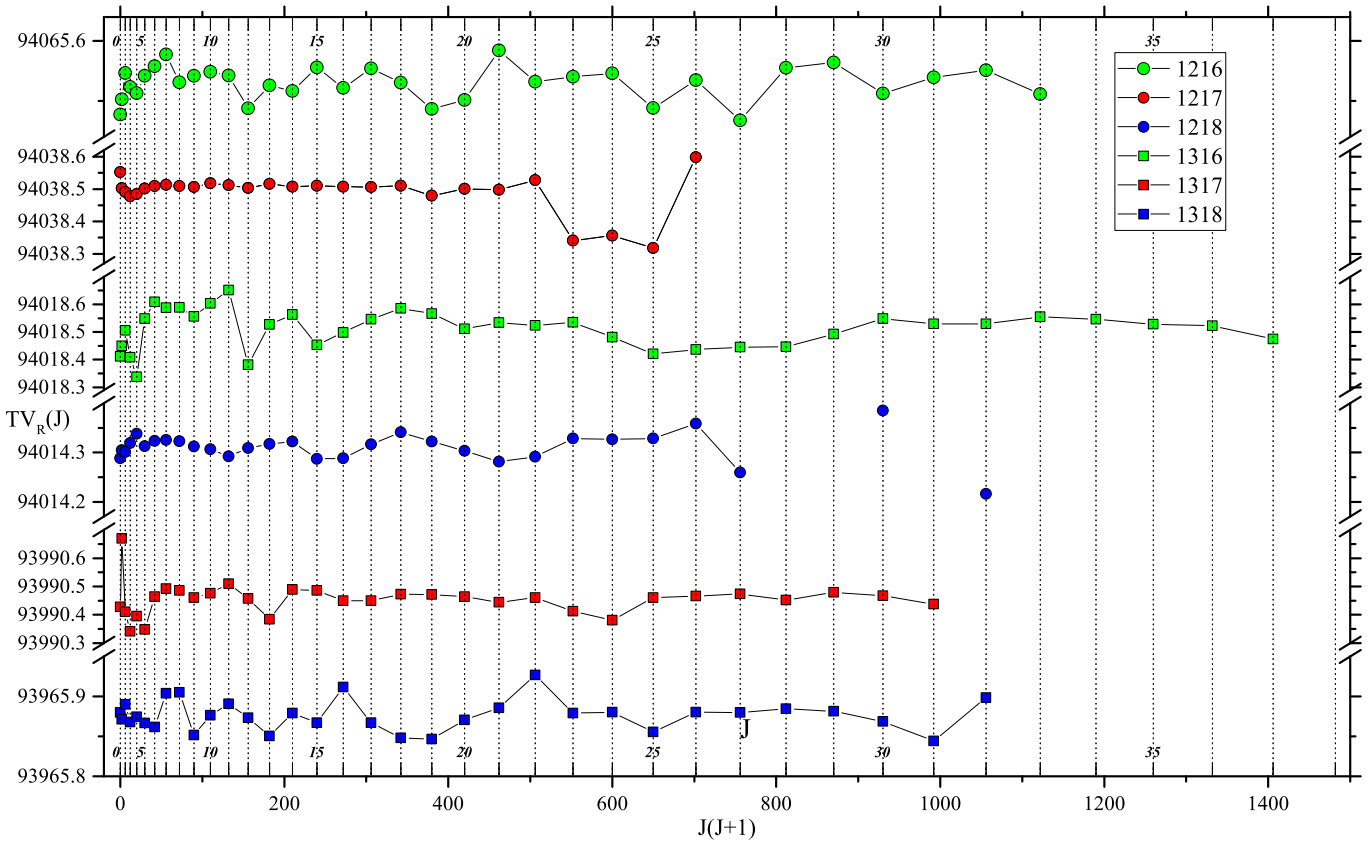

Fig. A.7. Reduced term values (cm^{-1}) of the $C^1\Sigma^+(v'=1)$ levels for six CO isotopologues.

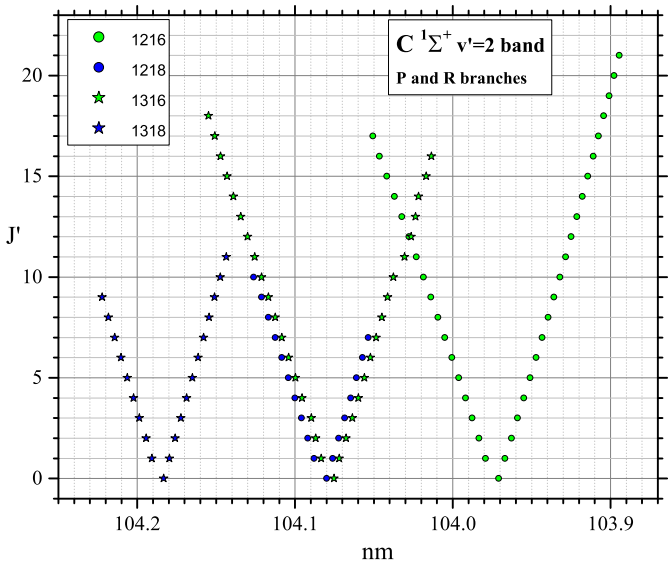

Fig. A.8. Transition wavelengths of the $C^1\Sigma^+(v'=2)$–$X^1\Sigma^+(v''=0)$ band for the four observed CO isotopologues.

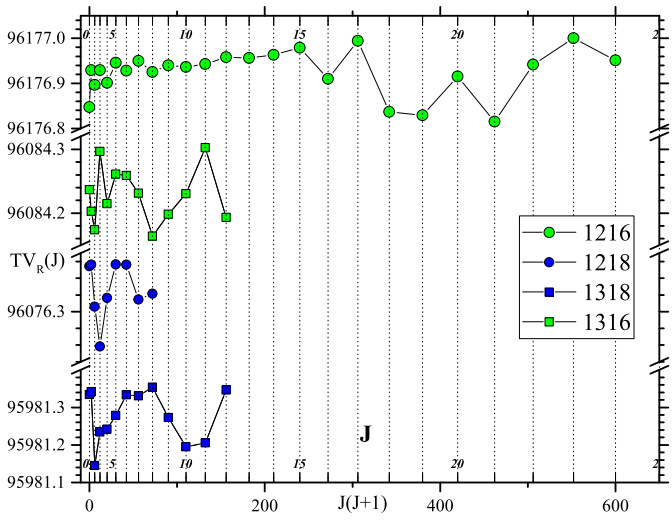

Fig. A.9. Reduced term values (cm^{-1}) of the $C^1\Sigma^+(v'=2)$ levels for the four observed CO isotopologues.

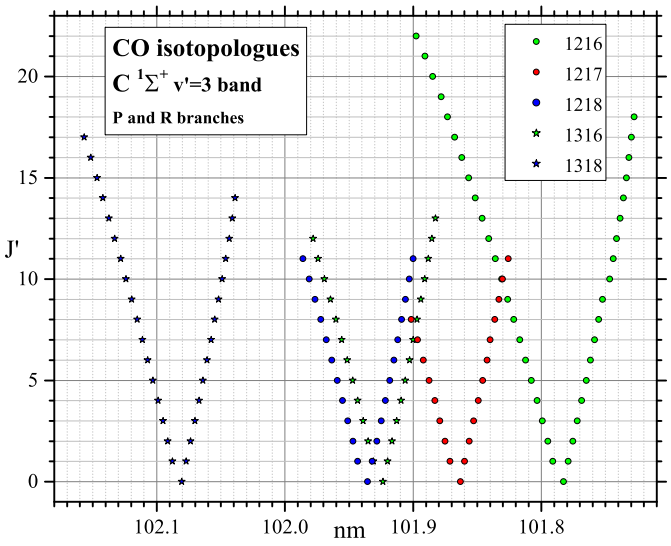

Fig. A.10. Transition wavelengths of the $C^1\Sigma^+(v'=3)$–$X^1\Sigma^+(v''=0)$ band for the four observed CO isotopologues.

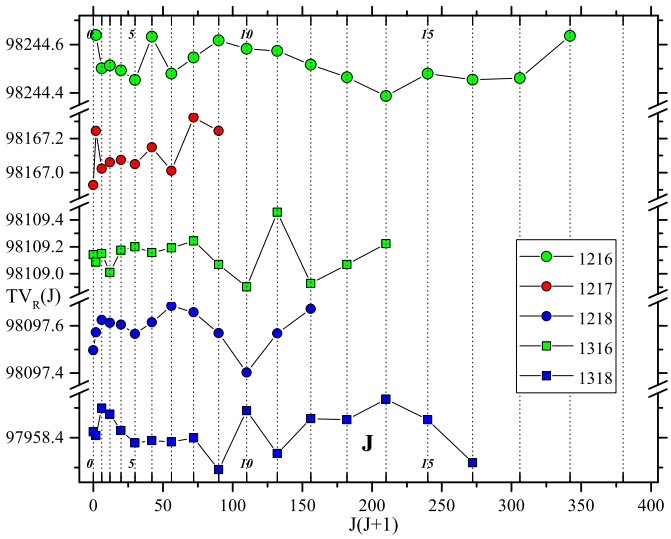

Fig. A.11. Reduced term values (cm^{-1}) of the $C^1\Sigma^+(v'=3)$ levels for the five observed CO isotopologues.

Table A.9. Transition wavelengths and wavenumbers of the $C^1\Sigma^+(v'=0)$–$X^1\Sigma^+(v''=0)$ band for $^{12}C^{16}O$, $^{12}C^{17}O$, and $^{12}C^{18}O$ (same column description as for Table A.1).

$C^1\Sigma^+(v'=0)$–$X^1\Sigma^+(v''=0)$															
	$^{12}C^{16}O$					$^{12}C^{17}O$					$^{12}C^{18}O$				
J''	R_{ms} (nm)	P_{ms} (nm)	R_{ms} (cm^{-1})	P_{ms} (cm^{-1})	δ_P	R_{ms} (nm)	P_{ms} (nm)	R_{ms} (cm^{-1})	P_{ms} (cm^{-1})	δ_P	R_{ms} (nm)	P_{ms} (nm)	R_{ms} (cm^{-1})	P_{ms} (cm^{-1})	δ_P
0	108.78678		91922.930			108.78708		91922.681			108.78724		91922.547		
1	108.78215	108.79595	91926.842	91915.182	−5	108.78251	108.79594	91926.542	91915.191	−52	108.78281	108.79595	91926.288	91915.189	−16
2	108.77744	108.80042	91930.823	91911.406	−10	108.77792	108.80026	91930.420	91911.542	−58	108.77832	108.80020	91930.082	91911.593	0
3	108.77274	108.80488	91934.795	91907.638	23	108.77334	108.80455	91934.295	91907.920	36	108.77379	108.80448	91933.910	91907.980	−6
4	108.76788	108.80935	91938.903	91903.863	−14	108.76864	108.80906	91938.264	91904.114	−76	108.76922	108.80864	91937.773	91904.463	−2
5	108.76309	108.81366	91942.952	91900.222	17	108.76391	108.81307	91942.265	91900.721	−20	108.76460	108.81279	91941.681	91900.960	1
6	108.75815	108.81797	91947.128	91896.582	−15	108.75912	108.81738	91946.310	91897.084	−13	108.75993	108.81689	91945.629	91897.496	0
7	108.75329	108.82220	91951.237	91893.010	17	108.75432	108.82153	91950.370	91893.581	−2	108.75523	108.82093	91949.599	91894.089	3
8	108.74826	108.82643	91955.490	91889.439	−17	108.74945	108.82563	91954.490	91890.114	3	108.75045	108.82492	91953.642	91890.714	−11
9	108.74324	108.83058	91959.735	91885.935	−11	108.74455	108.82970	91958.627	91886.678	2	108.74565	108.82885	91957.701	91887.395	6
10	108.73814	108.83465	91964.048	91882.498	−4	108.73957	108.83369	91962.839	91883.316	−12	108.74080	108.83277	91961.799	91884.091	−1
11	108.73304	108.83873	91968.362	91879.054	0	108.73458	108.83761	91967.067	91879.999	−11	108.73590	108.83660	91965.944	91880.852	−1
12	108.72786	108.84272	91972.743	91875.686	−27	108.72954	108.84149	91971.326	91876.729	−8	108.73096	108.84040	91970.125	91877.644	2
13	108.72261	108.84663	91977.184	91872.385	−19	108.72442	108.84534	91975.661	91873.477	−10	108.72596	108.84415	91974.353	91874.479	0
14	108.71735	108.85054	91981.634	91869.085	−9	108.71925	108.84914	91980.030	91870.267	−12	108.72094	108.84785	91978.605	91871.362	−8
15	108.71201	108.85438	91986.153	91865.845	4	108.71406	108.85285	91984.421	91867.137	−8	108.71585	108.85146	91982.909	91868.309	3
16	108.70667	108.85821	91990.671	91862.612	19	108.70883	108.85653	91988.847	91864.033	3	108.71071	108.85510	91987.255	91865.244	−1
17	108.70126	108.86196	91995.250	91859.448	7	108.70355	108.86019	91993.318	91860.944	−6	108.70556	108.85863	91991.613	91862.266	5
18	108.69584	108.86564	91999.837	91856.343	23	108.69821	108.86376	91997.836	91857.931	3	108.70035	108.86212	91996.023	91859.315	−5
19	108.69035	108.86931	92004.484	91853.246	17	108.69286	108.86731	92002.367	91854.934	7	108.69508	108.86556	92000.485	91856.413	−3
20	108.68478	108.87291	92009.199	91850.209	5	108.68745	108.87079	92006.945	91851.998	−1	108.68978	108.86896	92004.972	91853.542	−8
21	108.67920	108.87642	92013.923	91847.248	1	108.68200	108.87422	92011.558	91849.105	2	108.68442	108.87228	92009.510	91850.744	−6
22	108.67363	108.87986	92018.639	91844.346	0	108.67650	108.87762	92016.215	91846.243	−5	108.67905	108.87558	92014.058	91847.963	2
23	108.66790	108.88329	92023.491	91841.453	−31	108.67095	108.88094	92020.915	91843.442	−2	108.67360	108.87882	92018.672	91845.224	−8
24	108.66225	108.88665	92028.276	91838.619	9	108.66534	108.88422	92025.663	91840.671	−4	108.66812	108.88201	92023.306	91842.538	9
25	108.65644	108.89001	92033.197	91835.785	−18	108.65972	108.88744	92030.427	91837.960	5	108.66262	108.88517	92027.970	91839.871	6
26	108.65063	108.89328	92038.118	91833.027	−4	108.65404	108.89061	92035.234	91835.280	11	108.65704	108.88825	92032.690	91837.270	0
27	108.64483	108.89648	92043.032	91830.329	48	108.64831	108.89376	92040.089	91832.630	−43	108.65145	108.89129	92037.428	91834.712	6
28	108.63894	108.89976	92048.022	91827.563	−18	108.64258	108.89670	92044.945	91830.151	8	108.64580	108.89427	92042.216	91832.192	−6
29	108.63289	108.90276	92053.155	91825.033	−18	108.63676	108.89982	92049.875	91827.518	2	108.64013	108.89719	92047.018	91829.735	−5
30	108.62687	108.90582	92058.253	91822.457	37	108.63092	108.90280	92054.823	91825.006	−81	108.63436	108.90007	92051.910	91827.309	−5
31	108.62088	108.90883	92063.327	91819.920	62	108.62505	108.90549	92059.796	91822.732	−44	108.62858	108.90291	92056.804	91824.908	4
32	108.61481	108.91179	92068.473	91817.421	43	108.61894	108.90844	92064.974	91820.244	−22	108.62278	108.90567	92061.720	91822.585	4
33	108.60872	108.91467	92073.638	91814.992	47	108.61332	108.91132	92069.738	91817.820	99	108.61694	108.90839	92066.671	91820.291	4
34	108.60260	108.91751	92078.827	91812.600	66		108.91418		91815.413	−96	108.61103	108.91107	92071.678	91818.029	−10
35	108.59639	108.92035	92084.091	91810.205	47		108.91676		91813.231		108.60508	108.91367	92076.726	91815.838	−16
36	108.59017	108.92306	92089.363	91807.922	51						108.59913	108.91621	92081.772	91813.695	43
37	108.58389	108.92572	92094.690	91805.678	29							108.91885		91811.473	
38		108.92830		91803.503											

Table A.10. Transition wavelengths and wavenumbers of the $C^1\Sigma^+(v'=0)$–$X^1\Sigma^+(v''=0)$ band for $^{13}C^{16}O$, $^{13}C^{17}O$, and $^{13}C^{18}O$ (same column description as for Table A.1).

$C^1\Sigma^+(v'=0)$–$X^1\Sigma^+(v''=0)$															
	$^{13}C^{16}O$					$^{13}C^{17}O$					$^{13}C^{18}O$				
J''	R_{ms} (nm)	P_{ms} (nm)	R_{ms} (cm^{-1})	P_{ms} (cm^{-1})	δ_P	R_{ms} (nm)	P_{ms} (nm)	R_{ms} (cm^{-1})	P_{ms} (cm^{-1})	δ_P	R_{ms} (nm)	P_{ms} (nm)	R_{ms} (cm^{-1})	P_{ms} (cm^{-1})	δ_P
0	108.78698		91922.763			108.78732		91922.475			108.78749		91922.332		
1	108.78251	108.79570	91926.540	91915.398	12	108.78293	108.79581	91926.184	91915.307	−23	108.78326	108.79581	91925.906	91915.301	3
2	108.77804	108.80006	91930.317	91911.712	11	108.77861	108.79997	91929.841	91911.786	−28	108.77899	108.79990	91929.514	91911.848	9
3	108.77350	108.80429	91934.154	91908.138	−7	108.77414	108.80405	91933.613	91908.347	−3	108.77468	108.80395	91933.157	91908.426	−3
4	108.76887	108.80848	91938.068	91904.602	0	108.76968	108.80825	91937.386	91904.798	26	108.77032	108.80792	91936.842	91905.072	−5
5	108.76425	108.81266	91941.973	91901.075	16	108.76512	108.81232	91941.240	91901.356	69	108.76587	108.81187	91940.604	91901.736	−7
6	108.75954	108.81676	91945.955	91897.609	6	108.76059	108.81643	91945.073	91897.889	44	108.76142	108.81577	91944.365	91898.442	13
7	108.75488	108.82081	91949.893	91894.186	9	108.75597	108.82028	91948.978	91894.639	4	108.75691	108.81963	91948.178	91895.182	4
8	108.75008	108.82480	91953.956	91890.817	−35	108.75131	108.82411	91952.917	91891.401	33	108.75237	108.82342	91952.017	91891.982	−3
9	108.74523	108.82873	91958.056	91887.500	−1	108.74660	108.82802	91956.900	91888.099	−12	108.74776	108.82715	91955.915	91888.832	−2
10	108.74041	108.83269	91962.130	91884.153	0	108.74185	108.83171	91960.911	91884.980	−10	108.74316	108.83087	91959.804	91885.691	10
11	108.73546	108.83653	91966.319	91880.913	−14	108.73707	108.83547	91964.959	91881.814	−29	108.73846	108.83454	91963.779	91882.593	−11
12	108.73053	108.84036	91970.491	91877.680	1	108.73224	108.83913	91969.045	91878.722	−12	108.73372	108.83814	91967.788	91879.554	−5
13	108.72551	108.84412	91974.733	91874.506	−7	108.72732	108.84283	91973.203	91875.596	3	108.72894	108.84170	91971.831	91876.549	−6
14	108.72040	108.84784	91979.057	91871.365	−22	108.72242	108.84648	91977.349	91872.517	3	108.72411	108.84520	91975.918	91873.594	−1
15	108.71532	108.85146	91983.354	91868.311	24	108.71740	108.85000	91981.595	91869.542	−5	108.71925	108.84867	91980.029	91870.665	−6
16	108.71020	108.85512	91987.688	91865.222	3	108.71240	108.85352	91985.830	91866.574	1	108.71433	108.85206	91984.191	91867.804	−2
17	108.70501	108.85865	91992.080	91862.243	−11	108.70734	108.85694	91990.109	91863.684	3	108.70939	108.85544	91988.371	91864.952	1
18	108.69978	108.86215	91996.504	91859.293	−6	108.70223	108.86037	91994.430	91860.794	−2	108.70438	108.85875	91992.616	91862.158	−7
19	108.69448	108.86562	92000.988	91856.366	−5	108.69709	108.86372	91998.782	91857.967	−6	108.69936	108.86201	91996.865	91859.407	7
20	108.68917	108.86903	92005.489	91853.484	−1	108.69188	108.86702	92003.193	91855.184	−5	108.69426	108.86524	92001.176	91856.682	−4
21	108.68380	108.87238	92010.033	91850.661	−11	108.68663	108.87028	92007.634	91852.428	10	108.68914	108.86840	92005.510	91854.016	6
22	108.67837	108.87566	92014.628	91847.891	−8	108.68135	108.87351	92012.105	91849.707	7	108.68395	108.87153	92009.903	91851.375	−4
23	108.67291	108.87892	92019.251	91845.142	7	108.67604	108.87665	92016.604	91847.057	1	108.67876	108.87458	92014.297	91848.802	0
24	108.66746	108.88214	92023.871	91842.425	13	108.67065	108.87974	92021.164	91844.449	−6	108.67347	108.87759	92018.776	91846.265	−6
25	108.66189	108.88530	92028.583	91839.763	3	108.66525	108.88279	92025.736	91841.879	2	108.66817	108.88056	92023.267	91843.757	−4
26	108.65634	108.88842	92033.286	91837.133	22	108.65980	108.88579	92030.358	91839.346	−8	108.66284	108.88345	92027.778	91841.320	0
27	108.65071	108.89148	92038.051	91834.547	8	108.65426	108.88873	92035.049	91836.866	−28	108.65746	108.88632	92032.340	91838.900	0
28	108.64505	108.89447	92042.851	91832.025	5	108.64877	108.89158	92039.699	91834.463	11	108.65203	108.88915	92036.935	91836.513	−5
29	108.63934	108.89741	92047.685	91829.547	2	108.64318	108.89448	92044.437	91832.017	−9	108.64657	108.89190	92041.558	91834.194	−12
30	108.63359	108.90030	92052.558	91827.113	3	108.63753	108.89728	92049.219	91829.656	−2	108.64108	108.89460	92046.214	91831.919	4
31	108.62781	108.90314	92057.459	91824.715	4	108.63177	108.90003	92054.105	91827.337	1	108.63552	108.89731	92050.924	91829.634	1
32	108.62196	108.90593	92062.416	91822.364	−3	108.62609	108.90271	92058.917	91825.077	39	108.62992	108.89993	92055.671	91827.425	−4
33	108.61608	108.90866	92067.399	91820.064	8	108.62039	108.90534	92063.747	91822.860	27	108.62429	108.90247	92060.442	91825.285	−4
34	108.61017	108.91135	92072.405	91817.793	11	108.61468	108.90793	92068.583	91820.676		108.61863	108.90496	92065.241	91823.178	7
35	108.60422	108.91399	92077.453	91815.573	13	108.60882		92073.551		29	108.61291	108.90745	92070.086	91821.081	−4
36	108.59824	108.91658	92082.526	91813.387	−29	108.60289	108.91309	92078.579	91816.326	−1	108.60715	108.90984	92074.967	91819.065	2
37	108.59221	108.91901	92087.637	91811.339	−16	108.59743	108.91542	92083.214	91814.361	3	108.60135	108.91221	92079.883	91817.068	8
38	108.58615	108.92152	92092.778	91809.219		108.59170	108.91775	92088.071	91812.397		108.59553	108.91453	92084.825	91815.118	2
39	108.57990		92098.076								108.58971	108.91676	92089.754	91813.234	8
40											108.58376	108.91898	92094.807	91811.361	−27
41											108.57783	108.92111	92099.830	91809.568	*
42											108.57798	108.92439	92099.703	91806.803	
43											108.56635		92109.574		

Table A.11. Term values (cm^{-1}) of the $C^1\Sigma^+(v'=0)$ levels for six CO isotopologues.

	$C^1\Sigma^+(v'=0)$					
J'	$^{12}C^{16}O$	$^{12}C^{17}O$	$^{12}C^{18}O$	$^{13}C^{16}O$	$^{13}C^{17}O$	$^{13}C^{18}O$
0	91919.027	91918.939	91918.851	91919.074	91918.886	91918.794
1	91922.935 (−5)	91922.733 (−52)	91922.563 (−16)	91922.751 (12)	91922.499 (−23)	91922.329 (3)
2	91930.698 (−10)	91930.348 (−58)	91929.950 (0)	91930.204 (11)	91929.791 (−28)	91929.390 (9)
3	91942.334 (23)	91941.627 (36)	91941.074 (−6)	91941.352 (−7)	91940.580 (−3)	91939.995 (−3)
4	91957.879 (−14)	91956.858 (−76)	91955.883 (−2)	91956.209 (0)	91955.059 (26)	91954.118 (−5)
5	91977.334 (17)	91975.760 (−20)	91974.389 (1)	91974.809 (16)	91973.103 (69)	91971.775 (−7)
6	92000.638 (−15)	91998.492 (−13)	91996.606 (0)	91997.101 (6)	91994.873 (44)	91992.978 (13)
7	92027.846 (17)	92025.008 (−2)	92022.518 (3)	92023.131 (9)	92020.214 (4)	92017.701 (4)
8	92058.896 (−17)	92055.291 (3)	92052.127 (−11)	92052.837 (−35)	92049.134 (33)	92045.965 (−3)
9	92093.891 (−11)	92089.383 (2)	92085.437 (6)	92086.262 (−1)	92081.738 (−12)	92077.734 (−2)
10	92132.717 (−4)	92127.249 (−12)	92122.444 (−1)	92123.428 (0)	92117.912 (−10)	92113.041 (10)
11	92175.452 (0)	92168.915 (−11)	92163.141 (−1)	92164.253 (−14)	92157.710 (−29)	92151.859 (−11)
12	92222.056 (−27)	92214.337 (−8)	92207.535 (2)	92208.833 (1)	92201.079 (−12)	92194.222 (−5)
13	92272.528 (−19)	92263.533 (−10)	92255.623 (0)	92257.085 (−7)	92248.060 (3)	92240.111 (−6)
14	92326.890 (−9)	92316.541 (−12)	92307.416 (−8)	92309.080 (−22)	92298.695 (3)	92289.512 (−1)
15	92385.092 (4)	92373.313 (−8)	92362.863 (3)	92364.760 (24)	92352.893 (−5)	92342.447 (−6)
16	92447.188 (19)	92433.835 (3)	92422.025 (−1)	92424.142 (3)	92410.744 (1)	92398.878 (−2)
17	92513.139 (7)	92498.140 (−6)	92484.867 (5)	92487.214 (−11)	92472.151 (3)	92458.840 (1)
18	92582.947 (23)	92566.203 (3)	92551.379 (−5)	92553.982 (−6)	92537.171 (−2)	92522.307 (−7)
19	92656.609 (17)	92638.044 (7)	92621.572 (−3)	92624.441 (−5)	92605.790 (−6)	92589.290 (7)
20	92734.156 (5)	92713.634 (−1)	92695.465 (−8)	92698.610 (−1)	92677.993 (−5)	92659.775 (−4)
21	92815.581 (1)	92792.982 (2)	92773.012 (−6)	92776.462 (−11)	92753.795 (10)	92733.771 (6)
22	92900.825 (0)	92876.094 (−5)	92854.237 (2)	92857.991 (−8)	92833.197 (7)	92811.277 (−4)
23	92989.903 (−31)	92962.954 (−2)	92939.122 (−8)	92943.203 (7)	92916.182 (1)	92892.294 (0)
24	93082.854 (9)	93053.576 (−4)	93027.674 (9)	93032.096 (13)	93002.743 (−6)	92976.784 (−6)
25	93179.610 (−18)	93147.943 (5)	93119.891 (6)	93124.638 (3)	93092.894 (2)	93064.809 (−4)
26	93280.260 (−4)	93246.036 (11)	93215.764 (0)	93220.881 (22)	93186.615 (−8)	93156.301 (0)
27	93384.671 (48)	93347.935 (−43)	93315.298 (6)	93320.780 (8)	93283.933 (−28)	93251.270 (0)
28	93492.986 (−18)	93453.476 (8)	93418.485 (−6)	93424.358 (5)	93384.795 (11)	93349.746 (−5)
29	93605.101 (−18)	93562.769 (2)	93525.320 (−5)	93531.596 (2)	93489.206 (−9)	93451.704 (−12)
30	93721.089 (37)	93675.906 (−81)	93635.779 (−5)	93642.487 (3)	93597.205 (−2)	93557.111 (4)
31	93840.854 (62)	93792.627 (−44)	93749.921 (4)	93757.034 (4)	93708.777 (1)	93666.009 (1)
32	93964.415 (43)	93913.072 (−22)	93867.675 (4)	93875.231 (−3)	93823.936 (39)	93778.401 (−4)
33	94091.798 (47)	94037.302 (99)	93989.048 (4)	93997.075 (8)	93942.588 (27)	93894.258 (−4)
34	94222.951 (66)	94165.107 (−96)	94114.061 (−10)	94122.558 (11)	94064.784	94013.556 (7)
35	94357.931 (47)		94242.709 (−16)	94251.666 (13)	94190.438 (29)	94136.329 (−4)
36	94496.720 (51)		94374.916 (43)	94384.456 (−29)	94319.787 (−1)	94262.552 (2)
37	94639.295 (29)		94510.802	94520.809 (−16)	94452.659 (3)	94392.228 (8)
38	94785.681			94660.782	94588.641	94525.363 (2)
39				94804.384	94728.331	94661.919 (8)
40				94951.719		94801.907 (−27)
41						94944.865 (*)
42						95092.196
43						95237.275
44						95395.735

Notes. The δ_P value in parentheses (in units of the least significant digit) corresponds to the wavenumber correction applied to TV_P and TV_R. There is no value when the term value is derived from a single transition, either R or P. An asterisk indicates when both R- and P-branches are present at high J', either the potential presence of a perturbing state or that one of the lines shows a larger uncertainty than the other (see also Sect. 2.2.2).

Table A.12. Transition wavelengths and wavenumbers of the $C^1\Sigma^+(v'=1)$–$X^1\Sigma^+(v''=0)$ band for $^{12}C^{16}O$, $^{12}C^{17}O$, and $^{12}C^{18}O$ (same column description as for Table A.1).

$C^1\Sigma^+(v'=1)$–$X^1\Sigma^+(v''=0)$															
	$^{12}C^{16}O$					$^{12}C^{17}O$					$^{12}C^{18}O$				
J''	R_{ms} (nm)	P_{ms} (nm)	R_{ms} (cm^{-1})	P_{ms} (cm^{-1})	δ_P	R_{ms} (nm)	P_{ms} (nm)	R_{ms} (cm^{-1})	P_{ms} (cm^{-1})	δ_P	R_{ms} (nm)	P_{ms} (nm)	R_{ms} (cm^{-1})	P_{ms} (cm^{-1})	δ_P
0	106.30450		94069.392			106.33521		94042.231			106.36264		94017.971		
1	106.30013	106.31320	94073.259	94061.694	−7	106.33096	106.34360	94045.990	94034.805	−22	106.35852	106.37095	94021.613	94010.626	0
2	106.29575	106.31752	94077.135	94057.872	−12	106.32670	106.34787	94049.756	94031.033	−7	106.35433	106.37507	94025.318	94006.985	−25
3	106.29143	106.32183	94080.959	94054.059	23	106.32243	106.35213	94053.531	94027.265	15	106.35013	106.37918	94029.031	94003.353	−14
4	106.28705	106.32622	94084.836	94050.175	−3	106.31817	106.35640	94057.300	94023.493	22	106.34602	106.38330	94032.665	93999.713	2
5	106.28268	106.33053	94088.704	94046.363	3	106.31391	106.36062	94061.066	94019.761	10	106.34182	106.38742	94036.379	93996.073	−21
6	106.27830	106.33485	94092.582	94042.542	5	106.30965	106.36480	94064.835	94016.061	2	106.33763	106.39154	94040.084	93992.433	−4
7	106.27399	106.33917	94096.398	94038.722	13	106.30540	106.36900	94068.602	94012.353	−2	106.33344	106.39566	94043.790	93988.793	10
8	106.26961	106.34349	94100.276	94034.902	−10	106.30113	106.37320	94072.379	94008.641	−3	106.32933	106.39978	94047.425	93985.153	25
9	106.26523	106.34781	94104.155	94031.082	0	106.29685	106.37741	94076.165	94004.922	2	106.32513	106.40390	94051.140	93981.514	−26
10	106.26086	106.35213	94108.025	94027.263	11	106.29259	106.38162	94079.935	94001.204	1	106.32094	106.40795	94054.846	93977.937	−4
11	106.25654	106.35645	94111.851	94023.443	19	106.28833	106.38580	94083.704	93997.511	−3	106.31675	106.41207	94058.553	93974.299	14
12	106.25217	106.36077	94115.722	94019.624	7	106.28404	106.38998	94087.499	93993.810	−6	106.31256	106.41619	94062.260	93970.660	−1
13	106.24779	106.36509	94119.601	94015.806	−7	106.27976	106.39417	94091.294	93990.109	−5	106.30837	106.42023	94065.967	93967.093	−10
14	106.24342	106.36935	94123.473	94012.041	11	106.27548	106.39834	94095.082	93986.430	14	106.30419	106.42428	94069.666	93963.517	−18
15	106.23905	106.37367	94127.344	94008.223	−4	106.27122	106.40254	94098.852	93982.719	14	106.30000	106.42833	94073.374	93959.941	3
16	106.23467	106.37792	94131.225	94004.467	19	106.26695	106.40670	94102.639	93979.043	−1	106.29573	106.43245	94077.153	93956.304	−4
17	106.23036	106.38225	94135.044	94000.641	17	106.26267	106.41085	94106.428	93975.381	−2	106.29154	106.43649	94080.861	93952.738	30
18	106.22599	106.38651	94138.917	93996.877	−17	106.25840	106.41500	94110.206	93971.716	−7	106.28736	106.44054	94084.561	93949.163	−4
19	106.22162	106.39076	94142.790	93993.122	13	106.25410	106.41913	94114.012	93968.063	11	106.28317	106.44451	94088.271	93945.659	−5
20	106.21724	106.39509	94146.672	93989.296	16	106.24984	106.42333	94117.785	93964.360	4	106.27898	106.44856	94091.980	93942.085	1
21	106.21294	106.39935	94150.483	93985.533	−5	106.24554	106.42743	94121.600	93960.741	−13	106.27479	106.45261	94095.690	93938.511	10
22	106.20856	106.40354	94154.366	93981.832	−28	106.24127	106.43154	94125.379	93957.114	−23	106.27053	106.45666	94099.462	93934.937	−13
23	106.20419	106.40780	94158.240	93978.070	−7	106.23699	106.43561	94129.175	93953.519	*	106.26635	106.46063	94103.163	93931.434	−3
24	106.19989	106.41207	94162.053	93974.299	8	106.23275	106.44012	94132.927	93949.534	*	106.26216	106.46460	94106.873	93927.931	−24
25	106.19551	106.41633	94165.936	93970.537	−4	106.22787	106.44419	94137.251	93945.943	*	106.25797	106.46857	94110.584	93924.429	−42
26	106.19121	106.42059	94169.750	93966.775	6	106.22294	106.44832	94141.623	93942.297	*	106.25379	106.47254	94114.294	93920.933	−87
27	106.18684	106.42481	94173.625	93963.048	5	106.21782	106.45237	94146.158	93938.724		106.24946	106.47643	94118.122	93917.500	−4
28	106.18251	106.42908	94177.471	93959.280	−8	106.21327		94150.192			106.24534	106.48060	94121.778	93913.817	*
29	106.17821	106.43324	94181.283	93955.606	−6						106.24102	106.48385	94125.599	93910.957	*
30	106.17386	106.43746	94185.143	93951.883	−6						106.23680	106.48713	94129.342	93908.060	
31	106.16958	106.44171	94188.935	93948.135	9						106.23281		94132.877		
32	106.16526	106.44592	94192.771	93944.416	−33										
33		106.45007		93940.752											

Table A.13. Transition wavelengths and wavenumbers of the $C^1\Sigma^+(v'=1)$–$X^1\Sigma^+(v''=0)$ band for $^{13}C^{16}O$, $^{13}C^{17}O$, and $^{13}C^{18}O$ (same column description as for Table A.1).

$C^1\Sigma^+(v'=1)$–$X^1\Sigma^+(v''=0)$															
	$^{13}C^{16}O$					$^{13}C^{17}O$					$^{13}C^{18}O$				
J''	R_{ms} (nm)	P_{ms} (nm)	R_{ms} (cm^{-1})	P_{ms} (cm^{-1})	δ_P	R_{ms} (nm)	P_{ms} (nm)	R_{ms} (cm^{-1})	P_{ms} (cm^{-1})	δ_P	R_{ms} (nm)	P_{ms} (nm)	R_{ms} (cm^{-1})	P_{ms} (cm^{-1})	δ_P
0	106.35798		94022.091			106.38925		93994.456			106.41767		93969.353		
1	106.35378	106.36630	94025.804	94014.736	−38	106.38582	106.39786	93997.486	93986.849	79	106.41366	106.42556	93972.895	93962.387	−17
2	106.34953	106.37037	94029.561	94011.139	−63	106.38175	106.40159	94001.082	93983.562	−93	106.40972	106.42950	93976.374	93958.908	0
3	106.34565	106.37443	94032.992	94007.551	*	106.37762	106.40587	94004.732	93979.779	−18	106.40571	106.43344	93979.916	93955.430	−9
4	106.34108	106.37888	94037.033	94003.618	−81	106.37371	106.41007	94008.187	93976.069	−16	106.40177	106.43739	93983.396	93951.943	9
5	106.33689	106.38289	94040.738	94000.075	59	106.36942	106.41404	94011.979	93972.559	*	106.39776	106.44133	93986.938	93948.466	−25
6	106.33276	106.38695	94044.391	93996.488	9	106.36529	106.41802	94015.629	93969.049	−36	106.39369	106.44522	93990.533	93945.032	−6
7	106.32857	106.39096	94048.097	93992.945	−13	106.36123	106.42199	94019.222	93965.539	−19	106.38969	106.44916	93994.067	93941.555	13
8	106.32444	106.39509	94051.750	93989.296	−7	106.35716	106.42600	94022.816	93962.003	−27	106.38575	106.45304	93997.548	93938.131	8
9	106.32019	106.39922	94055.510	93985.648	−23	106.35309	106.43001	94026.414	93958.463	−20	106.38174	106.45693	94001.091	93934.699	−1
10	106.31593	106.40336	94059.278	93981.991	−15	106.34894	106.43405	94030.087	93954.896	−53	106.37768	106.46087	94004.679	93931.222	−31
11	106.31206	106.40743	94062.702	93978.397	−1	106.34480	106.43799	94033.744	93951.414	−33	106.37367	106.46469	94008.223	93927.852	−12
12	106.30756	106.41150	94066.684	93974.802	−17	106.34087	106.44197	94037.223	93947.905	53	106.36967	106.46857	94011.758	93924.429	−8
13	106.30337	106.41589	94070.392	93970.925	*	106.33658	106.44611	94041.013	93944.251	−22	106.36560	106.47246	94015.355	93920.997	−12
14	106.29943	106.41996	94073.878	93967.331	63	106.33246	106.45008	94044.661	93940.743	32	106.36154	106.47634	94018.944	93917.575	−9
15	106.29512	106.42396	94077.693	93963.800	−58	106.32845	106.45399	94048.203	93937.293	48	106.35747	106.48016	94022.542	93914.206	21
16	106.29080	106.42803	94081.516	93960.206	−8	106.32430	106.45797	94051.878	93933.781	−14	106.35347	106.48405	94026.078	93910.775	1
17	106.28655	106.43211	94085.278	93956.604	44	106.32013	106.46189	94055.563	93930.322	16	106.34946	106.48781	94029.623	93907.459	4
18	106.28236	106.43618	94088.988	93953.012	40	106.31598	106.46587	94059.239	93926.815	27	106.34540	106.49169	94033.213	93904.037	−12
19	106.27824	106.44019	94092.635	93949.472	39	106.31185	106.46978	94062.893	93923.362	49	106.34133	106.49551	94036.812	93900.669	−4
20	106.27399	106.44426	94096.398	93945.880	10	106.30773	106.47373	94066.538	93919.882	50	106.33721	106.49933	94040.455	93897.301	−16
21	106.26980	106.44833	94100.108	93942.288	14	106.30354	106.47764	94070.246	93916.428	48	106.33308	106.50309	94044.108	93893.986	24
22	106.26555	106.45234	94103.871	93938.749	−5	106.29947	106.48156	94073.843	93912.975	67	106.32914	106.50691	94047.593	93890.618	44
23	106.26137	106.45635	94107.573	93935.211	5	106.29532	106.48544	94077.520	93909.549	34	106.32508	106.51067	94051.184	93887.304	−17
24	106.25718	106.46036	94111.284	93931.672	14	106.29085	106.48933	94081.477	93906.123	56	106.32100	106.51443	94054.793	93883.990	−23
25	106.25293	106.46443	94115.048	93928.081	36	106.28666	106.49324	94085.185	93902.671	*	106.31694	106.51819	94058.387	93880.676	15
26	106.24875	106.46851	94118.751	93924.482	29	106.28244	106.49720	94088.921	93899.183	*	106.31286	106.52202	94062.002	93877.300	−14
27	106.24450	106.47246	94122.516	93920.997	−35	106.27825	106.50102	94092.626	93895.815	*	106.30881	106.52571	94065.581	93874.048	1
28	106.24032	106.47634	94126.219	93917.575	−34	106.27400	106.50484	94096.393	93892.448	*	106.30473	106.52947	94069.195	93870.735	−25
29	106.23611	106.48029	94129.953	93914.091	*	106.26982	106.50866	94100.095	93889.076	*	106.30066	106.53317	94072.791	93867.475	−8
30	106.23191	106.48405	94133.678	93910.775	*	106.26560	106.51242	94103.832	93885.766	*	106.29662	106.53692	94076.367	93864.171	
31	106.22771	106.48780	94137.398	93907.468	*	106.26062	106.51616	94108.237	93882.469	*	106.29249		94080.021		
32	106.22343	106.49169	94141.189	93904.037	*	106.25634	106.51995	94112.032	93879.129	*	106.28886		94083.236		
33	106.21927	106.49551	94144.877	93900.669	*	106.25206	106.52371	94115.823	93875.810	*					
34	106.21510	106.49933	94148.571	93897.301	*	106.24775	106.52743	94119.641	93872.532	*					
35	106.21083	106.50309	94152.357	93893.986	*	106.24347	106.53116	94123.433	93869.249	*					
36	106.20666	106.50685	94156.051	93890.671	*	106.23919	106.53490	94127.225	93865.957	*					
37		106.51067		93887.309	*	106.23485	106.53852	94131.067	93862.764						
38		106.51444		93883.980		106.23064		94134.799							
39		106.51829		93880.594		106.22641		94138.552							
40		106.52203		93877.296		106.22206		94142.402							
41		106.52577		93874.003		106.21780		94146.181							
42		106.52941		93870.787											
43		106.53316		93867.491											
44		106.53738		93863.773											
45		106.54105		93860.535											

Table A.14. Term values (cm^{-1}) of the $C^1\Sigma^+(v'=1)$ levels for six CO isotopologues.

	$C^1\Sigma^+(v'=1)$					
J'	$^{12}C^{16}O$	$^{12}C^{17}O$	$^{12}C^{18}O$	$^{13}C^{16}O$	$^{13}C^{17}O$	$^{13}C^{18}O$
0	94065.539	94038.553	94014.288	94018.412	93990.428	93965.880
1	94069.399 (−7)	94042.254 (−22)	94017.971 (0)	94022.129 (−38)	93994.252 (*)	93969.370 (−17)
2	94077.116 (−12)	94049.745 (−7)	94025.300 (−25)	94029.543 (−63)	94001.158 (−93)	93976.387 (0)
3	94088.647 (23)	94060.985 (15)	94036.317 (−14)	94040.482 (107)	94011.837 (−18)	93986.861 (−9)
4	94104.031 (−3)	94075.996 (22)	94050.999 (2)	94055.128 (−81)	94026.220 (−16)	94000.863 (9)
5	94123.281 (3)	94094.767 (10)	94069.303 (−21)	94073.731 (59)	94044.084 (*)	94018.347 (−25)
6	94146.370 (5)	94117.278 (2)	94091.307 (−4)	94095.863 (9)	94065.692 (−36)	94039.332 (−6)
7	94173.305 (13)	94143.533 (−2)	94116.965 (10)	94121.589 (−13)	94090.793 (−19)	94063.860 (13)
8	94204.050 (−10)	94173.529 (−3)	94146.282 (25)	94151.013 (−7)	94119.439 (−27)	94091.842 (8)
9	94238.667 (0)	94207.272 (2)	94179.252 (−26)	94184.078 (−23)	94151.645 (−20)	94123.265 (−1)
10	94277.122 (11)	94244.774 (1)	94215.887 (−4)	94220.897 (−15)	94187.469 (−53)	94158.259 (−31)
11	94319.409 (19)	94286.003 (−3)	94256.173 (14)	94261.389 (−1)	94226.890 (−33)	94196.734 (−12)
12	94365.511 (7)	94330.972 (−6)	94300.147 (−1)	94305.234 (−17)	94269.799 (53)	94238.669 (−8)
13	94415.494 (−7)	94379.701 (−5)	94347.768 (−10)	94353.165 (106)	94316.262 (−22)	94284.086 (−12)
14	94469.288 (11)	94432.149 (14)	94399.040 (−18)	94404.654 (63)	94366.475 (32)	94333.044 (−9)
15	94526.938 (−4)	94488.344 (14)	94453.924 (3)	94459.663 (−58)	94420.153 (48)	94385.446 (21)
16	94588.380 (19)	94548.269 (−1)	94512.494 (−4)	94518.492 (−8)	94477.368 (−14)	94441.388 (1)
17	94653.683 (17)	94611.929 (−2)	94574.739 (30)	94580.988 (44)	94538.186 (16)	94500.723 (4)
18	94722.782 (−17)	94679.323 (−7)	94640.626 (−4)	94647.134 (40)	94602.595 (27)	94563.564 (−12)
19	94795.693 (13)	94750.410 (11)	94710.113 (−5)	94716.881 (39)	94670.543 (49)	94629.898 (−4)
20	94872.451 (16)	94825.275 (4)	94783.241 (1)	94790.247 (10)	94742.049 (50)	94699.734 (−16)
21	94953.060 (−5)	94903.838 (−13)	94860.003 (10)	94867.346 (14)	94817.102 (48)	94773.033 (24)
22	95037.414 (−28)	94986.153 (−23)	94940.432 (−13)	94948.063 (−5)	94895.749 (67)	94849.828 (44)
23	95125.607 (−7)	95071.968 (*)	95024.520 (−3)	95032.448 (5)	94977.888 (34)	94930.001 (−17)
24	95217.604 (8)	95161.698 (*)	95112.198 (−24)	95120.416 (14)	95063.597 (56)	95013.686 (−23)
25	95313.372 (−4)	95255.084 (*)	95203.506 (−42)	95212.019 (36)	95152.969 (*)	95100.807 (15)
26	95412.990 (6)	95352.495 (*)	95298.465 (−87)	95307.339 (29)	95245.814 (*)	95191.435 (−14)
27	95516.346 (5)	95454.281	95396.912 (−4)	95406.288 (−35)	95342.207 (*)	95285.493 (1)
28	95623.569 (−8)	95559.553	95499.443 (*)	95508.862 (−34)	95442.113 (*)	95383.007 (−25)
29	95734.539 (−6)	95668.018	95605.477 (*)	95615.111 (*)	95545.608 (*)	95483.960 (−8)
30	95849.260 (−6)		95714.354	95724.997 (*)	95652.600 (*)	95588.347
31	95967.797 (9)		95827.358	95838.431 (*)	95763.109 (*)	95696.164
32	96090.099 (−33)		95943.752	95955.503 (*)	95877.478 (*)	95807.494
33	96216.142			96076.216 (*)	95995.073 (*)	95921.819
34				96200.504 (*)	96116.172 (*)	
35				96328.391 (*)	96240.783 (*)	
36				96459.893 (*)	96368.929 (*)	
37				96594.952 (*)	96501.308	
38				96734.237	96636.494	
39				96876.548	96775.059	
40				97022.430	96917.129	
41				97171.950	97062.777	
42				97324.945	97211.828	
43				97481.067		
44				97641.214		

Notes. See note to Table A.11.

Table A.15. Transition wavelengths and wavenumbers of the $C^1\Sigma^+(v'=2)$–$X^1\Sigma^+(v''=0)$ band for $^{12}C^{16}O$, $^{12}C^{18}O$, $^{13}C^{16}O$, and $^{13}C^{18}O$ (same column description as for Table A.1).

$C^1\Sigma^+(v'=2)$–$X^1\Sigma^+(v''=0)$															
	$^{12}C^{16}O$					$^{12}C^{17}O$					$^{12}C^{18}O$				
J''	R_{ms} (nm)	P_{ms} (nm)	R_{ms} (cm^{-1})	P_{ms} (cm^{-1})	δ_P	R_{ms} (nm)	P_{ms} (nm)	R_{ms} (cm^{-1})	P_{ms} (cm^{-1})	δ_P	R_{ms} (nm)	P_{ms} (nm)	R_{ms} (cm^{-1})	P_{ms} (cm^{-1})	δ_P
0	103.97097		96180.696								104.07997		96079.966		
1	103.96690	103.97929	96184.460	96173.002	−39						104.07616	104.08785	96083.483	96072.692	−10
2	103.96283	103.98335	96188.222	96169.239	−8						104.07236	104.09185	96086.992	96069.001	−21
3	103.95889	103.98767	96191.872	96165.252	−5						104.06851	104.09595	96090.547	96065.217	−4
4	103.95488	103.99192	96195.579	96161.320	−14						104.06469	104.10012	96094.074	96061.369	−10
5	103.95100	103.99627	96199.174	96157.299	2						104.06103	104.10419	96097.454	96057.613	8
6	103.94711	104.00060	96202.769	96153.289	7						104.05726	104.10834	96100.935	96053.784	−52
7	103.94335	104.00504	96206.251	96149.188	13						104.05355	104.11248	96104.362	96049.964	55
8	103.93953	104.00947	96209.789	96145.089	−9							104.11687		96045.915	75
9	103.93583	104.01397	96213.215	96140.933	27							104.12113		96041.985	
10	103.93213	104.01853	96216.641	96136.721	9							104.12620		96037.309	
11	103.92849	104.02308	96220.010	96132.508	20										
12	103.92491	104.02770	96223.324	96128.240	4										
13	103.92133	104.03232	96226.638	96123.971	−9										
14	103.91781	104.03700	96229.896	96119.647	7										
15	103.91441	104.04175	96233.040	96115.266	−2										
16	103.91090	104.04649	96236.298	96110.886	*										
17	103.90768	104.05062	96239.275	96107.066											
18	103.90435		96242.364												
19	103.90095		96245.509												
20	103.89780		96248.430												
21	103.89444		96251.540												

	$^{13}C^{16}O$					$^{13}C^{17}O$					$^{13}C^{18}O$				
J''	R_{ms} (nm)	P_{ms} (nm)	R_{ms} (cm^{-1})	P_{ms} (cm^{-1})	δ_P	R_{ms} (nm)	P_{ms} (nm)	R_{ms} (cm^{-1})	P_{ms} (cm^{-1})	δ_P	R_{ms} (nm)	P_{ms} (nm)	R_{ms} (cm^{-1})	P_{ms} (cm^{-1})	δ_P
0	104.07148		96087.808								104.18328		95984.695		
1	104.06751	104.07933	96091.474	96080.561	−35						104.17968	104.19072	95988.012	95977.841	−99
2	104.06364	104.08335	96095.047	96076.850	56						104.17596	104.19444	95991.440	95974.415	1
3	104.05977	104.08754	96098.621	96072.982	−60						104.17231	104.19864	95994.803	95970.546	−36
4	104.05604	104.09138	96102.066	96069.438	64						104.16865	104.20242	95998.176	95967.065	−23
5	104.05227	104.09574	96105.548	96065.414	−33						104.16506	104.20638	96001.484	95963.418	0
6	104.04856	104.09976	96108.974	96061.705	−10						104.16146	104.21035	96004.802	95959.762	−36
7	104.04497	104.10400	96112.291	96057.792	19						104.15793	104.21426	96008.056	95956.162	11
8	104.04133	104.10831	96115.653	96053.815	13						104.15445	104.21834	96011.264	95952.405	−23
9	104.03768	104.11266	96119.025	96049.802	−16						104.15098	104.22231	96014.463	95948.750	
10	104.03404	104.11691	96122.388	96045.881							104.14739		96017.772		
11	104.03063		96125.539								104.14362		96021.248		

Table A.16. Term values (cm^{-1}) of the $C^1\Sigma^+(v'=2)$ levels for $^{12}C^{16}O$, $^{12}C^{18}O$, $^{13}C^{16}O$ and $^{13}C^{18}O$.

	$C^1\Sigma^+(v'=2)$					
J'	$^{12}C^{16}O$	$^{12}C^{17}O$	$^{12}C^{18}O$	$^{13}C^{16}O$	$^{13}C^{17}O$	$^{13}C^{18}O$
0	96176.847		96076.354	96084.237		95981.334
1	96180.735 (−39)		96079.976 (−10)	96087.843 (−35)		95984.794 (−99)
2	96188.313 (−8)		96087.167 (−21)	96095.093 (56)		95991.504 (1)
3	96199.763 (−5)		96097.982 (−4)	96106.135 (−60)		96001.954 (−36)
4	96214.956 (−14)		96112.527 (−10)	96120.612 (64)		96015.782 (−23)
5	96234.026 (2)		96130.683 (8)	96138.856 (−33)		96033.102 (0)
6	96256.838 (7)		96152.430 (−52)	96160.691 (−10)		96053.908 (−36)
7	96283.492 (13)		96177.772 (55)	96186.140 (19)		96078.132 (11)
8	96313.902 (−9)		96206.804 (75)	96215.187 (13)		96105.863 (−23)
9	96348.152 (27)		96238.649	96247.974 (−16)		96136.979
10	96386.184 (9)			96284.397		96171.599
11	96428.026 (20)			96324.497		96209.816
12	96473.673 (4)			96368.054		96251.686
13	96523.099 (−9)					
14	96576.328 (7)					
15	96633.359 (−2)					
16	96694.441 (*)					
17	96758.774					
18	96826.996					
19	96899.153					
20	96975.186					
21	97054.812					
22	97138.442					

Notes. See note to Table A.11.

Table A.17. Transition wavelengths and wavenumbers of the $C^1\Sigma^+(v'=3)$–$X^1\Sigma^+(v''=0)$ band for $^{12}C^{16}O$, $^{12}C^{17}O$, $^{12}C^{18}O$, $^{13}C^{16}O$, and $^{13}C^{18}O$ (same column description as for Table A.1).

$C^1\Sigma^+(v'=3)$–$X^1\Sigma^+(v''=0)$															
	$^{12}C^{16}O$					$^{12}C^{17}O$					$^{12}C^{18}O$				
J''	R_{ms} (nm)	P_{ms} (nm)	R_{ms} (cm^{-1})	P_{ms} (cm^{-1})	δ_P	R_{ms} (nm)	P_{ms} (nm)	R_{ms} (cm^{-1})	P_{ms} (cm^{-1})	δ_P	R_{ms} (nm)	P_{ms} (nm)	R_{ms} (cm^{-1})	P_{ms} (cm^{-1})	δ_P
0	101.78276		98248.469			101.86301		98171.062			101.93560		98101.159		
1	101.77912	101.79108	98251.976	98240.438	78	101.85978	101.87119	98174.175	98163.179	*	101.93187	101.94321	98104.744	98093.834	8
2	101.77549	101.79487	98255.483	98236.778	65	101.85626	101.87502	98177.568	98159.489	−61	101.92835	101.94703	98108.129	98090.158	44
3	101.77189	101.79918	98258.962	98232.621	−4	101.85256	101.87910	98181.135	98155.558	*	101.92494	101.95099	98111.413	98086.346	27
4	101.76846	101.80337	98262.276	98228.577	26	101.84916	101.88313	98184.412	98151.675	10	101.92154	101.95505	98114.689	98082.443	−13
5	101.76485	101.80779	98265.758	98224.309	2	101.84564	101.88758	98187.806	98147.389	31	101.91818	101.95916	98117.920	98078.486	48
6	101.76171	101.81227	98268.790	98219.985	20	101.84237	101.89200	98190.958	98143.131	*	101.91499	101.96349	98120.995	98074.319	55
7	101.75845	101.81667	98271.935	98215.746	12	101.83925	101.89647	98193.966	98138.826	*	101.91191	101.96776	98123.961	98070.216	−38
8	101.75520	101.82147	98275.081	98211.110	−9	101.83629	101.90136	98196.821	98134.116		101.90893	101.97198	98126.827	98066.160	−70
9	101.75223	101.82613	98277.945	98206.618	56	101.83308		98199.916			101.90591	101.97643	98129.738	98061.876	−71
10	101.74933	101.83097	98280.744	98201.956	37	101.83026		98202.635			101.90293	101.98105	98132.605	98057.429	*
11	101.74660	101.83592	98283.385	98197.182	15	101.82568		98207.053			101.89995	101.98603	98135.471	98052.647	
12	101.74380	101.84093	98286.089	98192.352	−27										
13	101.74135	101.84605	98288.459	98187.409	76										
14	101.73857	101.85141	98291.144	98182.242	−43										
15	101.73601	101.85666	98293.615	98177.188	67										
16	101.73368	101.86204	98295.861	98171.996	*										
17	101.73165	101.86762	98297.827	98166.618	91										
18	101.72977	101.87307	98299.643	98161.366	*										
19	101.72763	101.87804	98301.712	98156.578	14										
20		101.88485		98150.022	34										
21		101.89066		98144.419											
22		101.89751		98137.827											
	$^{13}C^{16}O$					$^{13}C^{17}O$					$^{13}C^{18}O$				
J''	R_{ms} (nm)	P_{ms} (nm)	R_{ms} (cm^{-1})	P_{ms} (cm^{-1})	δ_P	R_{ms} (nm)	P_{ms} (nm)	R_{ms} (cm^{-1})	P_{ms} (cm^{-1})	δ_P	R_{ms} (nm)	P_{ms} (nm)	R_{ms} (cm^{-1})	P_{ms} (cm^{-1})	δ_P
0	101.92352		98112.780								102.08055		97961.854		
1	101.91994	101.93111	98116.226	98105.474	93						102.07698	102.08776	97965.280	97954.935	14
2	101.91646	101.93517	98119.577	98101.567	−31						102.07360	102.09150	97968.524	97951.347	−5
3	101.91288	101.93897	98123.023	98097.910	33						102.07027	102.09517	97971.720	97947.826	−23
4	101.90949	101.94326	98126.287	98093.782	−28						102.06700	102.09903	97974.859	97944.123	16
5	101.90619	101.94719	98129.465	98090.000	−50						102.06390	102.10306	97977.834	97940.257	56
6	101.90284	101.95139	98132.691	98085.959	−8						102.06075	102.10715	97980.858	97936.334	−43
7	101.89989	101.95581	98135.532	98081.707	82						102.05766	102.11112	97983.825	97932.526	−7
8	101.89694	101.96028	98138.373	98077.407	*						102.05480	102.11532	97986.571	97928.498	30
9	101.89399	101.96448	98141.214	98073.367	−81						102.05176	102.11958	97989.490	97924.413	44
10	101.89086	101.96930	98144.229	98068.731	55						102.04908	102.12402	97992.063	97920.155	6
11	101.88828	101.97426	98146.714	98063.961	*						102.04621	102.12817	97994.819	97916.176	46
12	101.88537	101.97805	98149.517	98060.317							102.04347	102.13284	97997.451	97911.699	92
13	101.88251		98152.273								102.04105	102.13733	97999.775	97907.395	*
14											102.03883	102.14212	98001.907	97902.803	58
15												102.14662		97898.490	−65
16												102.15140		97893.909	
17												102.15655		97888.974	

Table A.18. Term values (cm^{-1}) of the $C^1\Sigma^+(v'=3)$ levels for $^{12}C^{16}O$, $^{12}C^{17}O$, $^{12}C^{18}O$, $^{13}C^{16}O$ and $^{13}C^{18}O$.

	$C^1\Sigma^+(v'=3)$					
J'	$^{12}C^{16}O$	$^{12}C^{17}O$	$^{12}C^{18}O$	$^{13}C^{16}O$	$^{13}C^{17}O$	$^{13}C^{18}O$
0	98244.283	98166.927	98097.496	98109.150		97958.428
1	98248.391 (78)	98170.897 (*)	98101.151 (8)	98112.687 (93)		97961.839 (14)
2	98255.756 (65)	98177.984 (−61)	98108.361 (44)	98119.934 (−31)		97968.777 (−5)
3	98267.022 (−4)	98188.982 (*)	98119.088 (27)	98130.572 (33)		97979.025 (−23)
4	98282.005 (26)	98203.612 (10)	98133.397 (−13)	98145.106 (−28)		97992.660 (16)
5	98300.722 (2)	98221.858 (31)	98151.258 (48)	98163.094 (−50)		98009.729 (56)
6	98323.408 (20)	98243.884 (*)	98172.789 (55)	98184.608 (−8)		98030.266 (−43)
7	98349.513 (12)	98269.333 (*)	98197.924 (−38)	98209.794 (82)		98054.206 (−7)
8	98379.587 (−9)	98298.890	98226.549 (−70)	98238.590 (*)		98081.578 (30)
9	98413.415 (56)	98331.716	98258.699 (−71)	98270.759 (−81)		98112.243 (44)
10	98450.886 (37)	98368.526	98294.361 (*)	98306.531 (55)		98146.620 (6)
11	98492.133 (15)	98408.701	98333.946	98346.621 (*)		98184.062 (46)
12	98537.080 (−27)	98454.314	98377.064	98389.229		98225.166 (92)
13	98585.779 (76)			98436.105		98269.547 (*)
14	98638.200 (−43)			98486.598		98317.396 (58)
15	98694.538 (67)					98368.494 (−65)
16	98754.504 (*)					98422.903
17	98818.246 (91)					
18	98885.902 (*)					
19	98956.419 (14)					
20	99031.355 (34)					
21	99109.060					

Notes. See note to Table A.11.

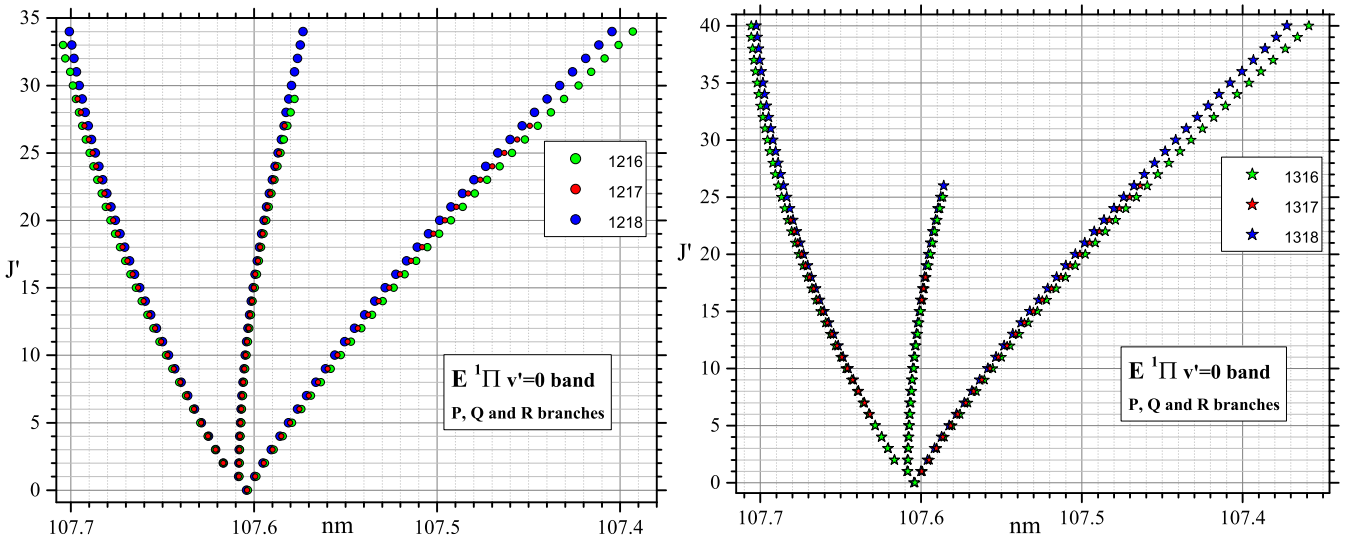

Fig. A.12. Transition wavelengths of the $E^1\Pi(v'=0)$–$X^1\Sigma^+(v''=0)$ band for six CO isotopologues.

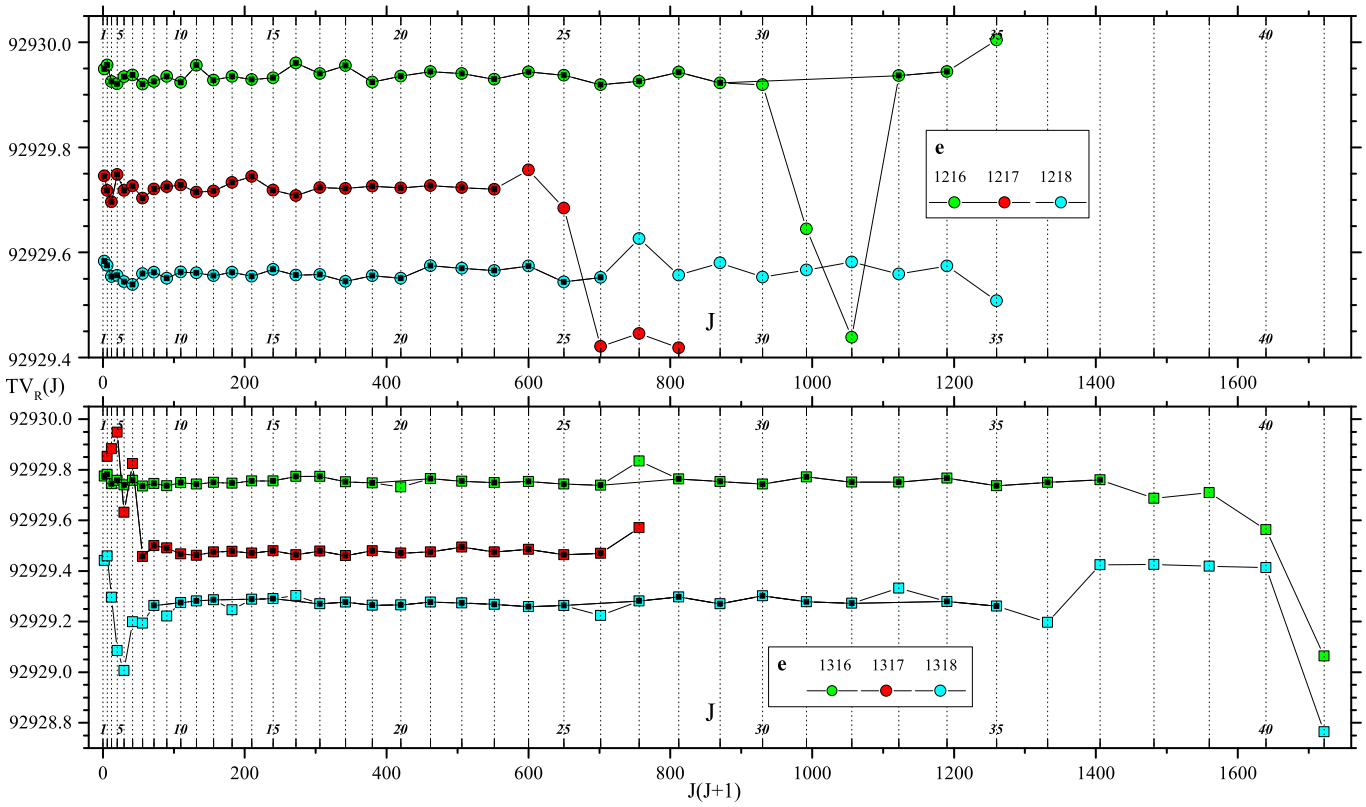

Fig. A.13. *e*-parity reduced term values (cm^{-1}) of the $E^1\Pi(v'=0)$ levels for six CO isotopologues. Data marked with a black center are kept to calculate molecular constants.

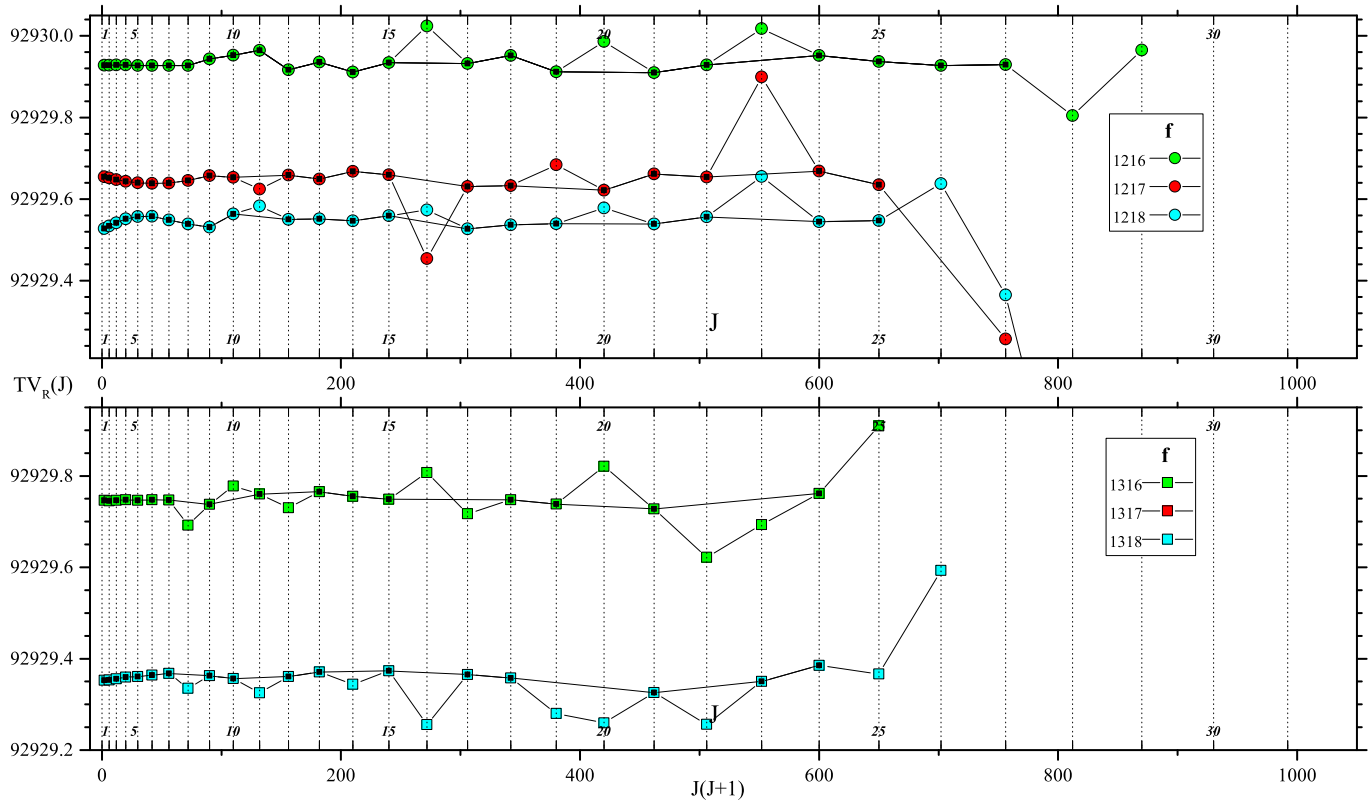

Fig. A.14. f-parity reduced term values (cm^{-1}) of the $E^1\Pi(v'=0)$ levels for six CO isotopologues (data marked with a black center are kept to calculate molecular constants).

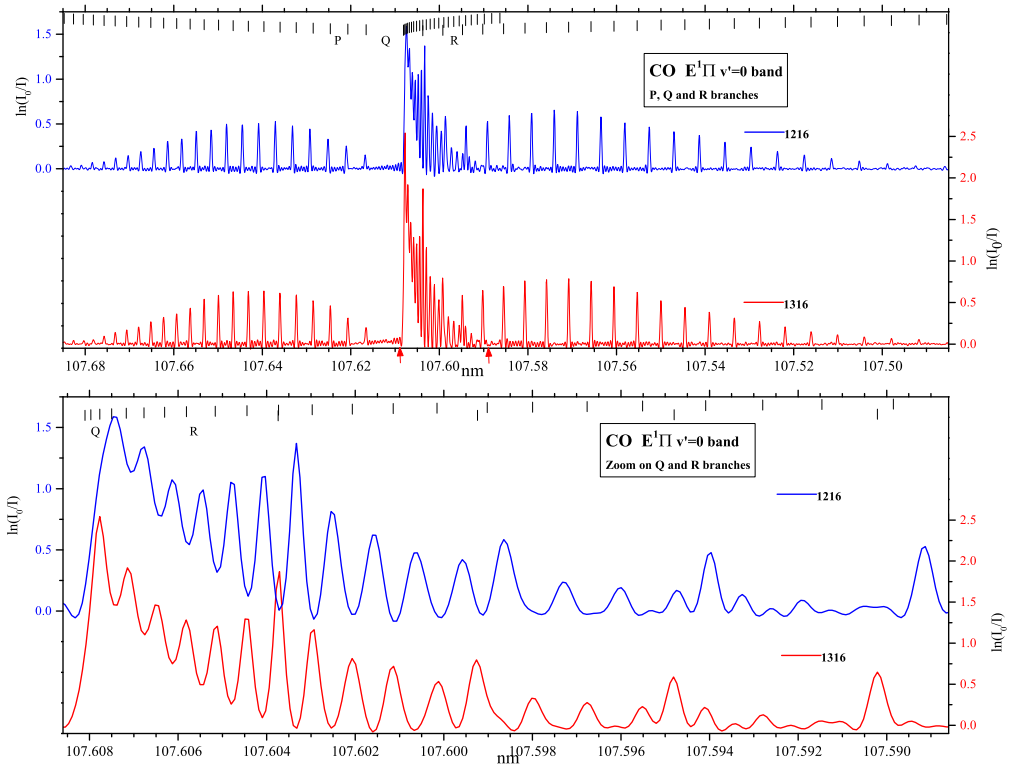

Fig. A.15. Spectra of the $E^1\Pi(v'=0)$–$X^1\Sigma^+(v''=0)$ band for $^{13}C^{16}O$ and $^{12}C^{16}O$. The lower graph shows a ×10 expanded scale on the Q-branch between the red arrows).

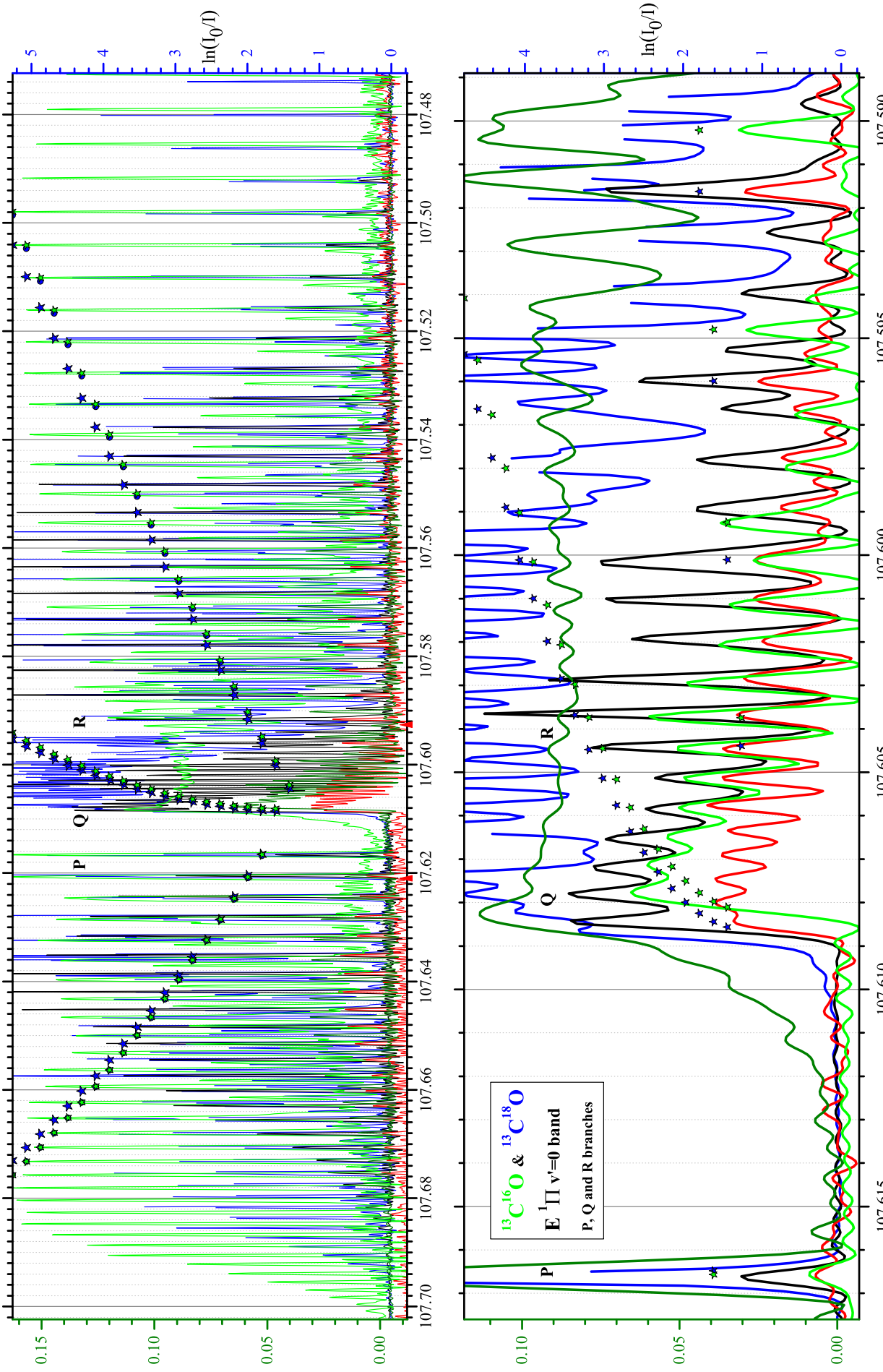

Fig. A.16. *Top*: spectra of the $E^1\Pi(v'=0)$–$X^1\Sigma^+(v''=0)$ band for $^{13}C^{18}O$ (three spectra at different pressures [saturated, half saturated, and no saturation]: 0.5/0.03/0.004 mbar, respectively, in blue/black/red colors; the scale to the right is valid for the highest pressure and has to be divided by 2 and 10 for the latter ones) and $^{13}C^{16}O$ (two spectra [saturated and no saturation]: 0.5/0.005 mbar respectively in olive/green colors; the scale to the left is the same for both pressures). *Bottom*: this is an ×8 expanded scale on the *Q*-branch between the red arrows (same color codes and same relative scales as above).

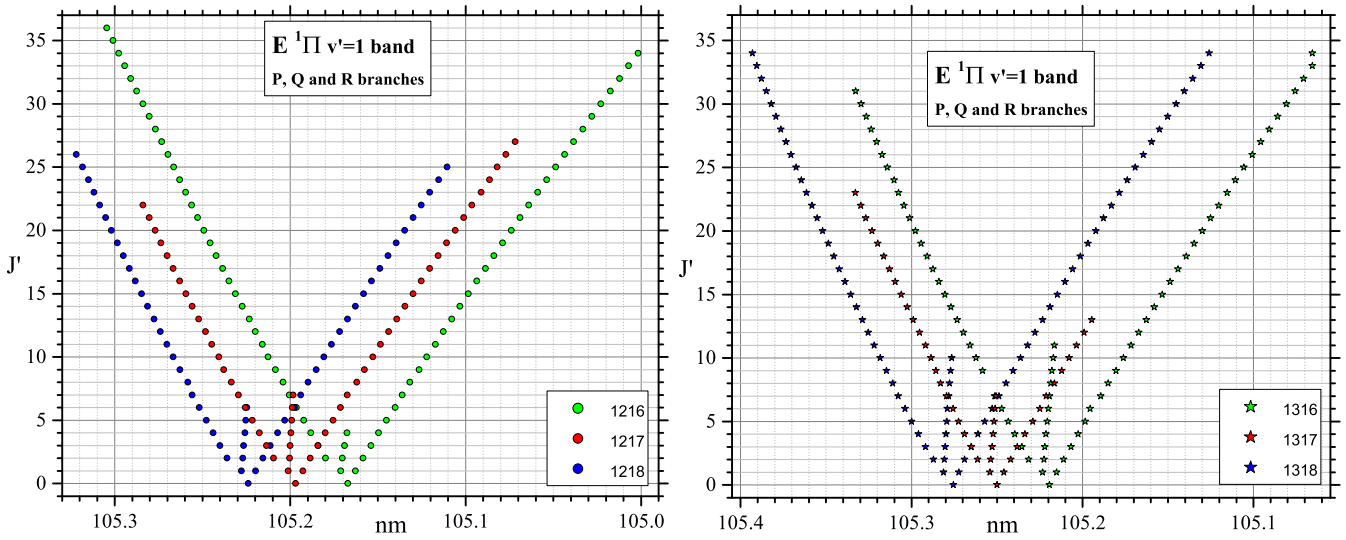

Fig. A.17. Transition wavelengths of the $E^1\Pi(v'=1)$–$X^1\Sigma^+(v''=0)$ band for six CO isotopologues.

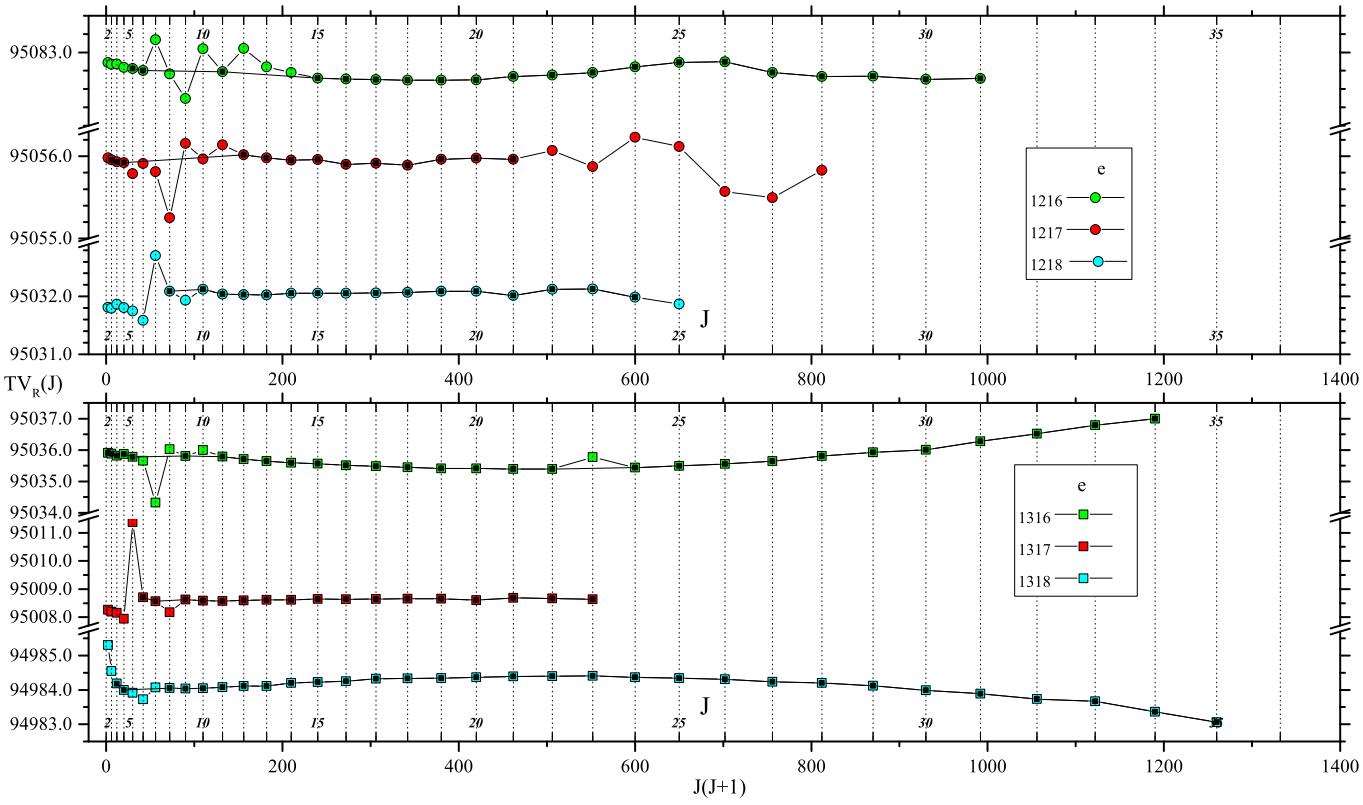

Fig. A.18. *e*-parity reduced term values (cm^{-1}) of the $E^1\Pi(v'=1)$ levels for six CO isotopologues (left). Data marked with a black center are kept to calculate molecular constants.

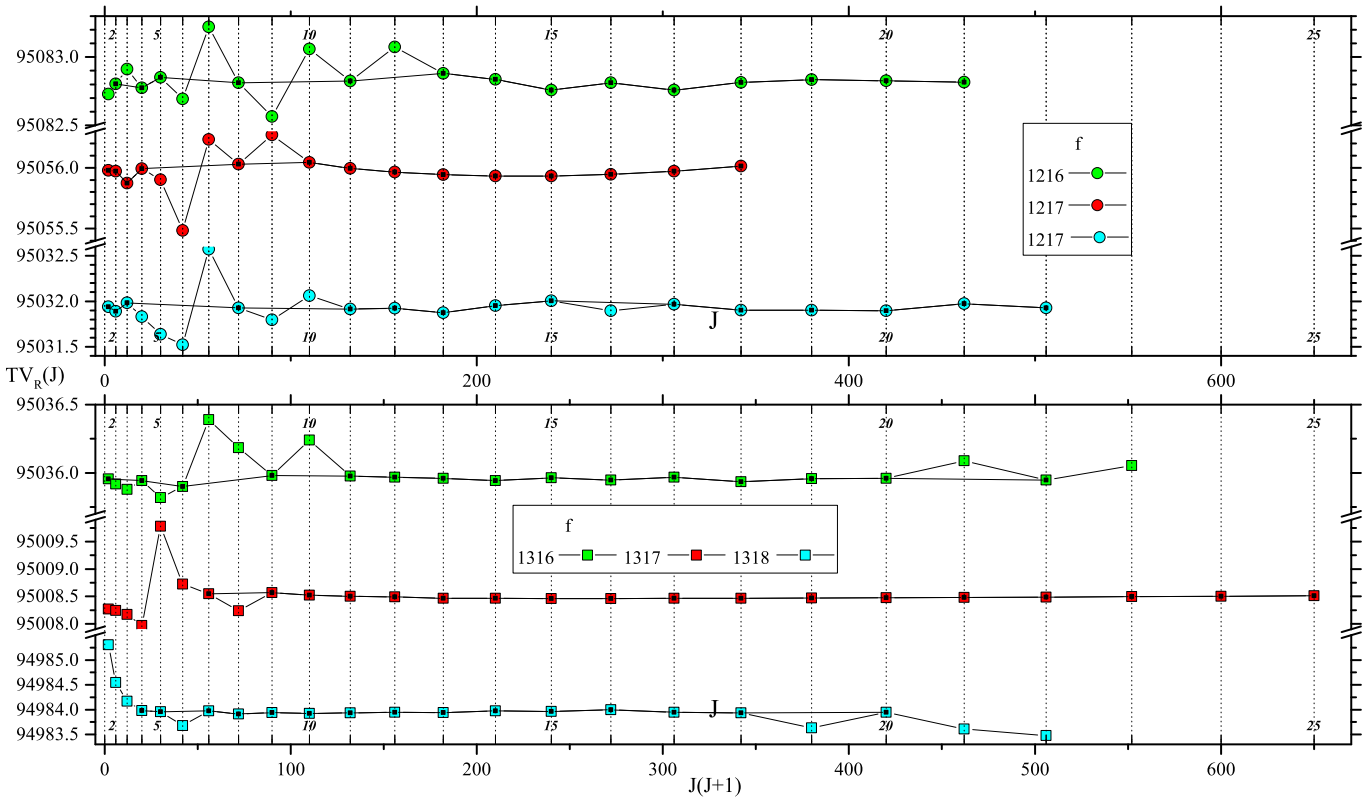

Fig. A.19. f-parity reduced term values (cm^{-1}) of the $E^1\Pi(v' = 1)$ levels for six CO isotopologues (data marked with a black center are kept to calculate molecular constants).

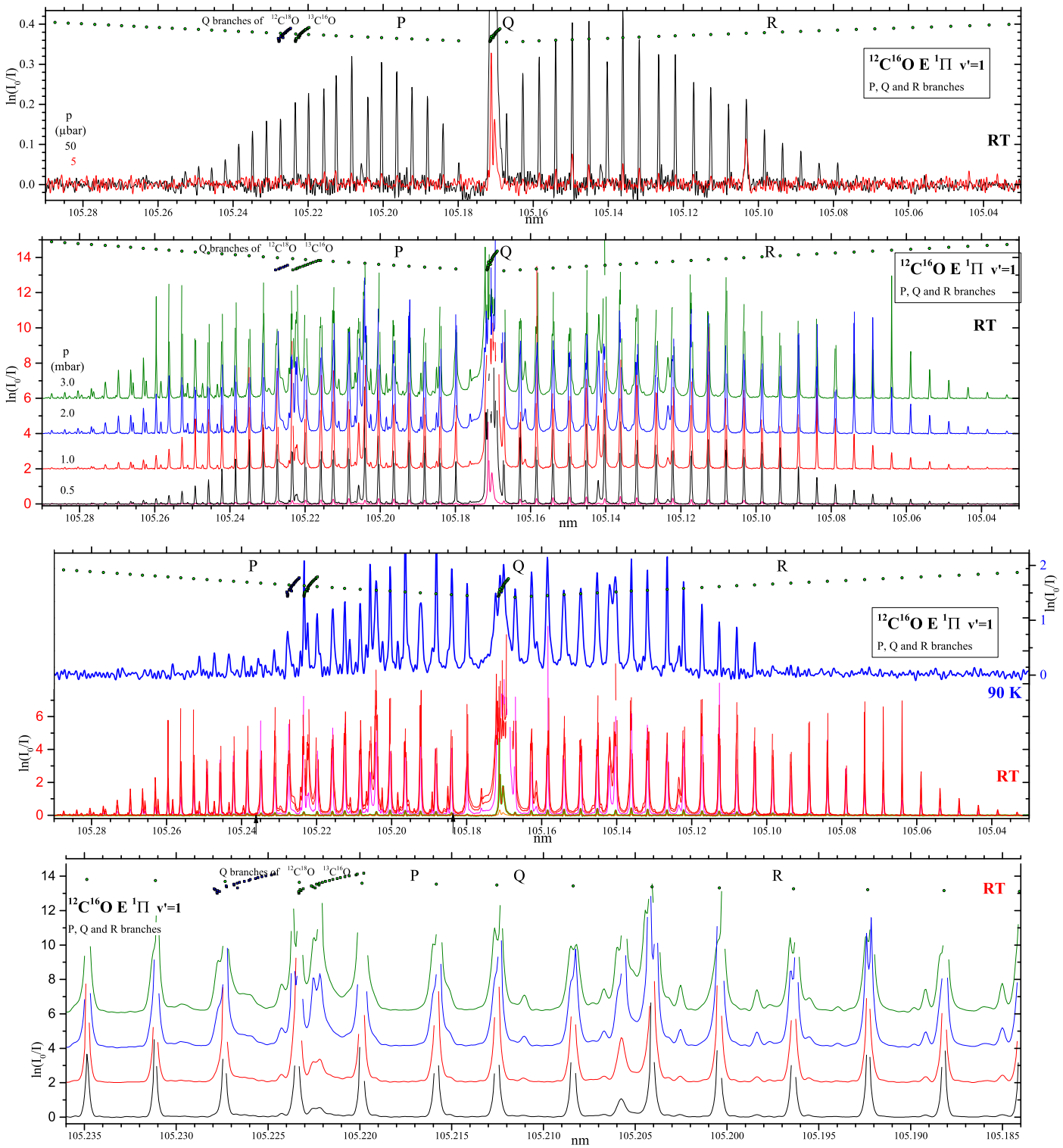

Fig. A.20. Spectra of the $E^1\Pi(v'=1)$–$X^1\Sigma^+(v''=0)$ band for $^{12}C^{16}O$. *Two upper panels*: RT spectra taken at different pressures. *Third panel*: comparison between 90 K (1 pressure) and room-temperature spectra (all pressures). *Lower panel*: ×5 expanded scale on the region indicated by black arrows on the above panel. This region contains among other lines those of the $k^3\Pi(v'=5)$ perturbing band (around 105.205 nm), while $k^3\Pi(v'=6)$ appears around 105.14 nm.

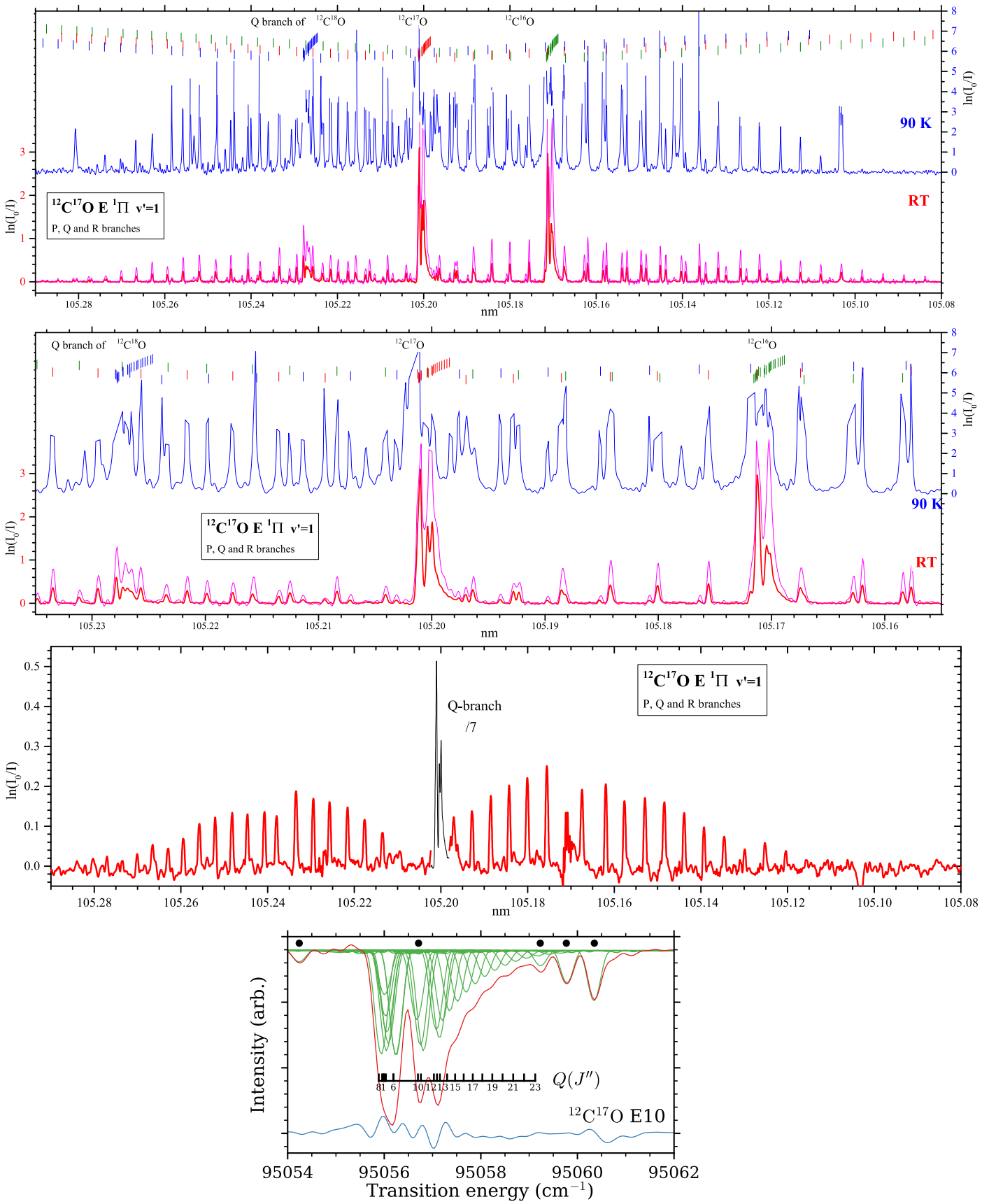

Fig. A.21. Spectra of the $E^1\Pi(v'=1)$–$X^1\Sigma^+(v''=0)$ band for $^{12}C^{17}O$ at 90 K and at room temperature (two pressures for the latter). *Second panel*: zoom of the central part of the *upper panel* (×3 zoom). *Third panel*: RT spectrum after weighted subtraction of $^{12}C^{16}O$ and $^{12}C^{18}O$ spectra (the signal in the *Q*-branch, in black, is divided by 7). *Lower panel*: simulated absorption spectrum of the *Q*-branch at room temperature.

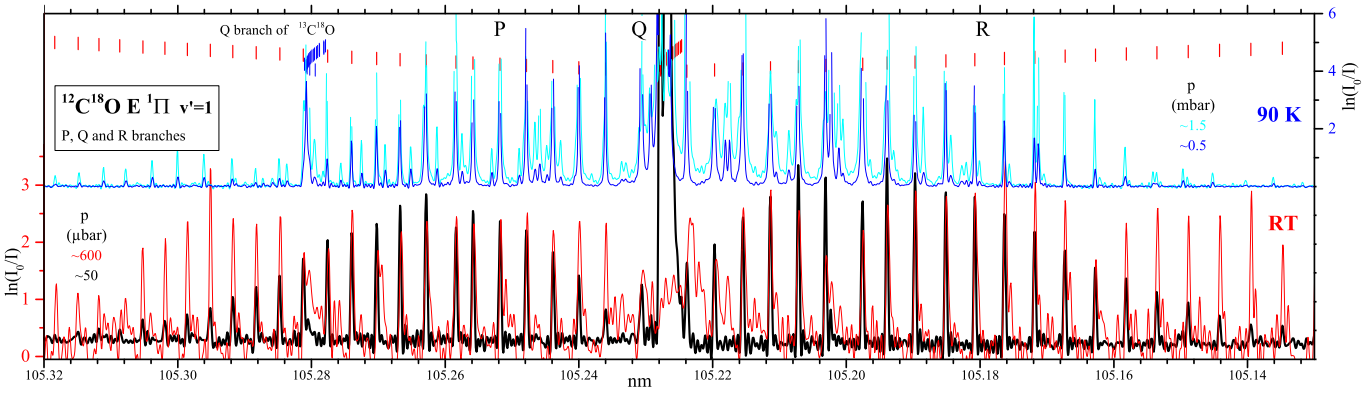

Fig. A.22. Spectra of the $E^1\Pi(v'=1)$–$X^1\Sigma^+(v''=0)$ band for $^{12}C^{18}O$ at 90 K and room temperature (both at two pressures).

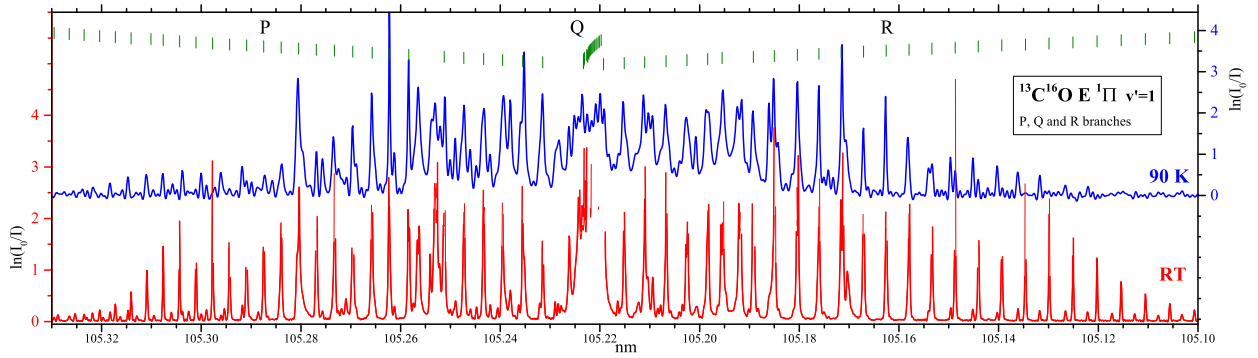

Fig. A.23. Spectra of the $E^1\Pi(v'=1)$–$X^1\Sigma^+(v''=0)$ band for $^{13}C^{16}O$ at 90 K and room temperature.

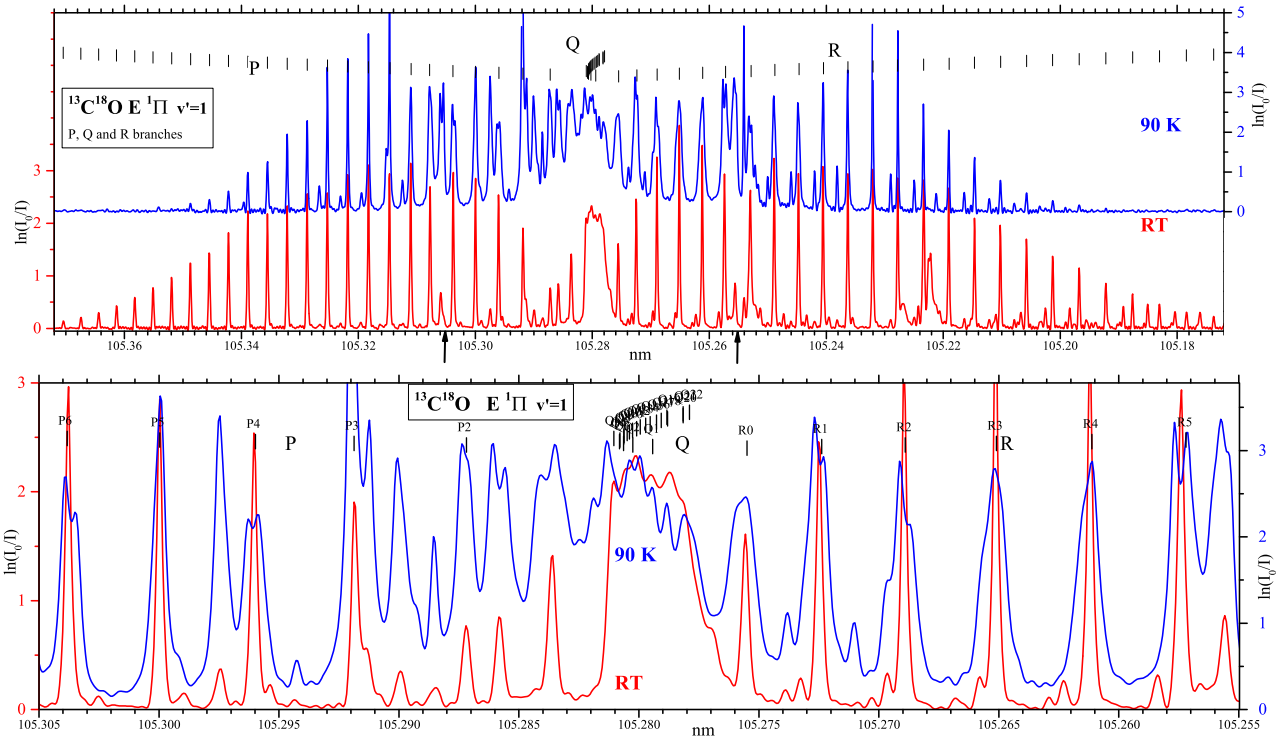

Fig. A.24. *Upper panel*: spectra of the $E^1\Pi(v'=1)$–$X^1\Sigma^+(v''=0)$ band for $^{13}C^{18}O$ at 90 K and room temperature. *Lower panel*: ×4 expanded scale on the Q-branch between the black arrows.

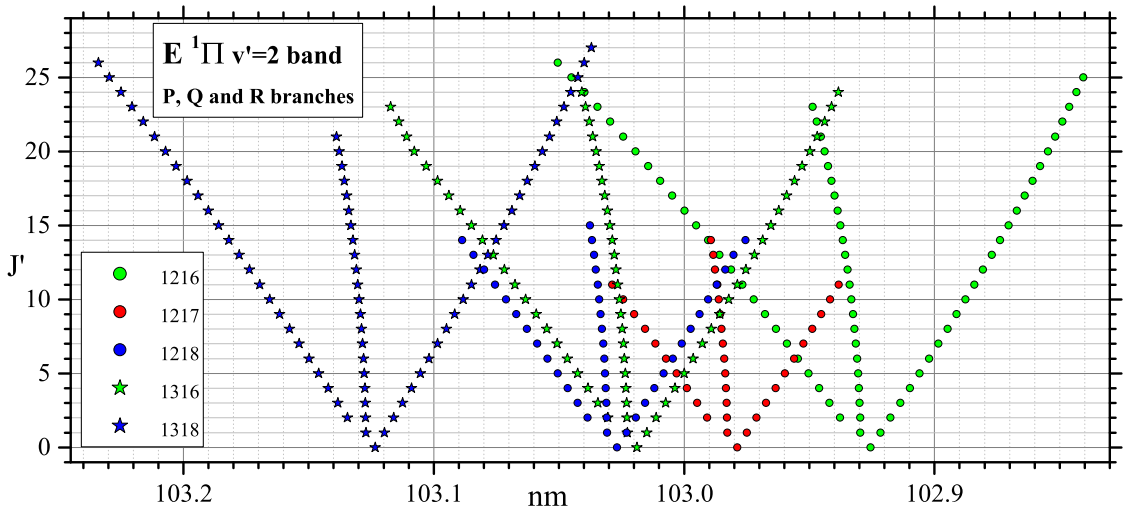

Fig. A.25. Transition wavelengths of the $E^1\Pi(v'=2)$–$X^1\Sigma^+(v''=0)$ band for five CO isotopologues.

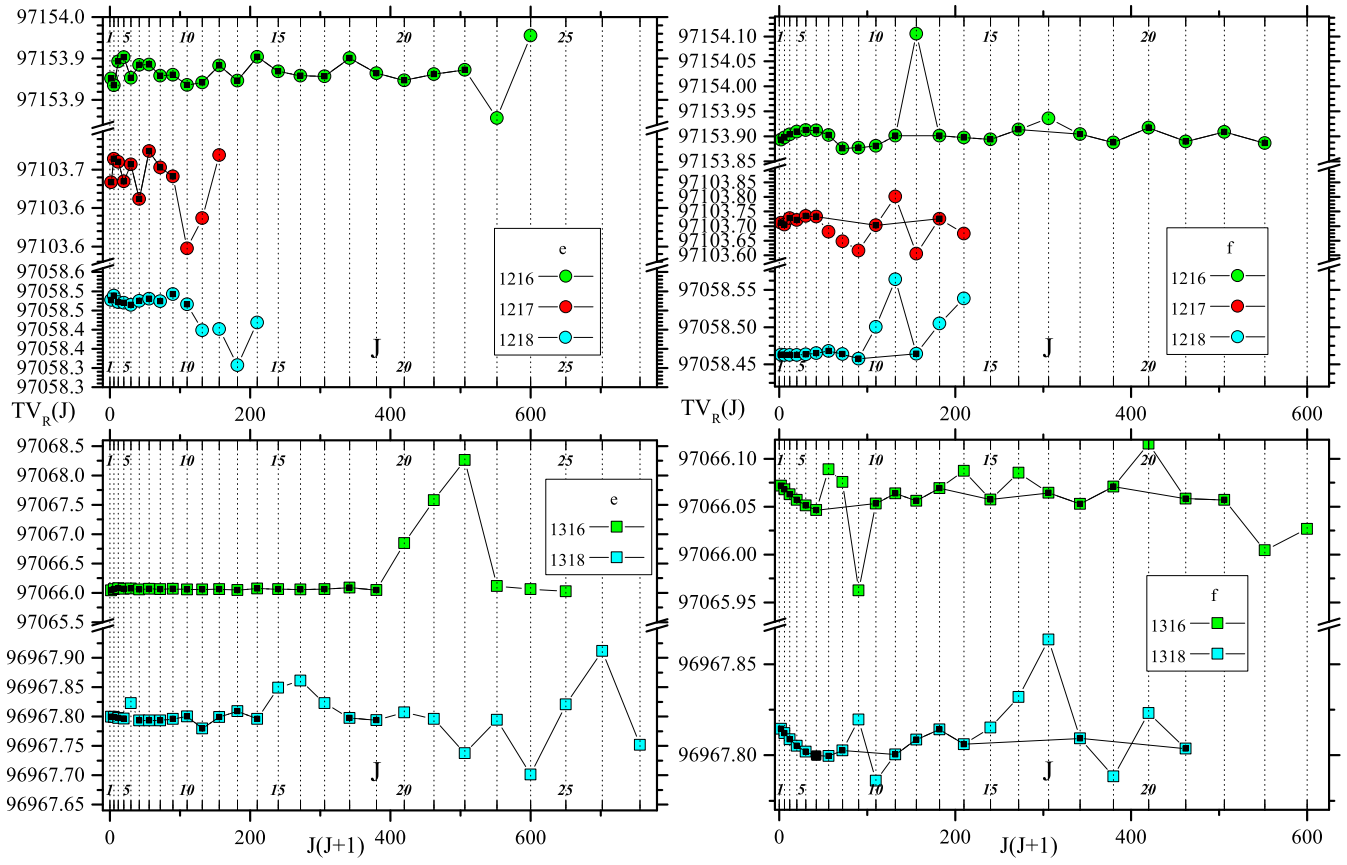

Fig. A.26. Reduced term values (cm^{-1}) of the $E^1\Pi(v'=2)$ levels for five CO isotopologues (*left*: *e*-parity and *right*: *f*-parity). Data marked with a black center are kept to calculate molecular constants.

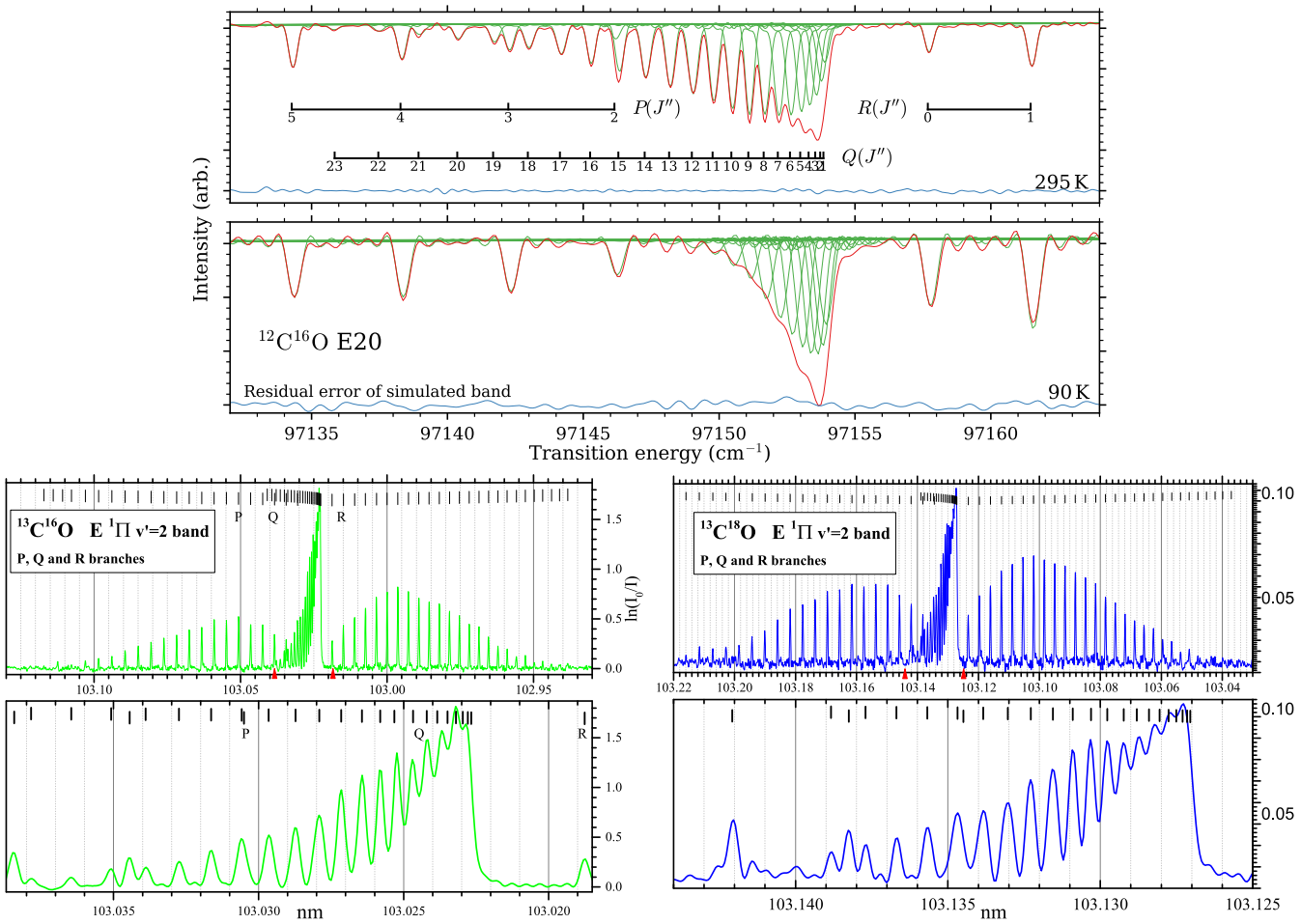

Fig. A.27. Spectra of the $E^1\Pi(v'=2)$–$X^1\Sigma^+(v''=0)$ band. *Upper panel*: Simulated absorption spectra of the Q-branch of the for $^{12}C^{16}O$ at 90 K and at room temperature. *Lower panels*: spectra of $^{13}C^{16}O$ (*left*) and $^{13}C^{18}O$ (*right*). *Lowest panel*: ×10 expanded scale on the Q-branch between the red arrows).

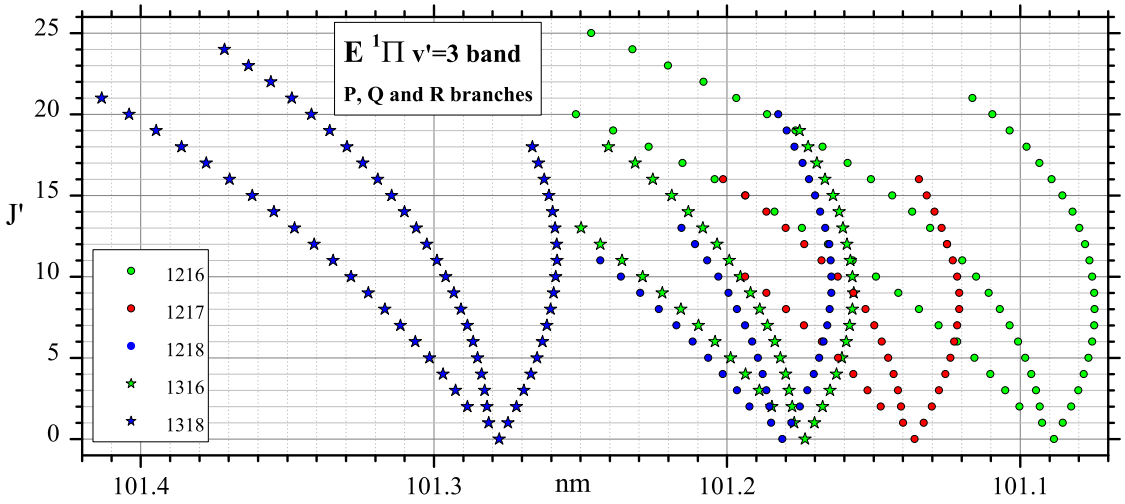

Fig. A.28. Transition wavelengths of the $E^1\Pi(v'=3)$–$X^1\Sigma^+(v''=0)$ band for the five observed CO isotopologues.

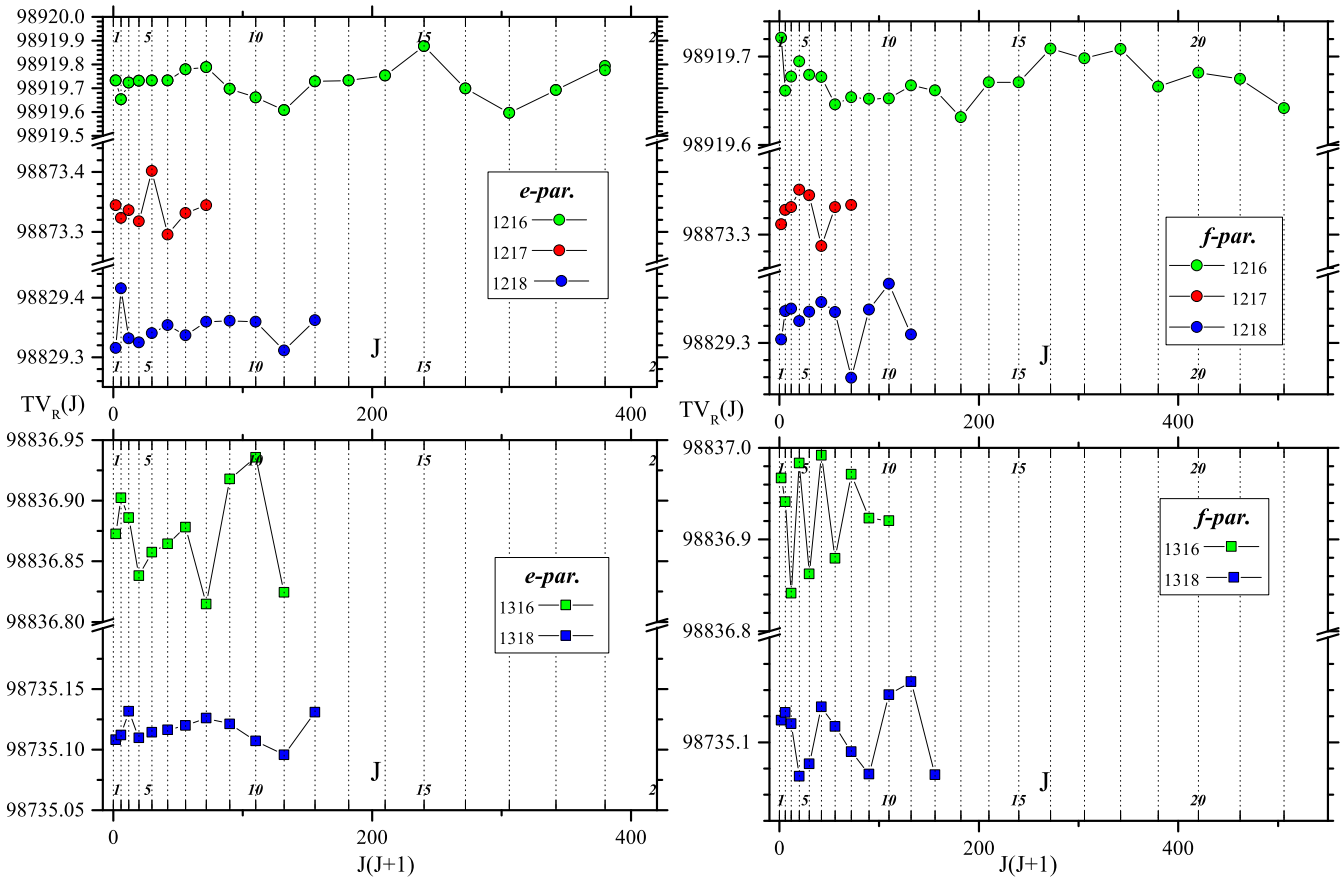

Fig. A.29. Reduced term values (cm^{-1}) of the $E^1\Pi(v'=3)$ levels for the five observed CO isotopologues (*left*: *e*-parity, and *right*: *f*-parity).

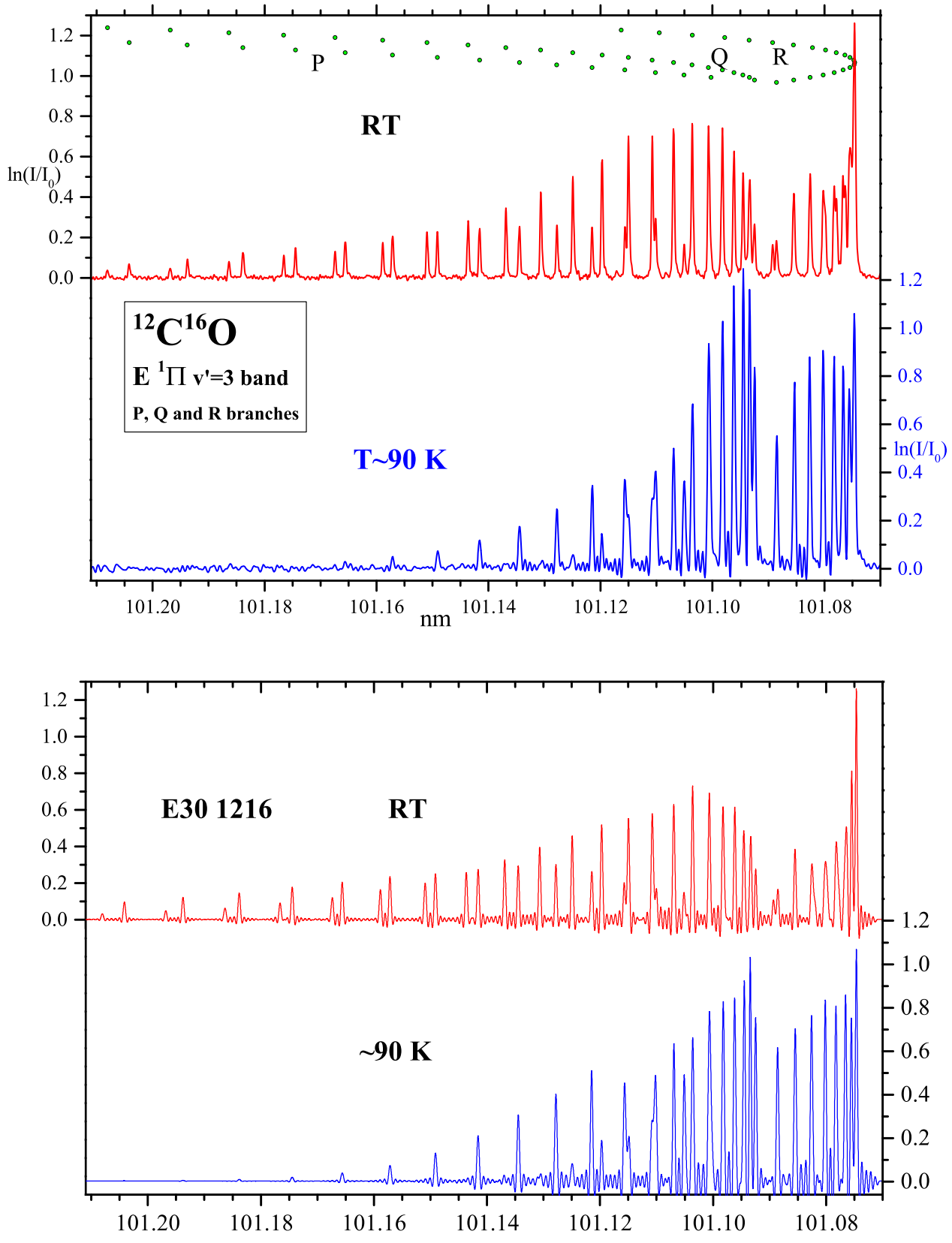

Fig. A.30. Spectra of the $E^1\Pi(v'=3)$–$X^1\Sigma^+(v''=0)$ band for $^{12}C^{16}O$ at room temperature (RT) and at ~90 K. Simulations below, in emission, of the upper experimental spectra (using classical Hönl–London factors).

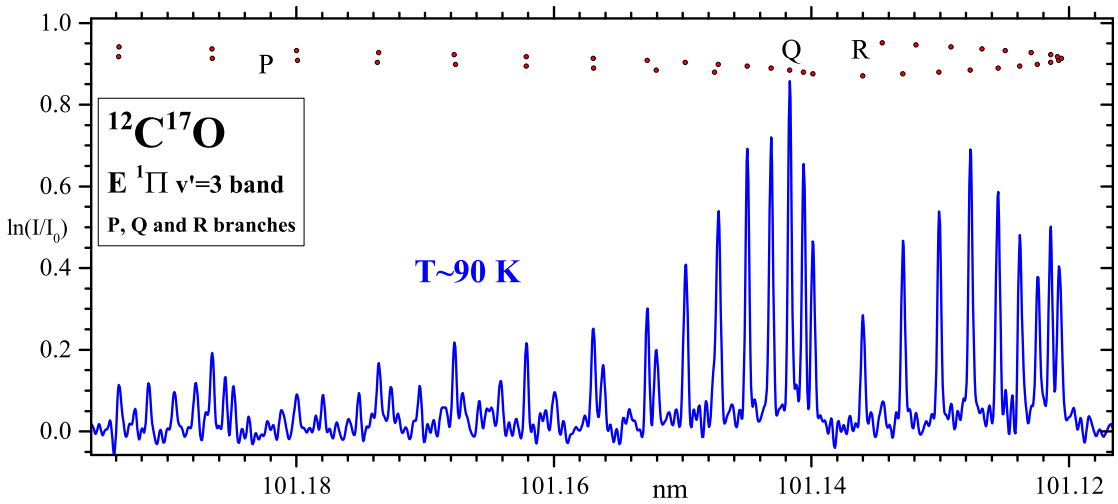

Fig. A.31. Spectra of the $E^1\Pi(v' = 3)$–$X^1\Sigma^+(v'' = 0)$ band for $^{12}C^{17}O$ at ~90 K. Traces of $^{12}C^{18}O$ are present around 101.185 nm.

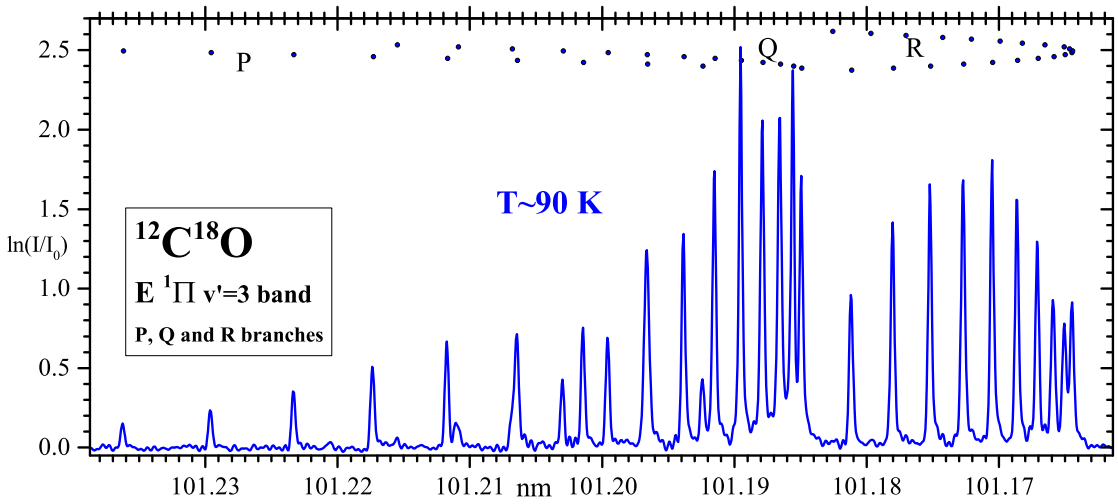

Fig. A.32. Spectra of the $E^1\Pi(v' = 3)$–$X^1\Sigma^+(v'' = 0)$ band for $^{12}C^{18}O$ at ~90 K.

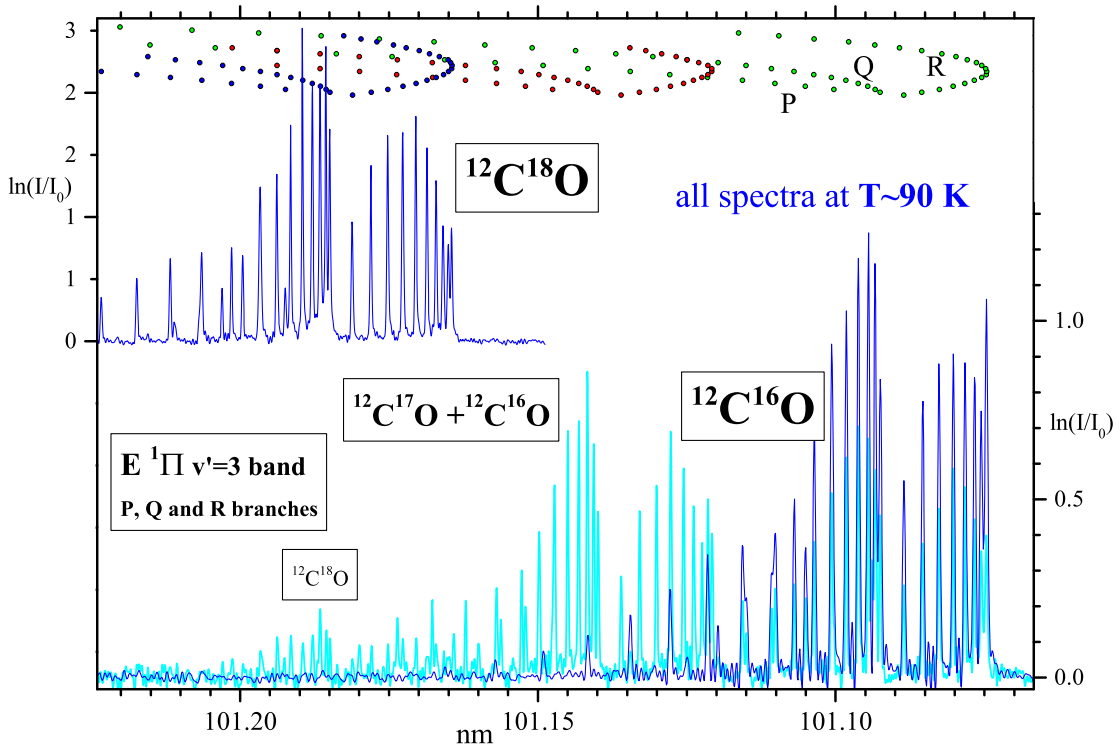

Fig. A.33. Spectra of the $E^1\Pi(v'=3)$–$X^1\Sigma^+(v''=0)$ band for $^{12}C^{16}O$, $^{12}C^{17}O$, and $^{12}C^{18}O$ at ~90 K. $^{12}C^{17}O$ is about equally mixed with $^{12}C^{16}O$, and traces of $^{12}C^{18}O$ are present.

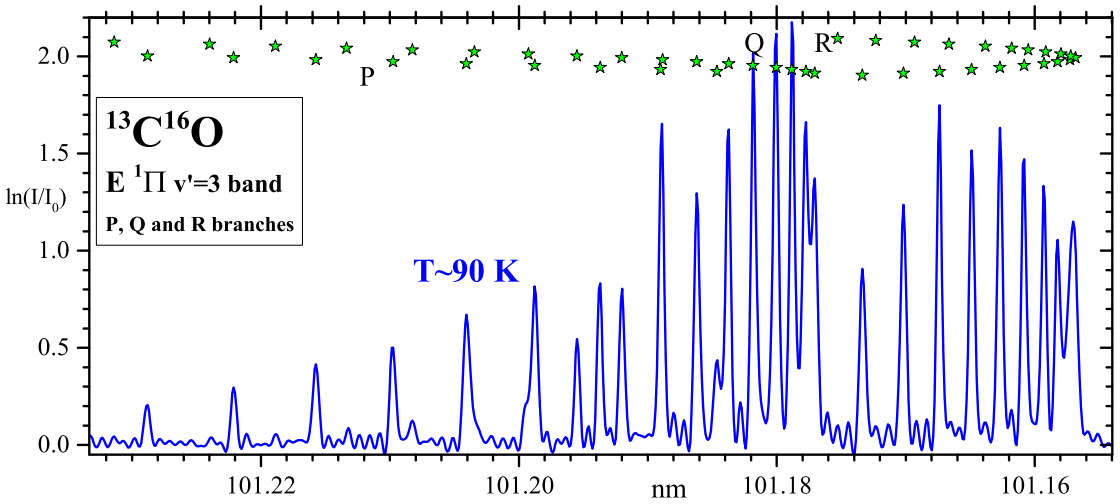

Fig. A.34. Spectrum of the $E^1\Pi(v'=3)$–$X^1\Sigma^+(v''=0)$ band for $^{13}C^{16}O$ at ~90 K.

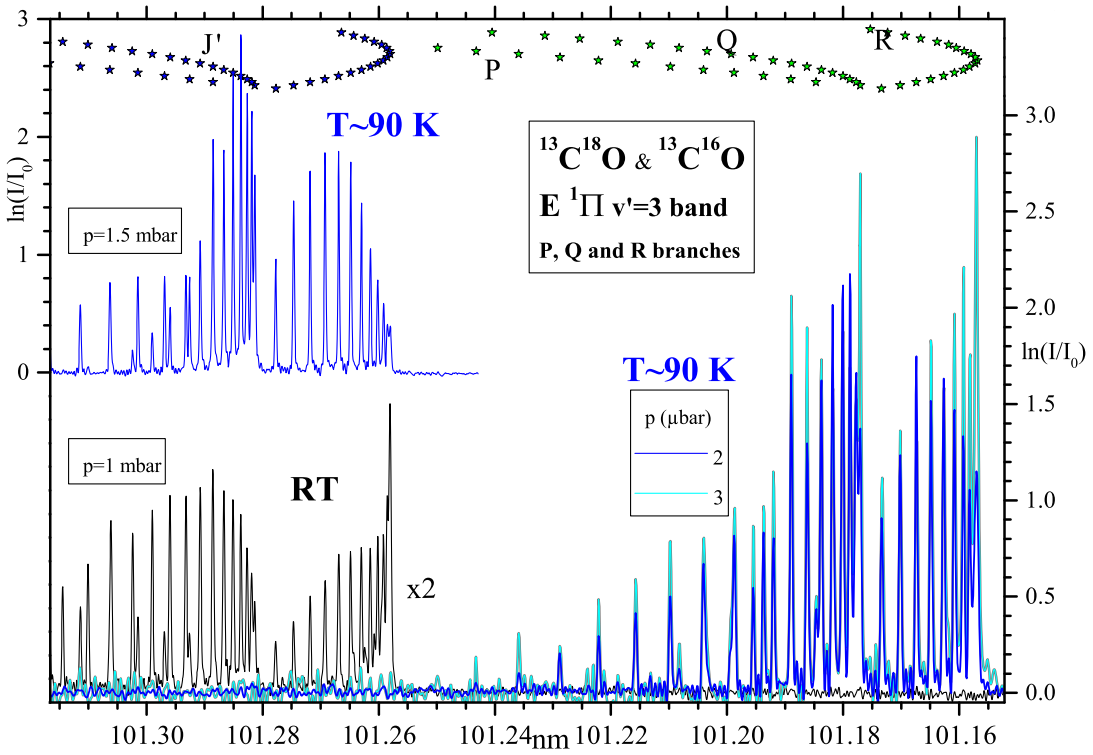

Fig. A.35. Spectra of the $E^1\Pi(v'=3)$–$X^1\Sigma^+(v''=0)$ band for $^{13}C^{16}O$ at ~90 K (at two pressures) and $^{13}C^{18}O$ at room temperature (in black) and ~90 K (with two different blues).

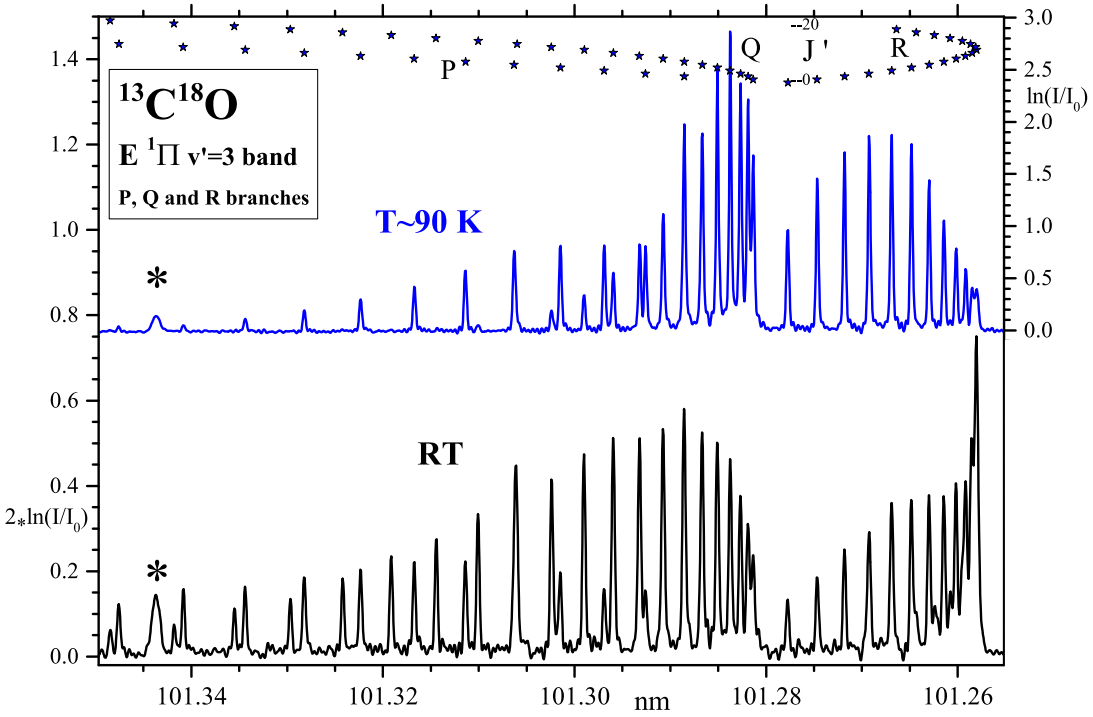

Fig. A.36. Spectra of the $E^1\Pi(v'=3)$–$X^1\Sigma^+(v''=0)$ band for $^{13}C^{18}O$ at room temperature (RT) and at ~90 K. The asterisk shows an impurity line in the gas filter.

Table A.19. Measured transition wavelengths and wavenumbers of the $E^1\Pi(v'=0)$–$X^1\Sigma^+(v''=0)$ band for $^{12}C^{16}O$, $^{12}C^{17}O$, and $^{12}C^{18}O$.

$E^1\Pi(v'=0)$–$X^1\Sigma^+(v''=0)$							
	$^{12}C^{16}O$						
J	R_{ms} (nm)	P_{ms} (nm)	R_{ms} (cm^{-1})	P_{ms} (cm^{-1})	δ_P	Q_{ms} (nm)	Q_{ms} (cm^{-1})
0	107.60335		92933.909		30		
1	107.59867		92937.954		55	107.60789	92929.988[a]
2	107.59401	107.61678	92941.976	92922.313	12	107.60775	92930.109[a]
3	107.58917	107.62106	92946.157	92918.619	17	107.60754	92930.291[a]
4	107.58424	107.62520	92950.416	92915.039	−1	107.60726	92930.532[a]
5	107.57921	107.62928	92954.762	92911.522	−6	107.60691	92930.832[a]
6	107.57410	107.63321	92959.183	92908.131	4	107.60649	92931.194[a]
7	107.56887	107.63706	92963.700	92904.801	3	107.60601	92931.616[a]
8	107.56354	107.64086	92968.305	92901.521	3	107.60545	92932.098[a]
9	107.55815	107.64453	92972.961	92898.358	−6	107.60480	92932.656
10	107.55260	107.64809	92977.759	92895.285	−1	107.60409	92933.268
11	107.54706	107.65157	92982.554	92892.285	−19	107.60331	92933.942
12	107.54134	107.65491	92987.495	92889.399	−7	107.60253	92934.616
13	107.53555	107.65820	92992.505	92886.561	5	107.60161	92935.417
14	107.52967	107.66138	92997.585	92883.814	−4	107.60066	92936.233
15	107.52367	107.66449	93002.782	92881.139	−1	107.59959	92937.157
16	107.51763	107.66745	93008.004	92878.579	−5	107.59838	92938.207
17	107.51145	107.67031	93013.348	92876.118	−3	107.59730	92939.134
18	107.50522	107.67311	93018.740	92873.700	15	107.59603	92940.232
19	107.49886	107.67578	93024.240	92871.397	18	107.59476	92941.330
20	107.49245	107.67842	93029.793	92869.116	−2	107.59329	92942.601
21	107.48592	107.68090	93035.440	92866.979	6	107.59192	92943.779
22	107.47935	107.68326	93041.133	92864.947	−13	107.59038	92945.111
23	107.47263	107.68556	93046.945	92862.960	−14	107.58869	92946.572
24	107.46583	107.68775	93052.831	92861.076	1	107.58711	92947.935
25	107.45898	107.68982	93058.762	92859.286	−5	107.58541	92949.408
26	107.45200	107.69184	93064.814	92857.544	9	107.58363	92950.943
27	107.44493	107.69376	93070.932	92855.895	2	107.58177	92952.549
28	107.43781	107.69556	93077.101	92854.336	8	107.58000	92954.083
29	107.43061	107.69724	93083.341	92852.893	−8	107.57782	92955.961
30	107.42264	107.69887	93090.243	92851.483	*		
31	107.41584	107.70036	93096.144	92850.198	*		
32	107.40839	107.70307	93102.593	92847.867			
33	107.40082	107.70427	93109.158	92846.831			
34	107.39310		93115.848				
	$^{12}C^{17}O$						
0	107.60371		92933.596		21		
1	107.59922		92937.478		19	107.60821	92929.714[e]
2	107.59460	107.61678	92941.469	92922.310	40	107.60807	92929.831[e]
3	107.58986	107.62096	92945.563	92918.701	8	107.60787	92930.006[e]
4	107.58509	107.62507	92949.679	92915.156	1	107.60760	92930.241[e]
5	107.58018	107.62893	92953.925	92911.820	2	107.60726	92930.536[e]
6	107.57519	107.63283	92958.234	92908.459	19	107.60684	92930.893[e]
7	107.57011	107.63659	92962.629	92905.211	1	107.60636	92931.311[e]
8	107.56492	107.64031	92967.111	92901.998	1	107.60580	92931.794[e]
9	107.55967	107.64385	92971.654	92898.942	−15	107.60517	92932.341
10	107.55431	107.64733	92976.282	92895.938	−10	107.60448	92932.931
11	107.54886	107.65070	92980.997	92893.032	−11	107.60376	92933.555
12	107.54328	107.65402	92985.817	92890.170	−3	107.60290	92934.301
13	107.53763	107.65721	92990.702	92887.413	−1	107.60202	92935.060
14	107.53193	107.66031	92995.630	92884.743	2	107.60104	92935.906
15	107.52614	107.66331	93000.646	92882.157	−2	107.60003	92936.781
16	107.52021	107.66625	93005.767	92879.615	−3	107.59917	92937.516
17	107.51422	107.66908	93010.952	92877.178	−2	107.59781	92938.691
18	107.50813	107.67178	93016.219	92874.846	−1	107.59659	92939.747
19	107.50198	107.67441	93021.547	92872.578	−8	107.59525	92940.908
20	107.49569	107.67694	93026.986	92870.397	12	107.59397	92942.010
21	107.48934	107.67937	93032.483	92868.300	21	107.59251	92943.269
22	107.48293	107.68173	93038.029	92866.264	3	107.59105	92944.536
23	107.47641	107.68399	93043.670	92864.314	−33	107.58923	92946.109
24	107.46983	107.68613	93049.368	92862.473	21	107.58790	92947.259
25	107.46316	107.68810	93055.144	92860.773	*	107.58628	92948.659
26	107.45625	107.69021	93061.134	92858.953	*		
27	107.44929	107.69267	93067.160	92856.831	*	107.58321	92951.304
28		107.69453		92855.225			
29		107.69638		92853.634			
	$^{12}C^{18}O$						
0	107.60400		92933.352		27		
1	107.59955		92937.192		55	107.60836	92929.585[e]
2	107.59511	107.61678	92941.031	92922.312	17	107.60822	92929.706[e]
3	107.59052	107.62088	92944.996	92918.772	3	107.60801	92929.887[e]
4	107.58584	107.62483	92949.035	92915.365	−2	107.60773	92930.126[e]
5	107.58106	107.62868	92953.167	92912.037	0	107.60739	92930.419[e]
6	107.57616	107.63247	92957.396	92908.765	−3	107.60699	92930.764[e]
7	107.57119	107.63617	92961.697	92905.573	5	107.60654	92931.157[e]
8	107.56615	107.63974	92966.048	92902.491	0	107.60602	92931.607[e]
9	107.56100	107.64325	92970.497	92899.461	−9	107.60543	92932.116
10	107.55577	107.64667	92975.020	92896.510	−7	107.60473	92932.722
11	107.55046	107.64997	92979.611	92893.665	−11	107.60397	92933.372
12	107.54503	107.65320	92984.303	92890.876	−2	107.60321	92934.028
13	107.53955	107.65634	92989.044	92888.170	−7	107.60235	92934.775
14	107.53393	107.65938	92993.904	92885.544	11	107.60143	92935.572
15	107.52828	107.66233	92998.790	92882.997	1	107.60042	92936.445
16	107.52252	107.66519	93003.776	92880.528	4	107.59934	92937.375
17	107.51670	107.66796	93008.808	92878.143	−9	107.59827	92938.302
18	107.51074	107.67063	93013.963	92875.837	3	107.59706	92939.341
19	107.50473	107.67321	93019.164	92873.614	1	107.59580	92940.430
20	107.49860	107.67569	93024.466	92871.470	−4	107.59443	92941.612
21	107.49242	107.67809	93029.814	92869.405	−8	107.59309	92942.772
22	107.48616	107.68035	93035.238	92867.451	−11	107.59162	92944.045
23	107.47978	107.68256	93040.760	92865.549	−3	107.58998	92945.456
24	107.47337	107.68468	93046.306	92863.725	−5	107.58853	92946.713
25	107.46683	107.68669	93051.971	92861.983	−1	107.58688	92948.140
26	107.46014	107.68865	93057.762	92860.293	−8	107.58506	92949.710
27	107.45351	107.69048	93063.499	92858.715	0	107.58360	92950.973
28	107.44672	107.69213	93069.388	92857.294	−4	107.58251	92951.910
29	107.43989	107.69387	93075.298	92855.794	−7	107.58105	92953.173
30	107.43292	107.69540	93081.335	92854.479	3	107.57945	92954.554
31	107.42591	107.69689	93087.414	92853.193	−17	107.57778	92955.999
32	107.41878	107.69826	93093.596	92852.013	33		
33	107.41161	107.69950	93099.802	92850.943			
34	107.40443	107.70077	93106.030	92849.846			

Notes. Column description (see also Sect. 2.2) for each isotopologue. Col. 1: J. Cols. 2 and 3: R_{ms} and P_{ms} wavelengths (nm). Cols. 4 and 5: R_{ms} and P_{ms} wavenumbers (cm^{-1}). Col. 6: δ_P wavenumber corrections applied to TV$_P$ in units of the least significant digit ($-\delta_P$ is applied to TV$_R$). No value means no measurement for one of the branches, either R or P. An asterisk indicates, when both R- and P-branches are present at high J', either the potential presence of a perturbing state or that one of the lines shows a larger uncertainty than the other. Cols. 7 and 8: Q_{ms} Q-branch wavelengths and wavenumbers. [(a)] Data from Cacciani & Ubachs (2004). [(e)] Data calculated from the e-parity levels.

Table A.20. Measured transition wavelengths and wavenumbers of the $E^1\Pi(v'=0)$–$X^1\Sigma^+(v''=0)$ band for $^{13}C^{16}O$, $^{13}C^{17}O$, and $^{13}C^{18}O$ (same column description as for Table A.19).

$E^1\Pi(v'=0)$–$X^1\Sigma^+(v''=0)$							
	$^{13}C^{16}O$						
J	R_{ms} (nm)	P_{ms} (nm)	R_{ms} (cm^{-1})	P_{ms} (cm^{-1})	δ_P	Q_{ms} (nm)	Q_{ms} (cm^{-1})
0	107.60376		92933.553		23		
1	107.59926		92937.440		68	107.60810	92929.804[a]
2	107.59482	107.61659	92941.275	92922.479	27	107.60797	92929.918[a]
3	107.59023	107.62070	92945.241	92918.925	−13	107.60777	92930.092[a]
4	107.58552	107.62468	92949.311	92915.492	3	107.60750	92930.323[a]
5	107.58070	107.62851	92953.476	92912.187	0	107.60717	92930.610[a]
6	107.57584	107.63234	92957.679	92908.877	−3	107.60677	92930.956[a]
7	107.57084	107.63602	92961.993	92905.701	−7	107.60630	92931.358[a]
8	107.56577	107.63966	92966.379	92902.565	4	107.60584	92931.763
9	107.56060	107.64316	92970.843	92899.543	−8	107.60518	92932.327
10	107.55535	107.64661	92975.381	92896.567	−4	107.60447	92932.942
11	107.54998	107.64991	92980.029	92893.715	20	107.60376	92933.557
12	107.54459	107.65316	92984.687	92890.910	−14	107.60299	92934.217
13	107.53905	107.65633	92989.481	92888.178	0	107.60209	92935.000
14	107.53343	107.65934	92994.338	92885.575	8	107.60117	92935.794
15	107.52774	107.66231	92999.260	92883.016	−13	107.60018	92936.650
16	107.52191	107.66519	93004.302	92880.535	27	107.59905	92937.628
17	107.51609	107.66791	93009.337	92878.182	7	107.59802	92938.514
18	107.51012	107.67064	93014.503	92875.829	23	107.59679	92939.579
19	107.50409	107.67323	93019.715	92873.598	23	107.59553	92940.661
20	107.49793	107.67574	93025.050	92871.427	22	107.59411	92941.891
21	107.49172	107.67816	93030.424	92869.342	28	107.59282	92943.003
22	107.48546	107.68043	93035.838	92867.385	−5	107.59148	92944.160
23	107.47906	107.68266	93041.382	92865.460	8	107.58987	92945.551
24	107.47261	107.68475	93046.965	92863.660	1	107.58820	92946.995
25	107.46605	107.68679	93052.640	92861.903	6	107.58637	92948.576
26	107.45931	107.68873	93058.477	92860.232	0		
27	107.45267	107.69058	93064.230	92858.636	5		
28	107.44588	107.69221	93070.108	92857.231	0		
29	107.43899	107.69395	93076.076	92855.727	14		
30	107.43201	107.69552	93082.124	92854.375	−2		
31	107.42497	107.69702	93088.224	92853.084	12		
32	107.41786	107.69834	93094.389	92851.942	−2		
33	107.41063	107.69967	93100.652	92850.799	−2		
34	107.40336	107.70084	93106.955	92849.785	11		
35	107.39595	107.70192	93113.383	92848.853	38		
36	107.38854	107.70298	93119.810	92847.940	−2		
37	107.38103	107.70392	93126.323	92847.136	58		
38	107.37346	107.70468	93132.882	92846.474			
39	107.36595	107.70557	93139.398	92845.709			
40	107.35877		93145.628				
	$^{13}C^{17}O$						
0							
1	107.59949		92937.243				
2	107.59504		92941.084				
3	107.59047		92945.036				
4	107.58645		92948.504		*		
5	107.58150		92952.785		*		
6	107.57715	107.63162	92956.546	92909.503	*		
7	107.57217	107.63505	92960.847	92906.536	−56		
8	107.56722	107.63901	92965.127	92903.125	−36		
9	107.56219	107.64246	92969.472	92900.146	−12		
10	107.55707	107.64583	92973.894	92897.238	−4		
11	107.55184	107.64913	92978.418	92894.390	12		
12	107.54657	107.65230	92982.973	92891.654	−4		
13	107.54120	107.65537	92987.614	92889.007	1		
14	107.53574	107.65832	92992.343	92886.459	3		
15	107.53022	107.66122	92997.115	92883.958	−2		
16	107.52458	107.66401	93001.993	92881.553	−1	107.59949	92937.247
17	107.51889	107.66672	93006.917	92879.208	4	107.59832	92938.251
18	107.51307	107.66932	93011.949	92876.965	8	107.59717	92939.246
19	107.50721	107.67188	93017.015	92874.763	2		
20	107.50127	107.67430	93022.154	92872.674	−16		
21	107.49522	107.67665	93027.391	92870.646	−22		
22	107.48910	107.67888	93032.686	92868.720			
23	107.48290	107.68103	93038.060	92866.871			
24	107.47664		93043.472				
25	107.47028		93048.979				
26	107.46373		93054.650				
	$^{13}C^{18}O$						
0	107.60441		92932.991		−19		
1	107.60012		92936.696		26	107.60856	92929.407[a]
2	107.59601	107.61650	92940.247	92922.550	22	107.60844	92929.516[a]
3	107.59165	107.62041	92944.020	92919.180	*	107.60825	92929.681[a]
4	107.58719	107.62438	92947.871	92915.754	*	107.60799	92929.902[a]
5	107.58258	107.62854	92951.852	92912.160	*	107.60767	92930.175[a]
6	107.57793	107.63231	92955.869	92908.903	*	107.60729	92930.504[a]
7	107.57319	107.63544	92959.963	92906.207	66	107.60685	92930.888[a]
8	107.56841	107.63888	92964.094	92903.230	76	107.60638	92931.291
9	107.56350	107.64207	92968.338	92900.478	31	107.60578	92931.809
10	107.55853	107.64539	92972.639	92897.613	16	107.60516	92932.348
11	107.55345	107.64845	92977.030	92894.973	19	107.60450	92932.917
12	107.54836	107.65151	92981.424	92892.334	−3	107.60370	92933.609
13	107.54305	107.65450	92986.015	92889.750	19	107.60286	92934.331
14	107.53773	107.65743	92990.620	92887.223	22	107.60200	92935.072
15	107.53234	107.66023	92995.282	92884.808	−1	107.60102	92935.925
16	107.52688	107.66297	93000.000	92882.449	6	107.60013	92936.688
17	107.52130	107.66557	93004.830	92880.203	15	107.59892	92937.735
18	107.51565	107.66817	93009.715	92877.957	26	107.59778	92938.722
19	107.50994	107.67065	93014.658	92875.823	11	107.59665	92939.697
20	107.50410	107.67306	93019.712	92873.744	27	107.59539	92940.786
21	107.49825	107.67534	93024.768	92871.778	−10	107.59396	92942.020
22	107.49230	107.67755	93029.921	92869.868	−17	107.59262	92943.178
23	107.48626	107.67963	93035.144	92868.072	−21	107.59102	92944.557
24	107.48010	107.68167	93040.480	92866.318	6	107.58943	92945.938
25	107.47394	107.68362	93045.815	92864.633	8	107.58782	92947.324
26	107.46758	107.68551	93051.319	92863.004	14	107.58586	92949.017
27	107.46122	107.68733	93056.824	92861.432	−6		
28	107.45480	107.68896	93062.384	92860.027	6		
29	107.44825	107.69053	93068.057	92858.679	6		
30	107.44170	107.69209	93073.734	92857.331	−1		
31	107.43503	107.69348	93079.514	92856.129	11		
32	107.42816	107.69485	93085.459	92854.951	58		
33	107.42148	107.69613	93091.251	92853.845	0		
34	107.41462	107.69730	93097.193	92852.841	−8		
35	107.40780	107.69838	93103.107	92851.904	−60		
36	107.40033	107.69940	93109.581	92851.025	91		
37	107.39327	107.70034	93115.701	92850.214	54		
38	107.38606	107.70110	93121.953	92849.564	93		
39	107.37894	107.70181	93128.133	92848.949			
40	107.37238	107.70254	93133.825	92848.319			

Notes. [a] Data from Cacciani & Ubachs (2004) (same column description as for Table A.19).

Table A.21. Term values (cm^{-1}) of the $E^1\Pi(v'=0)$ e- and f-parity levels for six CO isotopologues.

	$E^1\Pi(v'=0)$																	
	$^{12}C^{16}O$			$^{12}C^{17}O$			$^{12}C^{18}O$			$^{13}C^{16}O$			$^{13}C^{17}O$			$^{13}C^{18}O$		
J'	e-par. ($R\&P$)	f-par. (Q)	Λ_d	e-par. ($R\&P$)	f-par. (Q)	Λ_d	e-par. ($R\&P$)	f-par. (Q)	Λ_d	e-par. ($R\&P$)	f-par. (Q)	Λ_d	e-par. ($R\&P$)	f-par. (Q)	Λ_d	e-par. ($R\&P$)	f-par. (Q)	Λ_d
1	92933.878 (30)	92933.833[a]	0.045	92933.575 (21)	92933.462[e]	0.113	92933.325 (27)	92933.247[e]	0.077	92933.530 (23)	92933.480[a]	0.050				92933.010 (−19)	92932.900[a]	0.110
2	92941.744 (55)	92941.644[a]	0.100	92941.207 (19)	92941.075[e]	0.132	92940.798 (55)	92940.692[e]	0.106	92941.048 (68)	92940.946[a]	0.102	92940.821			92940.163 (26)	92939.994[a]	0.168
3	92953.499 (12)	92953.360[a]	0.139	92952.673 (40)	92952.493[e]	0.180	92952.000 (17)	92951.858[e]	0.142	92952.276 (27)	92952.147[a]	0.129	92951.820			92950.703 (22)	92950.637[a]	0.066
4	92969.209 (17)	92968.980[a]	0.229	92968.042 (8)	92967.718[e]	0.324	92966.964 (3)	92966.743[e]	0.221	92967.309 (−13)	92967.080[a]	0.229	92966.508			92964.762 (*)	92964.828[a]	−0.066
5	92988.865 (−1)	92988.502[a]	0.363	92987.156 (1)	92986.750[e]	0.406	92985.655 (−2)	92985.343[e]	0.311	92986.065 (3)	92985.744[a]	0.321	92984.470 (*)			92982.520 (*)	92982.563[a]	−0.043
6	93012.438 (−6)	93011.929[a]	0.508	93010.137 (2)	93009.589[e]	0.547	93008.091 (0)	93007.656[e]	0.435	93008.610 (0)	93008.141[a]	0.469	93006.594 (*)			93004.115 (125)	93003.844[a]	0.271
7	93039.915 (4)	93039.258[a]	0.657	93036.912 (19)	93036.235[e]	0.677	93034.290 (−3)	93033.675[e]	0.616	93034.867 (−3)	93034.267[a]	0.600	93031.813 (121)			93029.077 (*)	93028.671[a]	0.406
8	93071.339 (3)	93070.488[a]	0.851	93067.553 (1)	93066.689[e]	0.863	93064.209 (5)	93063.409[e]	0.800	93064.908 (−7)	93064.068	0.840	93061.093 (−56)			93057.680 (66)	93057.006	0.674
9	93106.692 (3)	93105.634	1.058	93102.005 (1)	93100.951	1.054	93097.850 (0)	93096.859	0.991	93098.680 (4)	93097.699	0.981	93093.972 (−36)			93089.733 (76)	93088.945	0.788
10	93145.946 (−6)	93144.672	1.274	93140.279 (−15)	93138.997	1.282	93135.249 (−9)	93134.063	1.186	93136.223 (−8)	93135.052	1.171	93130.487 (−12)			93125.443 (31)	93124.392	1.051
11	93189.164 (−1)	93187.609	1.555	93182.357 (−10)	93180.817	1.540	93176.368 (−7)	93174.965	1.403	93177.494 (−4)	93176.072	1.422	93170.667 (−4)			93164.667 (16)	93163.355	1.312
12	93236.240 (−19)	93234.382	1.858	93228.270 (−11)	93226.498	1.773	93221.214 (−11)	93219.526	1.688	93222.524 (20)	93220.805	1.719	93214.514 (12)			93207.449 (19)	93205.926	1.523
13	93287.268 (−7)	93285.114	2.154	93278.016 (−3)	93275.929	2.087	93269.803 (−2)	93267.830	1.973	93271.289 (−14)	93269.325	1.964	93261.994 (−4)			93253.743 (−3)	93252.010	1.733
14	93342.198 (5)	93339.694	2.504	93331.572 (−1)	93329.181	2.391	93322.106 (−7)	93319.833	2.272	93323.807 (0)	93321.522	2.285	93313.108 (1)			93303.675 (19)	93301.595	2.079
15	93401.050 (−4)	93398.212	2.839	93388.904 (2)	93386.198	2.707	93378.155 (11)	93375.560	2.595	93380.058 (8)	93377.441	2.617	93367.880 (3)			93357.121 (22)	93354.773	2.348
16	93463.838 (−1)	93460.682	3.156	93450.064 (−2)	93446.804	3.260	93437.905 (1)	93434.991	2.914	93440.065 (−13)	93437.142	2.922	93426.266 (−2)	93423.571	2.695	93414.130 (−1)	93411.338	2.793
17	93530.484 (−5)	93526.855	3.629	93515.058 (−3)	93511.579	3.479	93501.388 (4)	93498.062	3.326	93503.789 (27)	93500.410	3.379	93488.318 (−1)	93485.311	3.007	93474.644 (6)	93471.663	2.980
18	93601.072 (−3)	93597.021	4.050	93583.842 (−2)	93579.962	3.880	93568.577 (−9)	93564.887	3.690	93571.227 (7)	93567.511	3.715	93553.973 (4)	93550.600	3.373	93538.743 (15)	93535.404	3.340
19	93675.514 (15)	93671.007	4.507	93656.435 (−1)	93652.174	4.261	93639.506 (3)	93635.401	4.105	93642.412 (23)	93638.282	4.130	93623.295 (8)			93606.371 (26)	93602.603	3.768
20	93753.899 (18)	93748.983	4.916	93732.822 (−8)	93728.049	4.773	93714.135 (1)	93709.645	4.490	93717.314 (23)	93712.853	4.461	93696.218 (2)			93677.553 (11)	93673.387	4.166
21	93836.178 (−2)	93830.681	5.496	93813.013 (12)	93807.799	5.214	93792.503 (−4)	93787.501	5.002	93795.989 (22)	93790.953	5.036	93772.782 (−16)			93752.286 (27)	93747.784	4.503
22	93922.337 (6)	93916.344	5.993	93896.992 (21)	93891.273	5.719	93874.551 (−8)	93869.101	5.450	93878.345 (28)	93872.742	5.603	93852.983 (−22)			93830.541 (−10)	93825.568	4.973
23	94012.379 (−13)	94005.944	6.435	93984.762 (3)	93978.765	5.997	93960.305 (−11)	93954.467	5.838	93964.425 (−5)	93958.408	6.018	93936.765			93912.329 (−17)	93907.037	5.292
24	94106.331 (−14)	94099.250	7.081	94076.360 (−33)	94069.544	6.816	94049.774 (−3)	94043.304	6.470	94054.231 (8)	94047.766	6.465	94024.193			93997.645 (−21)	93991.966	5.679
25	94204.145 (1)	94196.467	7.678	94171.633 (21)	94164.280	7.353	94142.903 (−5)	94135.934	6.969	94147.735 (1)	94140.896	6.839	94115.203			94086.502 (6)	94080.358	6.144
26	94305.826 (−5)	94297.544	8.282	94270.495 (*)			94239.766 (−1)	94232.325	7.441	94244.954 (6)			94209.849			94178.841 (8)	94172.509	6.332
27	94411.406 (9)	94402.485	8.921	94373.422 (*)	94364.698	8.723	94340.385 (−8)	94332.024	8.361	94345.979 (0)			94308.197			94274.798 (14)		
28	94520.866 (2)	94511.144	9.722	94480.069 (*)			94444.550 (0)	94435.010	9.540	94450.537 (5)						94374.230 (−6)		
29	94634.154 (8)	94623.932	10.222				94552.491 (−4)	94541.928	10.563	94558.855 (0)						94477.134 (6)		
30	94751.320 (−8)						94664.061 (−7)	94652.570	11.491	94670.867 (14)						94583.607 (6)		
31	94872.072 (*)						94779.347 (3)	94766.874	12.473	94786.606 (−2)						94693.532 (−1)		
32	94996.743 (*)						94898.307 (−17)			94905.981 (12)						94806.976 (11)		
33	95125.965						95020.894 (33)			95029.057 (−2)						94923.983 (58)		
34	95258.538						95147.182			95155.825 (−2)						95044.372 (0)		
35	95395.000						95277.045			95286.218 (11)						95168.285 (−8)		
36										95420.319 (38)						95295.635 (−60)		
37										95558.078 (−2)						95426.758 (91)		
38										95699.410 (58)						95561.129 (54)		
39										95844.488						95698.962 (93)		
40										95993.041						95840.259		
41										96144.880						95984.375		

Notes. The δ_P value in parentheses (in units of the least significant digit) corresponds to the wavenumber correction applied to TV_P and TV_R. There is no value when the term value is derived from a single transition, either R or P. An asterisk indicates when both R- and P-branches are present at high J', either the potential presence of a perturbing state or that one of the lines shows a larger uncertainty than the other (see also Sect. 2.2.2). Each third column is the Λ-type doubling (cm^{-1}) of the $^1\Pi$ state: $\Lambda_d = TV_{R\&P} - TV_Q$. [(a)] Data from Cacciani & Ubachs (2004). [(*)] Data calculated from the e-parity levels.

Table A.22. Measured transition wavelengths and wavenumbers of the $E^1\Pi(v'=1)$–$X^1\Sigma^+(v''=0)$ band for $^{12}C^{16}O$, $^{12}C^{17}O$, and $^{12}C^{18}O$ (same column description as for Table A.19).

$E^1\Pi(v'=1)$–$X^1\Sigma^+(v''=0)$							
	$^{12}C^{16}O$						
J	R_{ms} (nm)	P_{ms} (nm)	R_{ms} (cm^{-1})	P_{ms} (cm^{-1})	δ_P	Q_{ms} (nm)	Q_{ms} (cm^{-1})
0	105.16712		95086.757		−11		
1	105.16277		95090.688		20	105.17156	95082.741[b]
2	105.15842	105.17985	95094.620	95075.244	−5	105.17145	95082.841[b]
3	105.15401	105.18408	95098.607	95071.424	26	105.17129	95082.987[b]
4	105.14960	105.18818	95102.595	95067.718	2	105.17138	95082.898[b]
5	105.14513	105.19234	95106.639	95063.954	6	105.17123	95083.036[b]
6	105.14016	105.19638	95111.132	95060.305	69	105.17133	95082.951[b]
7	105.13607	105.20042	95114.839	95056.654	19	105.17065	95083.564[b]
8	105.13178	105.20409	95118.714	95053.340	−1	105.17100	95083.249[b,u]
9	105.12651	105.20838	95123.488	95049.465	37	105.17115	95083.108[b]
10	105.12216	105.21254	95127.420	95045.702	−8	105.17048	95083.718[b,u]
11	105.11726	105.21584	95131.857	95042.726	−80	105.17060	95083.607[b,u]
12	105.11267	105.21988	95136.013	95039.074	−9	105.17018	95083.991[b]
13	105.10795	105.22330	95140.281	95035.985	8	105.17023	95083.938[b,u]
14	105.10324	105.22734	95144.549	95032.335	−2	105.17012	95084.042[b,u]
15	105.09840	105.23114	95148.930	95028.909	19	105.17004	95084.116[b,u]
16	105.09356	105.23487	95153.311	95025.540	14	105.16980	95084.331[b,u]
17	105.08872	105.23854	95157.692	95022.226	−16	105.16968	95084.442[b,u]
18	105.08382	105.24214	95162.129	95018.968	−15	105.16943	95084.664[b,u]
19	105.07886	105.24569	95166.622	95015.767	16	105.16922	95084.853[b,u]
20	105.07390	105.24924	95171.115	95012.565	−5	105.16904	95085.018[b,u]
21	105.06894	105.25278	95175.608	95009.364	−24	105.16886	95085.176[b,u]
22	105.06392	105.25621	95180.157	95006.275	−11		
23	105.05883	105.25963	95184.762	95003.186	5		
24	105.05381	105.26305	95189.311	95000.097	−31		
25	105.04867	105.26641	95193.973	94997.064	77		
26	105.04358	105.26971	95198.579	94994.087	*		
27	105.03844	105.27319	95203.240	94990.942	*		
28	105.03317	105.27687	95208.014	94987.628	*		
29	105.02804	105.28042	95212.665	94984.427	*		
30	105.02280	105.28396	95217.416	94981.226	*		
31		105.28745		94978.081			
32		105.29094		94974.936			
33		105.29437		94971.836			
34		105.29780		94968.743			
35		105.30108		94965.791			
36		105.30449		94962.708			
	$^{12}C^{17}O$						
0	105.19698		95059.762		−1		
1	105.19279		95063.545		−11	105.20115	95055.999[u]
2	105.18855	105.20942	95067.381	95048.522	−2	105.20111	95056.030[u]
3	105.18425	105.21351	95071.271	95044.828	13	105.20116	95055.989[e]
4	105.18008	105.21758	95075.037	95041.151	−4	105.20094	95056.184[e]
5	105.17557	105.22160	95079.115	95037.518	−1	105.20094	95056.188[e]
6	105.17126	105.22569	95083.007	95033.825	2	105.20128	95055.882[e]
7	105.16744	105.22948	95086.466	95030.408	4	105.20031	95056.754[e]
8	105.16198	105.23347	95091.405	95026.804	−7	105.20038	95056.693[e]
9	105.15765	105.23793	95095.312	95022.772	7	105.19994	95057.086[e]
10	105.15291	105.24073	95099.599	95020.248	10	105.20001	95057.023[e]
11	105.14848	105.24472	95103.611	95016.645	3	105.19988	95057.147[e]
12	105.14389	105.24826	95107.760	95013.447	17	105.19971	95057.297[e]
13	105.13929	105.25208	95111.926	95009.998	13	105.19953	95057.463[e]
14	105.13464	105.25579	95116.128	95006.647	−19	105.19933	95057.640[e]
15	105.12994	105.25944	95120.384	95003.353	40	105.19912	95057.828[e]
16	105.12522	105.26299	95124.654	95000.155	15	105.19890	95058.026[e]
17	105.12038	105.26667	95129.031	94996.833	*	105.19867	95058.232[e]
18	105.11566	105.27014	95133.302	94993.697	−20	105.19844	95058.445[e]
19	105.11079	105.27376	95137.713	94990.432	25		
20	105.10590	105.27699	95142.141	94987.519	90		
21	105.10102	105.28045	95146.554	94984.400			
22	105.09636	105.28392	95150.777	94981.263			
23	105.09106		95155.568				
24	105.08627		95159.911				
25	105.08194		95163.833				
26	105.07707		95168.244				
27	105.07174		95173.073				
	$^{12}C^{18}O$						
0	105.22385		95035.489		−15		
1	105.21971		95039.225		12	105.22776	95031.953[b]
2	105.21546	105.23598	95043.067	95024.533	24	105.22779	95031.929[b]
3	105.21136	105.24001	95046.773	95020.893	2	105.22764	95032.064[b]
4	105.20718	105.24389	95050.548	95017.388	15	105.22775	95031.968[b]
5	105.20308	105.24785	95054.254	95013.817	28	105.22789	95031.841[b]
6	105.19756	105.25181	95059.242	95010.244	17	105.22793	95031.804[b]
7	105.19390	105.25584	95062.545	95006.605	25	105.22666	95032.947[b]
8	105.18973	105.25840	95066.319	95004.297	8	105.22726	95032.407[b,u]
9	105.18510	105.26286	95070.497	95000.270	25	105.22728	95032.392[b,u]
10	105.18078	105.26674	95074.406	94996.765	11	105.22684	95032.784[b]
11	105.17638	105.27025	95078.383	94993.597	−36	105.22685	95032.775[b,u]
12	105.17183	105.27399	95082.494	94990.227	20	105.22668	95032.932[b,u]
13	105.16728	105.27757	95086.605	94986.992	11	105.22656	95033.041[b,u]
14	105.16274	105.28123	95090.717	94983.690	4	105.22629	95033.284[b]
15	105.15812	105.28474	95094.895	94980.523	32	105.22604	95033.509[b]
16	105.15357	105.28826	95099.006	94977.354	−39	105.22596	95033.579[b]
17	105.14887	105.29177	95103.253	94974.187	−6	105.22568	95033.835[b]
18	105.14418	105.29513	95107.498	94971.154	−11	105.22554	95033.959[b]
19	105.13950	105.29857	95111.731	94968.054	−41	105.22533	95034.154[b]
20	105.13479	105.30192	95115.994	94965.033	15	105.22512	95034.342[b]
21	105.12993	105.30522	95120.386	94962.055	−14	105.22482	95034.616[b]
22	105.12524	105.30867	95124.632	94958.942	*	105.22465	95034.769[b]
23	105.12047	105.31179	95128.953	94956.132	−8		
24	105.11541	105.31491	95133.534	94953.320	*		
25	105.11054	105.31838	95137.938	94950.187	*		
26		105.32201		94946.914			
27		105.32201		94946.914			

Notes. [b]Data from Baker et al. (1993). [u]Data from Ubachs et al. (2000). [e]Data calculated from the *e*-parity levels.

Table A.23. Measured transition wavelengths and wavenumbers of the $E^1\Pi(v'=1)$–$X^1\Sigma^+(v''=0)$ band for $^{13}C^{16}O$, $^{13}C^{17}O$, and $^{13}C^{18}O$ (same column description as for Table A.19).

$E^1\Pi(v'=1)$–$X^1\Sigma^+(v''=0)$							
	$^{13}C^{16}O$						
J	R_{ms} (nm)	P_{ms} (nm)	R_{ms} (cm^{-1})	P_{ms} (cm^{-1})	δ_P	Q_{ms} (nm)	Q_{ms} (cm^{-1})
0	105.21928		95039.616		−2		
1	105.21515		95043.351		5	105.22332	95035.969[b]
2	105.21101	105.23149	95047.086	95028.592	12	105.22333	95035.958[b]
3	105.20672	105.23551	95050.961	95024.962	2	105.22333	95035.961[b]
4	105.20255	105.23953	95054.730	95021.333	1	105.22320	95036.078[b]
5	105.19838	105.24335	95058.502	95017.877	−2	105.22326	95036.021[b]
6	105.19549	105.24732	95061.111	95014.300		105.22308	95036.180[b]
7	105.18922	105.25127	95066.774	95010.732	−9	105.22244	95036.763[b,u]
8	105.18501		95070.579		15	105.22255	95036.662[b,u]
9	105.18037	105.25836	95074.771	95004.330	−28	105.22265	95036.575[b,u]
10	105.17608	105.26233	95078.656	95000.745	−2	105.22222	95036.962[b,u]
11	105.17161	105.26572	95082.692	94997.685	16	105.22236	95036.836[b,u]
12	105.16712	105.26961	95086.751	94994.181	8	105.22220	95036.978[b,u]
13	105.16257	105.27330	95090.869	94990.850	20	105.22204	95037.126[b,u]
14	105.15799	105.27690	95095.006	94987.595	−4	105.22187	95037.276[b,u]
15	105.15340	105.28049	95099.162	94984.363	−6	105.22165	95037.472[b,u]
16	105.14874	105.28396	95103.377	94981.227	−2	105.22147	95037.640[b,u]
17	105.14408	105.28746	95107.593	94978.069	−6	105.22124	95037.849[b,u]
18	105.13937	105.29091	95111.847	94974.964	−1	105.22106	95038.011[b,u]
19	105.13463	105.29433	95116.141	94971.878	1	105.22081	95038.235[b,u]
20	105.12988	105.29772	95120.433	94968.820	−7	105.22058	95038.441[b,u]
21	105.12510	105.30105	95124.765	94965.811	−6	105.22021	95038.775[b,u]
22	105.12027	105.30436	95129.135	94962.826	*	105.22014	95038.842[b,u]
23	105.11542	105.30764	95133.520	94959.868	5	105.21979	95039.160[u]
24	105.11058	105.31010	95137.901	94957.656	−23		
25	105.10568	105.31410	95142.338	94954.048	−18		
26	105.10072	105.31724	95146.831	94951.216	8		
27	105.09575	105.32038	95151.324	94948.381	−26		
28	105.09078	105.32350	95155.823	94945.569	−16		
29	105.08578	105.32648	95160.353	94942.884	63		
30	105.08074	105.32955	95164.920	94940.122			
31	105.07567	105.33272	95169.508	94937.264			
32	105.07059		95174.114				
33	105.06558		95178.646				
34	105.06558		95178.646				
	$^{13}C^{17}O$						
0	105.25000		95011.872		−2		
1	105.24604		95015.447		3	105.25399	95008.279[u]
2	105.24203	105.26189	95019.067	95001.140	−1	105.25399	95008.279[u]
3	105.23816	105.26587	95022.562	94997.548		105.25402	95008.246[u]
4		105.26978		94994.020		105.25419	95008.095[u]
5	105.22903		95030.806		0	105.25212	95009.966[u]
6	105.22499	105.27384	95034.455	94990.356	−1	105.25321	95008.983[u]
7	105.22120	105.28056	95037.878	94984.293	−1	105.25330	95008.896[u]
8	105.21645	105.28444	95042.168	94980.792	0	105.25354	95008.681[u]
9	105.21220	105.28857	95046.007	94977.067	−2	105.25305	95009.127[u]
10	105.20789	105.29174	95049.901	94974.207	−3	105.25296	95009.203[u]
11	105.20351	105.29540	95053.858	94970.906	−2	105.25284	95009.312[u]
12	105.19910	105.29900	95057.843	94967.659	−4	105.25269	95009.447[u]
13	105.19468	105.30253	95061.837	94964.476	−4	105.25254	95009.581[x]
14	105.19019	105.30602	95065.895	94961.328	2	105.25236	95009.746[x]
15	105.18572	105.30950	95069.935	94958.190	−3	105.25216	95009.924[x]
16	105.18119	105.31292	95074.029	94955.107	−2	105.25195	95010.114[x]
17	105.17662	105.31633	95078.160	94952.032	−2	105.25173	95010.316[x]
18	105.17204	105.31969	95082.301	94949.003	−1	105.25149	95010.529[x]
19	105.16747	105.32300	95086.432	94946.019	−1	105.25125	95010.753[x]
20	105.16272	105.32630	95090.727	94943.044	2	105.25098	95010.988[x]
21	105.15806	105.32960	95094.941	94940.069		105.25071	95011.233[x]
22	105.15337	105.33272	95099.183	94937.257		105.25043	95011.488[x]
23						105.25014	95011.754[x]
24						105.24983	95012.029[x]
25						105.24952	95012.313[x]
	$^{13}C^{18}O$						
0	105.27550		94988.861		35		
1	105.27239		94991.669		58	105.27943	94985.317[u]
2	105.26890	105.28719	94994.815	94978.312	−8	105.28026	94984.570[b,u]
3	105.26511	105.29187	94998.240	94974.090	10	105.28065	94984.220[b,u]
4	105.26112	105.29598	95001.835	94970.383	57	105.28082	94984.067[b,u]
5	105.25720	105.29997	95005.373	94966.789	*	105.28079	94984.086[b,u]
6	105.25285	105.30383	95009.305	94963.307	41	105.28104	94983.860[b,u]
7	105.24880	105.30782	95012.955	94959.712	6	105.28064	94984.227[b,u]
8	105.24464	105.31099	95016.718	94956.848	56	105.28062	94984.240[b,u]
9	105.24047	105.31461	95020.481	94953.590	52	105.28049	94984.358[b,u]
10	105.23630	105.31828	95024.246	94950.277	−7	105.28040	94984.441[b,u]
11	105.23201	105.32183	95028.119	94947.075	19	105.28026	94984.564[b,u]
12	105.22778	105.32526	95031.938	94943.986	−10	105.28010	94984.710[b,u]
13	105.22337	105.32875	95035.926	94940.841	19	105.27994	94984.853[b,u]
14	105.21901	105.33218	95039.858	94937.752	22	105.27973	94985.049[b,u]
15	105.21466	105.33554	95043.789	94934.719	−1	105.27953	94985.225[b,u]
16	105.21018	105.33891	95047.832	94931.687	6	105.27927	94985.459[b,u]
17	105.20577	105.34221	95051.820	94928.710	−14	105.27908	94985.634[b,u]
18	105.20129	105.34545	95055.864	94925.789	−2	105.27881	94985.874[b,u]
19	105.19676	105.34869	95059.964	94922.869	11	105.27884	94985.849[b]
20	105.19222	105.35193	95064.064	94919.948	−1	105.27816	94986.464[b]
21	105.18762	105.35511	95068.220	94917.084	18	105.27816	94986.462[b]
22	105.18302	105.35823	95072.376	94914.276	11	105.27790	94986.695[b]
23	105.17843	105.36135	95076.532	94911.468	7		
24	105.17377	105.36440	95080.744	94908.716	6		
25	105.16911	105.36746	95084.957	94905.964	−20		
26	105.16439	105.37045	95089.225	94903.268	14		
27	105.15960	105.37338	95093.550	94900.629	23		
28	105.15488	105.37637	95097.818	94897.932	−22		
29	105.15010	105.37924	95102.143	94895.349	1		
30	105.14526	105.38205	95106.522	94892.822	2		
31	105.14043	105.38493	95110.887	94890.225	0		
32	105.13554	105.38770	95115.311	94887.732	−73		
33	105.13070	105.39047	95119.694	94885.239			
34	105.12588	105.39301	95124.053	94882.956			

Notes. [b]Data from Baker et al. (1993). [u]Data from Ubachs et al. (2000). [e]Data calculated from the *e*-parity levels. [x]Data calculated from the *e*-parity levels using the deperturbation described in Ubachs et al. (2000).

Table A.24. Term values (cm^{-1}) of the $E^1\Pi(v'=1)$ *e*- and *f*-parity levels for six CO isotopologues (see note to Table A.21).

	$E^1\Pi(v'=1)$																	
	$^{12}C^{16}O$			$^{12}C^{17}O$			$^{12}C^{18}O$			$^{13}C^{16}O$			$^{13}C^{17}O$			$^{13}C^{18}O$		
J'	*e*-par. (*R*&*P*)	*f*-par. (*Q*)	Λ_d	*e*-par. (*R*&*P*)	*f*-par. (*Q*)	Λ_d	*e*-par. (*R*&*P*)	*f*-par. (*Q*)	Λ_d	*e*-par. (*R*&*P*)	*f*-par. (*Q*)	Λ_d	*e*-par. (*R*&*P*)	*f*-par. (*Q*)	Λ_d	*e*-par. (*R*&*P*)	*f*-par. (*Q*)	Λ_d
1	95086.768 (−11)	95086.586[b]	0.182	95059.764 (−1)	95059.746[u]	0.017	95035.504 (−15)	95035.615[b]	−0.111	95039.617 (−2)	95039.645[b]	−0.028	95011.874 (−2)	95011.857[u]	0.017	94988.826 (35)	94988.809[u]	0.016
2	95094.514 (20)	95094.376[b]	0.137	95067.304 (−11)	95067.273[u]	0.031	95042.876 (12)	95042.915[b]	−0.039	95047.022 (5)	95046.985[b]	0.037	95019.023 (3)	95019.015[u]	0.008	94995.104 (58)	94995.048[b,u]	0.056
3	95106.160 (−5)	95106.056[b]	0.104	95078.626 (−2)	95078.475[e]	0.151	95054.029 (24)	95054.035[b]	−0.006	95058.102 (12)	95058.015[b]	0.086	95029.804 (−1)	95029.718[u]	0.087	95005.301 (−8)	95005.176[b,u]	0.125
4	95121.651 (26)	95121.346[b]	0.305	95093.745 (13)	95093.661[e]	0.084	95068.743 (2)	95068.585[b]	0.158	95073.014 (2)	95072.835[b]	0.178	95044.034	95043.880[u]	0.153	95019.186 (10)	95018.993[b,u]	0.193
5	95141.042 (2)	95140.706[b]	0.335	95112.518 (−4)	95112.401[e]	0.116	95087.151 (15)	95086.765[b]	0.386	95091.486 (1)	95091.155[b]	0.331	95065.501	95063.643[u]	1.859	95036.704 (57)	95036.474[b,u]	0.230
6	95164.303 (6)	95163.686[b]	0.617	95135.330 (−1)	95134.578[e]	0.752	95109.150 (28)	95108.695[b]	0.455	95113.638 (−2)	95113.365[b]	0.273	95084.483 (0)	95084.128[u]	0.355	95057.628 (*)	95057.200[b,u]	0.428
7	95191.799 (69)	95191.206[b]	0.592	95161.701 (2)	95161.677[e]	0.024	95136.116 (17)	95135.465[b]	0.651	95138.296	95139.672[b,u]	−1.376	95109.601 (−1)	95109.085[u]	0.516	95082.604 (41)	95082.010[b,u]	0.594
8	95222.462 (19)	95221.640[b,u]	0.823	95191.386 (4)	95191.588[e]	−0.202	95165.038 (25)	95164.209[b,u]	0.829	95169.692 (−9)	95168.967[b,u]	0.726	95138.068 (−1)	95137.490[u]	0.579	95110.732 (6)	95109.955[b,u]	0.777
9	95257.105 (−1)	95256.086[b]	1.019	95226.307 (−7)	95225.695[e]	0.612	95198.113 (8)	95197.135[b,u]	0.978	95202.869 (15)	95201.948[b,u]	0.922	95170.977 (0)	95170.129[u]	0.848	95142.377 (56)	95141.494[b,u]	0.883
10	95296.429 (37)	95295.122[b,u]	1.307	95263.914 (7)	95263.088[e]	0.826	95235.215 (25)	95234.125[b]	1.090	95240.172 (−28)	95239.071[b,u]	1.101	95207.012 (−2)	95205.972[u]	1.040	95177.565 (52)	95176.485[b,u]	1.080
11	95338.832 (−8)	95337.275[b,u]	1.557	95305.654 (10)	95304.408[e]	1.246	95275.736 (11)	95274.368[b,u]	1.368	95280.767 (−2)	95279.350[b,u]	1.416	95246.673 (−3)	95245.420[u]	1.254	95216.296 (−7)	95215.002[b,u]	1.294
12	95385.603 (−80)	95383.756[b]	1.847	95350.870 (3)	95349.493[e]	1.376	95320.011 (−36)	95318.430[b,u]	1.581	95325.191 (16)	95323.565[b,u]	1.626	95289.968 (−2)	95288.464[u]	1.505	95258.539 (19)	95257.027[b,u]	1.512
13	95435.787 (−9)	95433.635[b,u]	2.152	95399.940 (17)	95398.331[e]	1.609	95367.972 (20)	95366.096[b,u]	1.876	95373.330 (8)	95371.452[b,u]	1.879	95336.864 (−4)	95335.075[x]	1.789	95304.265 (−10)	95302.532[b,u]	1.733
14	95489.971 (8)	95487.503[b,u]	2.468	95452.782 (13)	95450.915[e]	1.867	95419.649 (11)	95417.545[b]	2.104	95425.175 (20)	95423.004[b,u]	2.171	95387.336 (−4)	95385.285[x]	2.051	95353.586 (19)	95351.572[b,u]	2.014
15	95548.013 (−2)	95545.171[b,u]	2.842	95509.424 (−19)	95507.244[e]	2.180	95474.974 (4)	95472.625[b]	2.349	95480.738 (−4)	95478.264[b,u]	2.474	95441.433 (2)	95439.074[x]	2.359	95406.358 (22)	95404.072[b,u]	2.287
16	95609.965 (19)	95606.806[b,u]	3.159	95569.761 (40)	95567.313[e]	2.448	95533.979 (32)	95531.195[b]	2.784	95539.959 (−6)	95537.154[b,u]	2.805	95499.088 (−3)	95496.438[x]	2.651	95462.637 (−1)	95460.109[b,u]	2.528
17	95675.772 (14)	95672.162[b,u]	3.609	95633.927 (15)	95631.120[e]	2.807	95596.661 (−39)	95593.595[b]	3.066	95602.894 (−2)	95599.745[b,u]	3.149	95560.355 (−2)	95557.375[x]	2.980	95522.476 (6)	95519.563[b,u]	2.914
18	95745.428 (−16)	95741.453[b,u]	3.975	95701.809 (111)	95698.660[e]	3.149	95663.019 (−6)	95659.505[b]	3.514	95669.495 (−6)	95665.943[b,u]	3.551	95625.222 (−2)	95621.883[x]	3.339	95585.762 (−14)	95582.555[b,u]	3.207
19	95818.933 (−15)	95814.531[b,u]	4.402	95773.538 (−20)			95733.055 (−11)	95729.125[b]	3.930	95739.780 (−1)	95735.856[b,u]	3.924	95693.656 (−1)	95689.958[x]	3.697	95652.547 (−2)	95648.756[b]	3.792
20	95896.283 (16)	95891.400[b,u]	4.883	95848.955 (25)			95806.743 (−41)	95802.375[b]	4.368	95813.762 (1)	95809.403[b,u]	4.359	95765.639 (−1)	95761.600[x]	4.039	95722.859 (11)	95719.066[b]	3.793
21	95977.503 (−5)	95972.079[b,u]	5.424	95928.090 (90)			95884.013 (15)	95879.345[b]	4.668	95891.402 (−7)	95886.725[b,u]	4.677	95841.338 (2)	95836.803[x]	4.534	95796.666 (−1)	95792.226[b]	4.440
22	96062.534 (−24)			96011.085			95965.129 (−14)	95959.825[b]	5.304	95972.720 (−6)	95967.425[b,u]	5.295	95920.512	95915.566[x]	4.946	95873.966 (18)	95869.086[b]	4.880
23	96151.401 (−11)			96097.514			96049.800 (112)			96058.072 (*)	96052.017[u]	6.056	96003.261	95997.887[x]	5.375	95954.755 (11)		
24	96244.129 (5)			96188.225			96137.973 (−8)			96146.373 (5)				96083.760[x]		96039.005 (7)		
25	96340.657 (−31)			96282.196			96229.827 (*)			96238.694 (−23)				96173.183[x]		96126.766 (6)		
26	96440.956 (77)			96379.454			96326.848 (*)			96334.675 (−18)						96218.010 (−20)		
27	96544.934 (*)			96480.902						96434.325 (8)						96312.703 (14)		
28	96652.787 (*)			96586.468						96537.662 (−26)						96410.928 (23)		
29	96764.482 (*)									96644.586 (−16)						96512.597 (−22)		
30	96879.924 (*)									96755.095 (63)						96617.699 (1)		
31	96999.193 (*)									96869.400						96726.316 (2)		
32	97121.216									96987.277						96838.360 (0)		
33	97247.894									97108.781						96953.966 (−73)		
34	97378.471									97233.816						97072.814		
35	97512.670									97357.920						97195.137		

Notes. [(b)] Data from Baker et al. (1993). [(u)] Data from Ubachs et al. (2000). [(*)] Data calculated from the *e*-parity levels. [(x)] Data calculated from the *e*-parity levels using the deperturbation described in Ubachs et al. (2000).

Table A.25. Measured transition wavelengths and wavenumbers of the $E^1\Pi(v'=2)$–$X^1\Sigma^+(v''=0)$ band for $^{12}C^{16}O$, $^{12}C^{17}O$, and $^{12}C^{18}O$ (same column description as for Table A.19).

$E^1\Pi(v'=2)$–$X^1\Sigma^+(v''=0)$							
	$^{12}C^{16}O$						
J	R_{ms} (nm)	P_{ms} (nm)	R_{ms} (cm^{-1})	P_{ms} (cm^{-1})	δ_P	Q_{ms} (nm)	Q_{ms} (cm^{-1})
0	102.92548		97157.676		−6		
1	102.92149		97161.438		0	102.92955	97153.831
2	102.91750	102.93769	97165.201	97146.152	9	102.92968	97153.712
3	102.91364	102.94186	97168.852	97142.214	−30	102.92987	97153.531
4	102.90977	102.94604	97172.503	97138.271	2	102.93012	97153.288
5	102.90596	102.95023	97176.098	97134.311	−21	102.93045	97152.979
6	102.90216	102.95458	97179.692	97130.212	13	102.93085	97152.604
7	102.89847	102.95887	97183.174	97126.168	−9	102.93132	97152.156
8	102.89478	102.96327	97186.656	97122.012	−1	102.93189	97151.626
9	102.89116	102.96768	97190.082	97117.856	9	102.93249	97151.060
10	102.88759	102.97214	97193.452	97113.644	−8	102.93315	97150.430
11	102.88402	102.97667	97196.821	97109.375	4	102.93387	97149.752
12	102.88058	102.98120	97200.079	97105.106	−9	102.93447	97149.189
13	102.87707	102.98578	97203.392	97100.782	35	102.93557	97148.150
14	102.87374	102.99043	97206.538	97096.401	8	102.93653	97147.243
15	102.87041	102.99514	97209.684	97091.965	20	102.93757	97146.265
16	102.86714	102.99986	97212.772	97087.508	23	102.93865	97145.240
17	102.86394	103.00467	97215.802	97082.977	−1	102.93981	97144.145
18	102.86080	103.00951	97218.770	97078.413	9	102.94111	97142.922
19	102.85773	103.01436	97221.671	97073.848		102.94247	97141.638
20	102.85469	103.01933	97224.538	97069.158		102.94386	97140.325
21	102.85173		97227.342			102.94540	97138.875
22	102.84890		97230.019			102.94697	97137.393
23	102.84597		97232.789			102.94867	97135.788
	$^{12}C^{17}O$						
0	102.97878		97107.382		35		
1	102.97490		97111.046		−8	102.98274	97103.654
2	102.97105	102.99078	97114.672	97096.067	−20	102.98287	97103.531
3	102.96724	102.99475	97118.266	97092.324	−5	102.98303	97103.379
4	102.96340	102.99883	97121.892	97088.479	30	102.98328	97103.140
5	102.95975	103.00300	97125.334	97084.550	−12	102.98358	97102.863
6	102.95602	103.00718	97128.850	97080.612	−48	102.98395	97102.511
7	102.95236	103.01139	97132.309	97076.647	−17	102.98444	97102.052
8	102.94873	103.01553	97135.732	97072.747	11	102.98497	97101.553
9	102.94524	103.01987	97139.025	97068.657	36	102.98556	97100.995
10	102.94172	103.02424	97142.346	97064.539		102.98608	97100.498
11	102.93817	103.02873	97145.697	97060.302		102.98666	97099.952
12						102.98762	97099.053
13						102.98830	97098.409
14						102.98923	97097.534
	$^{12}C^{18}O$						
0	103.02681		97062.114		8		
1	103.02299		97065.713		2	103.03074	97058.409
2	103.01924	103.03849	97069.246	97051.112	−9	103.03086	97058.302
3	103.01548	103.04243	97072.789	97047.401	8	103.03103	97058.141
4	103.01179	103.04643	97076.267	97043.634	−2	103.03126	97057.927
5	103.00809	103.05048	97079.754	97039.820	17	103.03154	97057.658
6	103.00446	103.05454	97083.175	97035.997	8	103.03188	97057.336
7	103.00088	103.05865	97086.549	97032.127	1	103.03228	97056.959
8	102.99731	103.06277	97089.914	97028.248	−6	103.03275	97056.518
9	102.99379	103.06694	97093.233	97024.322	21	103.03328	97056.019
10	102.99036	103.07112	97096.466	97020.387	41	103.03382	97055.511
11	102.98695	103.07542	97099.677	97016.340	3	103.03440	97054.964
12	102.98357	103.07979	97102.866	97012.227	78	103.03522	97054.194
13	102.98017	103.08406	97106.070	97008.209		103.03595	97053.502
14	102.97550	103.08859	97110.479	97003.946		103.03676	97052.741
15						103.03759	97051.957

Table A.26. Measured transition wavelengths and wavenumbers of the $E^1\Pi(v'=2)$–$X^1\Sigma^+(v''=0)$ band for $^{13}C^{16}O$, $^{13}C^{17}O$, and $^{13}C^{18}O$ (same column description as for Table A.19).

$E^1\Pi(v'=2)$–$X^1\Sigma^+(v''=0)$							
	$^{13}C^{16}O$						
J	R_{ms} (nm)	P_{ms} (nm)	R_{ms} (cm^{-1})	P_{ms} (cm^{-1})	δ_P	Q_{ms} (nm)	Q_{ms} (cm^{-1})
0	103.01876		97069.703		22		
1	103.01491		97073.325		13	103.02267	97066.018
2	103.01111	103.03051	97076.906	97058.631	3	103.02278	97065.907
3	103.00738	103.03445	97080.427	97054.919	−6	103.02296	97065.740
4	103.00364	103.03843	97083.951	97051.171	10	103.02320	97065.518
5	102.99998	103.04248	97087.394	97047.358	−1	103.02349	97065.241
6	102.99633	103.04657	97090.837	97043.502	−3	103.02384	97064.911
7	102.99272	103.05069	97094.242	97039.620	6	103.02420	97064.573
8	102.98915	103.05483	97097.605	97035.724	4	103.02468	97064.124
9	102.98565	103.05903	97100.908	97031.767	−6	103.02532	97063.518
10	102.98217	103.06325	97104.192	97027.792	−4	103.02581	97063.059
11	102.97870	103.06752	97107.459	97023.776	10	103.02644	97062.463
12	102.97533	103.07183	97110.642	97019.722	3	103.02715	97061.790
13	102.97195	103.07618	97113.828	97015.629	−1	103.02791	97061.079
14	102.96865	103.08057	97116.936	97011.496	−1	103.02872	97060.313
15	102.96538	103.08496	97120.023	97007.364	11	103.02965	97059.438
16	102.96217	103.08943	97123.050	97003.152	1	103.03058	97058.559
17	102.95903	103.09396	97126.017	96998.896	−49	103.03164	97057.568
18	102.95588	103.09849	97128.985	96994.630	21	103.03275	97056.522
19	102.95282	103.10300	97131.871	96990.389	*	103.03389	97055.441
20	102.94978	103.10776	97134.739	96985.913	*	103.03508	97054.320
21	102.94691	103.11073	97137.450	96983.118	*	103.03646	97053.028
22	102.94389	103.11393	97140.297	96980.108		103.03784	97051.724
23	102.94110	103.11717	97142.928	96977.056		103.03936	97050.297
24	102.93836		97145.520			103.04087	97048.873
	$^{13}C^{17}O$						
0	103.07389		97017.780		*		
1	103.06991		97021.526		*	103.07767	97014.220
2		103.08426		97008.020			
3		103.08762		97004.859			
4		103.09098		97001.697			
5		103.09442		96998.460			
6		103.09783		96995.252			
7		103.10130		96991.987			
8		103.10479		96988.704			
9		103.10830		96985.403			
10		103.11187		96982.045			
11		103.11544		96978.687			
12		103.11906		96975.283			
	$^{13}C^{18}O$						
0	103.12332		96971.277		12		
1	103.11968		96974.703		2	103.12705	96967.768
2	103.11603	103.13449	96978.129	96960.774	20	103.12715	96967.673
3	103.11245	103.13825	96981.499	96957.237	10	103.12730	96967.530
4	103.10887	103.14208	96984.868	96953.642	1	103.12751	96967.341
5	103.10535	103.14590	96988.182	96950.047	21	103.12776	96967.104
6	103.10188	103.14973	96991.440	96946.453	−15	103.12806	96966.822
7	103.09842	103.15367	96994.697	96942.746	−22	103.12841	96966.495
8	103.09496	103.15755	96997.955	96939.096	0	103.12880	96966.123
9	103.09156	103.16150	97001.156	96935.389	−4	103.12923	96965.717
10	103.08821	103.16550	97004.302	96931.626	−8	103.12977	96965.212
11	103.08487	103.16951	97007.446	96927.863	−19	103.13031	96964.706
12	103.08153	103.17357	97010.591	96924.044	14	103.13091	96964.145
13	103.07831	103.17762	97013.625	96920.243	−8	103.13156	96963.531
14	103.07506	103.18176	97016.679	96916.358	−40	103.13228	96962.853
15	103.07188	103.18589	97019.671	96912.473	−56	103.13304	96962.141
16	103.06875	103.18998	97022.617	96908.632	−30	103.13384	96961.385
17	103.06568	103.19417	97025.511	96904.702	−30	103.13468	96960.592
18	103.06260	103.19849	97028.409	96900.645	−9	103.13568	96959.659
19	103.05955	103.20280	97031.282	96896.593	13	103.13669	96958.706
20	103.05660	103.20716	97034.059	96892.506	5	103.13770	96957.754
21	103.05368	103.21153	97036.804	96888.399	56	103.13883	96956.691
22	103.05083	103.21594	97039.488	96884.260	−23		
23	103.04801	103.22051	97042.147	96879.976	68		
24	103.04519	103.22485	97044.804	96875.897	−5		
25	103.04237	103.22958	97047.462	96871.456			
26	103.03987	103.23396	97049.812	96867.351			
27	103.03702		97052.493				

Table A.27. Measured transition wavelengths and wavenumbers of the $E^1\Pi(v'=3)$–$X^1\Sigma^+(v''=0)$ band for $^{12}C^{16}O$, $^{12}C^{17}O$, and $^{12}C^{18}O$ (same column description as for Table A.19).

$E^1\Pi(v'=3)$–$X^1\Sigma^+(v''=0)$							
	$^{12}C^{16}O$						
J	R_{ms} (nm)	P_{ms} (nm)	R_{ms} (cm^{-1})	P_{ms} (cm^{-1})	δ_P	Q_{ms} (nm)	Q_{ms} (cm^{-1})
0	101.08858		98923.141		−59		
1	101.08548		98926.174		−34	101.09248	98919.326
2	101.08256	101.10025	98929.039	98911.724	53	101.09335	98918.475
3	101.08020	101.10506	98931.341	98907.018	26	101.09455	98917.301
4	101.07825	101.11017	98933.250	98902.019	3	101.09616	98915.725
5	101.07665	101.11562	98934.815	98896.689	33	101.09822	98913.710
6	101.07544	101.12148	98936.003	98890.958	41	101.10069	98911.293
7	101.07469	101.12780	98936.739	98884.777	49	101.10362	98908.427
8	101.07459	101.13446	98936.838	98878.266	−60	101.10695	98905.169
9	101.07475	101.14158	98936.679	98871.305	−48	101.11074	98901.462
10	101.07544	101.14911	98936.003	98863.945	−94	101.11499	98897.305
11	101.07630	101.15715	98935.160	98856.087	−22	101.11970	98892.698
12	101.07785	101.16560	98933.644	98847.830	−36	101.12492	98887.594
13	101.07978	101.17446	98931.754	98839.173	47	101.13067	98881.971
14	101.08211	101.18383	98929.473	98830.021	*	101.13687	98875.909
15	101.08552	101.19378	98926.134	98820.303	0	101.14365	98869.281
16	101.08923	101.20415	98922.503	98810.177	31	101.15095	98862.146
17	101.09327	101.21512	98918.550	98799.468	*	101.15888	98854.396
18	101.09779	101.22674	98914.131	98788.127	*	101.16739	98846.081
19	101.10357	101.23877	98908.472	98776.388		101.17658	98837.102
20	101.10950	101.25154	98902.677	98763.930		101.18636	98827.549
21	101.11626		98896.065			101.19684	98817.315
22						101.20805	98806.370
23						101.22003	98794.674
24						101.23283	98782.180
25						101.24633	98769.012
	$^{12}C^{17}O$						
0	101.13600		98876.756		2		
1	101.13290		98879.787		−16	101.13989	98872.957
2	101.13009	101.14751	98882.538	98865.508	−8	101.14060	98872.263
3	101.12768	101.15204	98884.898	98861.081	−20	101.14169	98871.197
4	101.12550	101.15691	98887.031	98856.321	−17	101.14313	98869.790
5	101.12383	101.16214	98888.661	98851.211	17	101.14497	98867.991
6	101.12245	101.16763	98890.008	98845.846	−25	101.14724	98865.772
7	101.12142	101.17370	98891.019	98839.916	−30	101.14978	98863.290
8	101.12078	101.17990	98891.639	98833.859	83	101.15275	98860.387
9	101.12077	101.18652	98891.648	98827.393		101.15692	98856.312
10	101.12142	101.19378	98891.019	98820.303		101.16215	98851.201
11	101.12294		98889.535			101.16773	98845.749
12	101.12494		98887.576			101.17359	98840.023
13	101.12675		98885.803			101.17997	98833.791
14	101.12915		98883.455			101.18654	98827.374
15	101.13187		98880.802			101.19376	98820.323
16	101.13448		98878.242			101.20130	98812.960
	$^{12}C^{18}O$						
0	101.18111		98832.677		1		
1	101.17796		98835.754		−81	101.18489	98828.985
2	101.17514	101.19236	98838.509	98821.690	3	101.18551	98828.380
3	101.17264	101.19654	98840.951	98817.608	4	101.18649	98827.423
4	101.17044	101.20139	98843.101	98812.872	0	101.18782	98826.124
5	101.16857	101.20639	98844.928	98807.990	−8	101.18946	98824.522
6	101.16702	101.21168	98846.442	98802.826	24	101.19144	98822.588
7	101.16582	101.21729	98847.615	98797.350	2	101.19379	98820.293
8	101.16497	101.22330	98848.445	98791.484	−4	101.19656	98817.588
9	101.16445	101.22955	98848.953	98785.384	14	101.19953	98814.688
10	101.16440	101.23618	98849.002	98778.915	−25	101.20292	98811.378
11	101.16463	101.24319	98848.777	98772.075	−73	101.20678	98807.610
12	101.16505	101.25055	98848.367	98764.896		101.21085	98803.636
13	101.16650	101.25817	98846.950	98757.462		101.21547	98799.126
14	101.16820		98845.289			101.22059	98794.127
15	101.16989		98843.638				
16	101.17207		98841.508				
17	101.17424		98839.388				
18	101.17702		98836.673				
19	101.17967		98834.084				
20	101.18946		98824.522				
21	101.18255		98831.271				

Table A.28. Measured transition wavelengths and wavenumbers of the $E^1\Pi(v'=3)$–$X^1\Sigma^+(v''=0)$ band for $^{13}C^{16}O$, $^{13}C^{17}O$, and $^{13}C^{18}O$ (same column description as for Table A.19).

$E^1\Pi(v'=3)$–$X^1\Sigma^+(v''=0)$							
	$^{13}C^{16}O$						
J	R_{ms} (nm)	P_{ms} (nm)	R_{ms} (cm^{-1})	P_{ms} (cm^{-1})	δ_P	Q_{ms} (nm)	Q_{ms} (cm^{-1})
0	101.17336		98840.250		1		
1	101.17017		98843.366		13	101.17705	98836.643
2	101.16738	101.18465	98846.091	98829.220	−14	101.17774	98835.969
3	101.16489	101.18901	98848.525	98824.961	8	101.17884	98834.895
4	101.16270	101.19369	98850.667	98820.391	−13	101.18003	98833.732
5	101.16080	101.19877	98852.516	98815.430	11	101.18183	98831.974
6	101.15927	101.20406	98854.014	98810.265	11	101.18372	98830.128
7	101.15821	101.20974	98855.048	98804.720	−30	101.18621	98827.696
8	101.15725	101.21573	98855.992	98798.872	31	101.18885	98825.118
9	101.15683	101.22211	98856.401	98792.645	16	101.19200	98822.041
10	101.15720	101.22879	98856.039	98786.126	*	101.19548	98818.643
11	101.15795	101.23586	98855.302	98779.227	*	101.19927	98814.942
12	101.15914	101.24320	98854.145	98772.066		101.20345	98810.861
13	101.16051	101.24981	98852.807	98765.617		101.20825	98806.174
14	101.16179		98851.554			101.21322	98801.323
15	101.16382		98849.572			101.21881	98795.866
16	101.16664		98846.813			101.22533	98789.503
17	101.16932		98844.197			101.23138	98783.599
18	101.17231		98841.274			101.24046	98774.739
19	101.17528		98838.371				
	$^{13}C^{17}O$						
0							
1						101.13448	98878.242[t]
	$^{13}C^{18}O$						
0	101.27772		98738.403		41		
1	101.27466		98741.379		1	101.28135	98734.861
2	101.27178	101.28855	98744.187	98727.842	18	101.28187	98734.354
3	101.26925	101.29258	98746.658	98723.914	−17	101.28267	98733.574
4	101.26689	101.29690	98748.961	98719.704	1	101.28377	98732.502
5	101.26482	101.30146	98750.983	98715.260	−8	101.28509	98731.215
6	101.26297	101.30630	98752.780	98710.544	11	101.28665	98729.694
7	101.26142	101.31137	98754.297	98705.604	8	101.28855	98727.842
8	101.26015	101.31673	98755.532	98700.382	2	101.29074	98725.708
9	101.25917	101.32233	98756.487	98694.927	−3	101.29322	98723.291
10	101.25848	101.32821	98757.161	98689.200	−11	101.29592	98720.659
11	101.25801	101.33438	98757.615	98683.191	3	101.29898	98717.677
12	101.25813	101.34083	98757.499	98676.910	*	101.30244	98714.305
13	101.25864	101.34755	98757.004	98670.367	*	101.30596	98710.875
14	101.25951	101.35460	98756.160	98663.504	*	101.31006	98706.881
15	101.26078	101.36193	98754.922	98656.369	*	101.31444	98702.613
16	101.26242	101.36964	98753.321	98648.866	*	101.31912	98698.054
17	101.26433	101.37766	98751.456	98641.062	*	101.32420	98693.106
18	101.26639	101.38603	98749.448	98632.918	*	101.32965	98687.798
19		101.39478		98624.407		101.33550	98682.101
20		101.40394		98615.498		101.34180	98675.966
21		101.41328		98606.415		101.34846	98669.482
22						101.35561	98662.521
23						101.36318	98655.153
24						101.37144	98647.114

Notes. [t] A small signal for $^{13}C^{17}O$ may be indicative of the Q-branch position.

Table A.29. Term values (cm^{-1}) of the $E^1\Pi(v'=2)$ e- and f-parity levels for six CO isotopologues (see note to Table A.21).

	$E^1\Pi(v'=2)$																	
	$^{12}C^{16}O$			$^{12}C^{17}O$			$^{12}C^{18}O$			$^{13}C^{16}O$			$^{13}C^{17}O$			$^{13}C^{18}O$		
J'	e-par. ($R\&P$)	f-par. (Q)	Λ_d	e-par. ($R\&P$)	f-par. (Q)	Λ_d	e-par. ($R\&P$)	f-par. (Q)	Λ_d	e-par. ($R\&P$)	f-par. (Q)	Λ_d	e-par. ($R\&P$)	f-par. (Q)	Λ_d	e-par. ($R\&P$)	f-par. (Q)	Λ_d
1	97157.681 (−6)	97157.676	0.005	97107.346 (35)	97107.402	−0.055	97062.106 (8)	97062.071	0.035	97069.681 (22)	97069.694	−0.013	97018.268 (*)	97017.799	0.469	96971.265 (12)	96971.261	0.004
2	97165.283 (0)	97165.246	0.037	97114.802 (−8)	97114.775	0.028	97069.373 (2)	97069.288	0.086	97076.987 (13)	97076.934	0.053	97025.718 (*)			96978.195 (2)	96978.151	0.043
3	97176.728 (9)	97176.600	0.127	97125.935 (−20)	97125.866	0.069	97080.242 (−9)	97080.112	0.129	97087.931 (3)	97087.795	0.136	97037.483			96988.588 (20)	96988.486	0.102
4	97191.952 (−30)	97191.736	0.216	97140.758 (−5)	97140.617	0.142	97094.752 (8)	97094.544	0.208	97102.487 (−6)	97102.275	0.212	97052.137			97002.445 (10)	97002.267	0.179
5	97210.949 (2)	97210.650	0.300	97159.339 (30)	97159.076	0.262	97112.886 (−2)	97112.582	0.304	97120.697 (10)	97120.376	0.322	97070.397			97019.794 (1)	97019.492	0.302
6	97233.789 (−21)	97233.339	0.450	97181.559 (−12)	97181.208	0.352	97134.661 (17)	97134.227	0.434	97142.528 (−1)	97142.096	0.432	97092.177			97040.549 (21)	97040.162	0.387
7	97260.415 (13)	97259.798	0.617	97207.594 (−48)	97206.976	0.618	97160.058 (8)	97159.476	0.582	97168.025 (−3)	97167.482	0.543	97117.514			97064.796 (−15)	97064.278	0.518
8	97290.825 (−9)	97290.016	0.809	97237.250 (−17)	97236.448	0.802	97189.066 (1)	97188.320	0.746	97197.145 (6)	97196.429	0.716	97146.406			97092.502 (−22)	97091.838	0.664
9	97325.047 (−1)	97324.038	1.009	97270.616 (11)	97269.605	1.011	97221.722 (−6)	97220.762	0.960	97229.906 (4)	97228.890	1.016	97178.814			97123.670 (0)	97122.853	0.817
10	97363.051 (9)	97361.834	1.217	97307.599 (36)	97306.563	1.036	97257.954 (21)	97256.851	1.103	97266.286 (−6)	97265.168	1.117	97214.795			97158.296 (−4)	97157.256	1.040
11	97404.864 (−8)	97403.419	1.445	97348.412	97347.213	1.198	97297.766 (41)	97296.557	1.209	97306.305 (−4)	97304.978	1.328	97254.300			97196.353 (−8)	97195.144	1.209
12	97450.484 (4)	97448.955	1.530	97392.959	97391.250	1.709	97341.267 (3)	97339.692	1.575	97349.964 (10)	97348.378	1.586				97237.903 (−19)	97236.462	1.442
13	97499.853 (−9)	97497.848	2.006		97439.278		97388.286 (78)	97386.557	1.729	97397.226 (3)	97395.405	1.822				97282.895 (14)	97281.210	1.685
14	97553.054 (35)	97550.704	2.350		97490.810		97439.125	97437.002	2.122	97448.154 (−1)	97446.040	2.114				97331.312 (−8)	97329.376	1.936
15	97609.991 (8)	97607.320	2.671				97494.740	97491.072	3.668	97502.665 (−1)	97500.229	2.436				97383.242 (−40)	97380.988	2.253
16	97670.718 (20)	97667.716	3.002							97560.803 (11)	97558.074	2.730				97438.574 (−56)	97436.035	2.539
17	97735.224 (23)	97731.866	3.359							97622.564 (1)	97619.464	3.100				97497.296 (−30)	97494.520	2.776
18	97803.524 (−1)	97799.711	3.813							97687.962 (−49)	97684.455	3.507				97559.469 (−30)	97556.341	3.129
19	97875.550 (9)	97871.316	4.234							97756.896 (21)	97753.063	3.834				97625.099 (−9)	97621.612	3.486
20	97951.348	97946.708	4.641							97830.280 (*)	97825.282	4.998				97694.176 (13)	97690.355	3.821
21	98030.921	98025.778	5.143							97907.196 (*)	97900.978	6.218				97766.655 (5)	97762.455	4.201
22	98114.244	98108.626	5.618							97987.656 (*)	97980.306	7.350				97842.511 (56)		
23	98201.252	98195.160	6.092							98068.880	98063.154	5.726				97921.902 (−23)		
24	98292.161									98155.785	98149.643	6.142				98004.558 (68)		
25										98246.290						98090.838 (−5)		
26																98180.495		
27																98273.304		
28																98369.894		

Table A.30. Term values (cm^{-1}) of the $E^1\Pi(v'=3)$ e- and f-parity levels for six CO isotopologues (see note to Table A.21).

	$E^1\Pi(v'=3)$																	
	$^{12}C^{16}O$			$^{12}C^{17}O$			$^{12}C^{18}O$			$^{13}C^{16}O$			$^{13}C^{17}O$			$^{13}C^{18}O$		
J'	e-par. ($R\&P$)	f-par. (Q)	Λ_d	e-par. ($R\&P$)	f-par. (Q)	Λ_d	e-par. ($R\&P$)	f-par. (Q)	Λ_d	e-par. ($R\&P$)	f-par. (Q)	Λ_d	e-par. ($R\&P$)	f-par. (Q)	Λ_d	e-par. ($R\&P$)	f-par. (Q)	Λ_d
1	98923.200 (−59)	98923.171	0.029	98876.754 (2)	98876.705	0.049	98832.676 (1)	98832.647	0.029	98840.249 (1)	98840.319	−0.071		98881.821		98738.362 (41)	98738.354	0.008
2	98930.053 (−34)	98930.010	0.044	98883.551 (−16)	98883.507	0.045	98839.498 (−81)	98839.365	0.132	98847.029 (13)	98846.997	0.032				98744.871 (1)	98744.832	0.039
3	98940.521 (53)	98940.370	0.150	98893.790 (−8)	98893.684	0.106	98849.492 (3)	98849.393	0.099	98857.134 (−14)	98856.950	0.184				98754.648 (18)	98754.530	0.118
4	98954.385 (26)	98954.174	0.211	98907.404 (−20)	98907.267	0.138	98862.919 (4)	98862.741	0.178	98870.572 (8)	98870.490	0.083				98767.631 (−17)	98767.428	0.203
5	98971.696 (3)	98971.380	0.316	98924.525 (−17)	98924.205	0.321	98879.718 (0)	98879.446	0.271	98887.437 (−13)	98887.108	0.329				98783.886 (1)	98783.603	0.283
6	98992.453 (33)	98992.029	0.424	98944.857 (17)	98944.468	0.388	98899.860 (−8)	98899.480	0.380	98907.639 (11)	98907.313	0.326				98803.379 (−8)	98803.035	0.344
7	99016.697 (41)	99016.069	0.628	98968.729 (−25)	98968.213	0.516	98923.310 (24)	98922.811	0.499	98931.188 (11)	98930.605	0.583				98826.109 (11)	98825.625	0.484
8	99044.332 (49)	99043.560	0.772	98995.973 (−30)	98995.282	0.691	98950.130 (2)	98949.390	0.740	98957.987 (−30)	98957.423	0.565				98852.071 (8)	98851.423	0.648
9	99075.288 (−60)	99074.440	0.848	99026.452 (83)	99024.921	1.530	98980.251 (−4)	98979.431	0.820	98988.266 (31)	98987.413	0.853				98881.246 (2)	98880.427	0.819
10	99109.706 (−48)	99108.709	0.996	99060.258	99057.266	2.991	99013.682 (14)	99012.719	0.964	99021.758 (16)	99020.752	1.006				98913.626 (−3)	98912.703	0.923
11	99147.501 (−94)	99146.366	1.135	99097.085	99093.010	4.075	99050.368 (−25)	99049.202	1.166	99058.401 (*)	99057.457	0.944				98949.216 (−11)	98948.115	1.101
12	99188.849 (−22)	99187.359	1.490	99136.797	99132.220	4.577	99090.444 (−73)	99089.134	1.309	99098.880 (*)	99097.448	1.432				98988.050 (3)	98986.622	1.428
13	99233.446 (−36)	99231.669	1.777	99179.773	99174.660	5.113	99133.865	99132.181	1.684	99140.733	99140.500	0.233				99029.922 (106)	99028.555	1.367
14	99281.404 (47)	99279.371	2.034	99226.672	99220.649	6.022	99180.005	99178.388	1.617	99187.133	99187.050	0.083				99074.950 (*)	99073.404	1.546
15	99332.793 (*)	99330.336	2.458	99276.730	99269.739	6.992	99229.551			99237.281	99236.657	0.624				99123.099 (*)	99121.461	1.639
16	99387.189 (0)	99384.621	2.567	99330.218	99322.248	7.970	99282.754			99290.363	99289.017	1.346				99174.379 (*)	99172.704	1.676
17	99444.947 (31)	99502.870	3.298				99399.149			99406.093	99402.671	3.422				99286.348 (*)	99284.479	1.869
19	99570.616 (103)	99566.780	3.836				99462.219			99469.206						99347.114 (*)	99345.007	2.107
20	99638.149	99633.932	4.217				99529.055			99535.993						99412.179	99408.567	3.612
21	99709.060	99704.217	4.842				99592.555										99475.245	
22	99782.967	99777.603	5.364				99676.000										99544.912	
23		99854.046															99617.632	
24		99933.495															99693.142	
25		100016.071																

Table A.31. Molecular constants T_v, B_v, and D_v of the six CO isotopologues for each state, $B^1\Sigma^+$, $C^1\Sigma^+$, and $E^1\Pi$ for e- and f-parity (D_v is always kept as a free parameter in the fitting process).

	T_0	B_0	$-D_0$ ($\times 10^{-6}$)								
		X0									
1216	0.0000 (0)	1.92253 (0)	−6.121 (0)								
1217	0.0000 (0)	1.87396 (0)	−5.815 (0)								
1218	0.0000 (0)	1.83098 (0)	−5.551 (0)								
1316	0.0000 (0)	1.83797 (0)	−5.593 (0)								
1317	0.0000 (0)	1.78940 (0)	−5.301 (0)								
1318	0.0000 (0)	1.74641 (0)	−5.049 (0)								
	T_v	B_v	$-D_v$ ($\times 10^{-6}$)	T_v	B_v	$-D_v$ ($\times 10^{-6}$)	T_v	B_v	$-D_v$ ($\times 10^{-6}$)	T_v	B_v	$-D_v$ ($\times 10^{-6}$)
		B00			**C00**			**E00$_e$**			**E00$_f$**	
1216	86916.1484 (32)	1.94814 (1)	−6.739(11)	91919.0328 (53)	1.94336 (2)	−6.363(16)	92929.9358 (40)	1.96456 (2)	−6.516(19)	92929.9317 (54)	1.95270 (4)	−6.454(62)
1217	86916.4584 (102)	1.89904 (8)	−6.584(117)	91918.9284 (85)	1.89464 (4)	−5.914(40)	92929.7231 (53)	1.91479 (6)	−6.304(108)	92929.6481 (53)	1.90387 (5)	−6.801(82)
1218	86916.7386 (54)	1.85548 (3)	−6.196(28)	91918.8543 (25)	1.85142 (1)	−5.641(8)	92929.5590 (44)	1.87052 (4)	−5.871(55)	92929.5452 (45)	1.85972 (4)	−5.752(69)
1316	86916.8158 (83)	1.86254 (5)	−6.191(44)	91919.0551 (37)	1.85845 (1)	−5.690(10)	92929.7536 (39)	1.87768 (2)	−5.918(13)	92929.7481 (43)	1.86675 (5)	−5.676(84)
1317	86917.1248 (168)	1.81312 (18)	−5.437(356)	91918.8853 (80)	1.80969 (3)	−5.404(27)	92929.4750 (87)	1.82811 (6)	−5.989(78)			
1318	86917.3644 (69)	1.76980 (4)	−5.639(46)	91918.7947 (23)	1.76641 (1)	−5.130(5)	92929.2758 (76)	1.78395 (3)	−5.516(22)	92929.3602 (56)	1.77352 (6)	−4.245(105)
		B10			**C10**			**E10$_e$**			**E10$_f$**	
1216	88998.3150 (97)	1.92199 (5)	−7.408(41)	94065.5649 (47)	1.92385 (3)	−6.337(24)	95082.7605 (454)	1.94090 (20)	−9.042(190)	95082.8140 (227)	1.92879 (24)	−8.616(523)
1217	88972.9899 (174)	1.87334 (19)	−4.528(371)	94038.5061 (64)	1.87569 (8)	−5.761(162)	95055.9480 (237)	1.89129 (24)	−7.715(522)	95055.9701 (259)	1.88372 (40)	−13.559(1204)
1218	88950.2474 (34)	1.83120 (2)	−6.593(24)	94014.3118 (77)	1.83317 (6)	−5.644(88)	95032.0645 (469)	1.84697 (33)	−6.089(480)	95031.9316 (228)	1.83783 (23)	−7.989(453)
1316	88954.0973 (40)	1.83818 (3)	−6.715(35)	94018.5116 (213)	1.83959 (9)	−5.051(72)	95035.6846 (2739)	1.85712 (121)	−9.292(1008)	95035.9422 (127)	1.84490 (12)	−7.970(242)
1317	88928.1002 (139)	1.78966 (17)	−5.212(352)	93990.4543 (194)	1.79134 (12)	−4.405(130)	95008.6131 (296)	1.80440 (24)	−4.433(413)	95008.5805 (140)	1.79498 (10)	−5.009(136)
1318	88904.7410 (31)	1.74738 (2)	−5.975(27)	93965.8762 (64)	1.74951 (4)	−5.280(38)	94984.1816 (2353)	1.75965 (93)	−3.196(715)	94983.9515 (176)	1.75065 (20)	−0.856(856)
		B20			**C20**			**E20$_e$**			**E20$_f$**	
1216	90988.2294 (126)	1.87355 (47)	9.682(3169)	96176.9248 (190)	1.90283 (19)	−5.197(343)	97153.8834 (48)	1.90270 (5)	−9.413(114)	97153.8983 (54)	1.89151 (6)	−9.328(113)
1217							97103.6477 (162)	1.85644 (95)	−12.927(10413)	97103.7201 (88)	1.84493 (36)	−6.806(1930)
1218	90899.3726 (195)	1.78362 (155)	39.098(*)	96076.3267 (238)	1.80991 (190)	32.499(*)	97058.4759 (70)	1.81424 (34)	−6.456(3105)	97058.4630 (18)	1.80427 (6)	−9.835(410)
1316	90906.3225 (105)	1.79341 (47)	12.410(3659)	96084.2280 (245)	1.81989 (92)	−1.736(*)	97066.0611 (57)	1.82118 (9)	−8.275(237)	97066.0601 (37)	1.81106 (4)	−8.390(90)
1317												
1318	90815.2393 (1206)	1.69520 (235)	37.719(8152)	95981.2762 (379)	1.72615 (143)	43.594(9531)	96967.7962 (33)	1.73261 (5)	−7.524(132)	96967.8062 (26)	1.72321 (4)	−6.896(82)
					C30			**E30$_e$**			**E30$_e$**	
1216				98244.5110 (415)	1.87571 (72)	−1.933(*)	98919.7206 (317)	1.73377 (48)	−55.337(1319)	98919.6726 (103)	1.72512 (12)	−58.382(246)
1217				98167.0437 (798)	1.82668 (813)	8.705(*)	98873.3367 (289)	1.70479 (209)	−22.505(28193)	98873.3289 (198)	1.69637 (144)	−37.152(19329)
1218				98097.5876 (428)	1.78947 (161)	9.638(*)	98829.3477 (188)	1.68059 (66)	−44.847(4302)	98829.3276 (205)	1.67165 (85)	−43.920(6431)
1316				98109.1420 (705)	1.79608 (198)	4.310(*)	98836.8720 (271)	1.68816 (112)	−72.393(8489)	98836.9281 (406)	1.67623 (199)	−45.754(17962)
1317												
1318				97958.4479 (263)	1.71070 (65)	−8.017(2855)	98735.1160 (71)	1.62678 (25)	−35.294(1614)	98735.1064 (170)	1.61846 (60)	−38.301(3880)

Notes. Standard errors are given in parentheses in units of the least significant digit, and for D_v, an asterisk indicates that the standard error is higher than 50% of the value. A ninth-order polynomial is used for the ground state X0.

Table A.32. Molecular constants $T_v(1)$, q_v, and q_{Dv} of the six CO isotopologues for the $E^1\Pi$ state, calculated from the previous table: $T_v(J=1)$ is the average of T_v for e- and f-parity, $q_v = B_e - B_f$, and $q_{Dv} = D_e - D_f$.

Species	$T_v(1)$	q_v	q_{Dv} ($\times 10^{-6}$)
		E00	
1216	92929.9338(47)	0.01186(3)	−0.06(4)
1217	92929.6856(53)	0.01092(5)	0.50(10)
1218	92929.5521(44)	0.01080(4)	−0.12(6)
1316	92929.7509(41)	0.01093(3)	−0.24(5)
1317	92929.4750(87)		
1318	92929.3180(66)	0.01043(4)	−1.27(6)
		E10	
1216	95082.7873(341)	0.01211(22)	−0.43(36)
1217	95055.9591(248)	0.00757(32)	5.84(86)
1218	95031.9981(348)	0.00914(28)	1.90(47)
1316	95035.8134(1433)	0.01222(67)	−1.32(63)
1317	95008.5968(218)	0.00942(17)	0.58(27)
1318	94984.0666(1264)	0.00900(57)	−2.34(79)
		E20	
1216	97153.8909(51)	0.01119(6)	−0.09(11)
1217	97103.6839(125)	0.01151(65)	−6.12(617)
1218	97058.4695(44)	0.00997(20)	3.38(176)
1316	97066.0606(47)	0.01012(6)	0.12(16)
1317			
1318	96967.8012(29)	0.00940(4)	−0.63(11)
		E30	
1216	98919.6966(210)	0.00865(30)	3.04(78)
1217	98873.3328(243)	0.00842(177)	14.65(2376)
1218	98829.3377(197)	0.00894(75)	−0.93(537)
1316	98836.9001(338)	0.01193(156)	−26.64(1323)
1317			
1318	98735.1112(120)	0.00832(42)	3.01(275)

Notes. The standard errors, in parentheses, are expressed in units of the least significant digit.

Table A.33. Molecular constants q_v and q_{Dv} of the six CO isotopologues for the $E^1\Pi$ state, obtained from a second-order regression through the data.

Species	N	q_v	q_{Dv} ($\times 10^{-6}$)
		E00	
1216	29	0.01173(9)	0.10(12)
1217	26	0.01082(21)	0.61(31)
1218	26	0.01084(10)	−0.27(15)
1316	25	0.01107(19)	−0.54(32)
1317			
1318	26	0.01112(35)	−2.41(53)
		E10	
1216	21	0.01133(29)	0.55(67)
1217	18	0.00848(60)	2.75(183)
1218	22	0.01025(37)	0.23(76)
1316	22	0.01140(208)	−1.13(434)
1317	22	0.00996(15)	−0.21(32)
1318	22	0.00943(36)	0.13(74)
		E20	
1216	23	0.01108(20)	0.09(38)
1217	12	0.01128(185)	−4.08(1198)
1218	14	0.00967(67)	0.33(328)
1316	21	0.00998(14)	0.51(25)
1317			
1318	21	0.00947(10)	−0.80(23)
		E30	
1216	22	0.00832(38)	4.11(79)
1217	8	0.00842(183)	14.69(2463)
1218	11	0.00958(104)	−6.38(793)
1316	13	0.00792(96)	5.96(279)
1317			
1318	12	0.00832(76)	3.05(494)

Notes. The standard errors, in parentheses, are expressed in units of the least significant digit. N is the number of data.

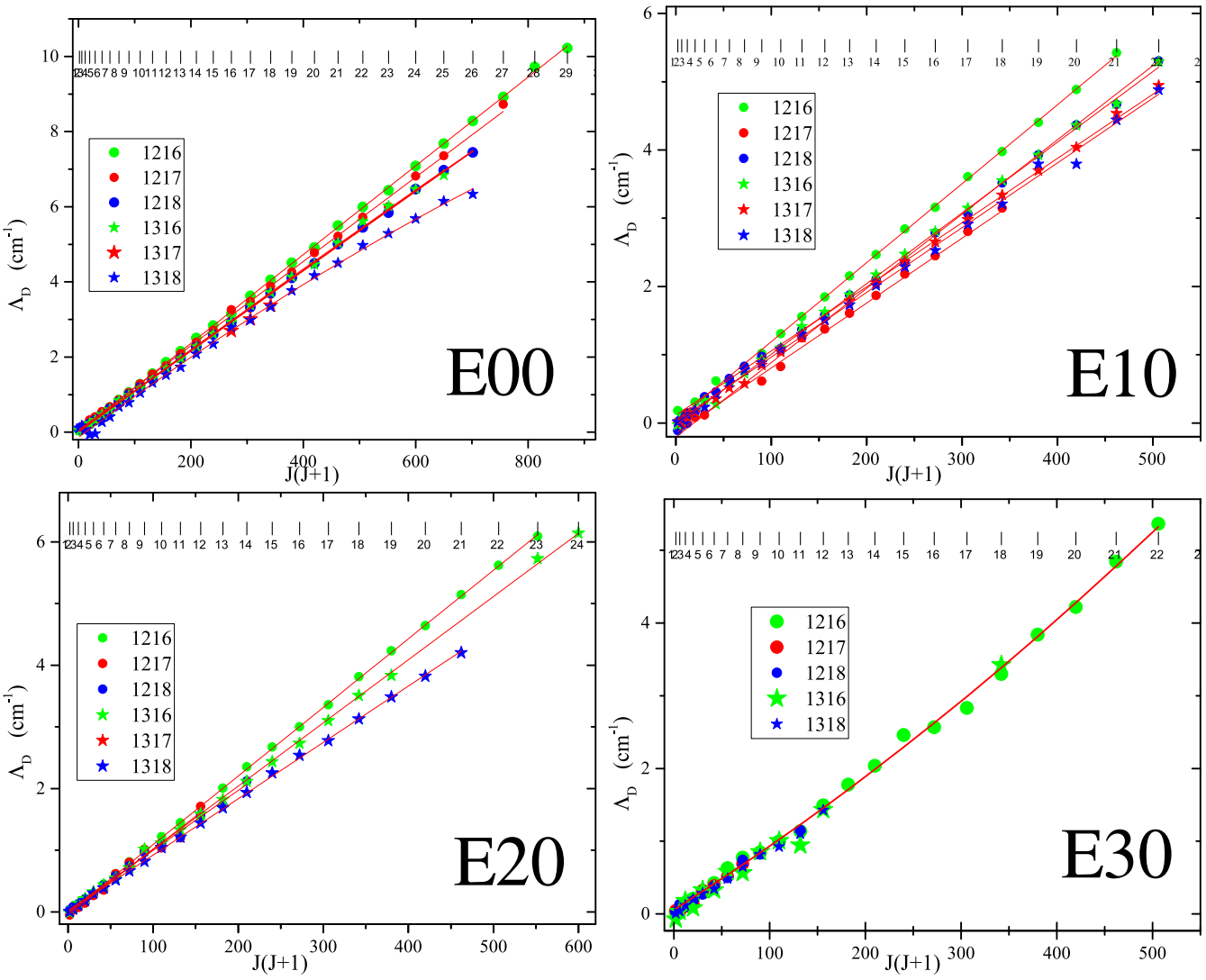

Fig. A.37. Λ-type doubling (in cm^{-1}) vs. $J \times (J + 1)$ of E00, E10, and E20 for the six isotopologues and of E30 for five isotopologues. For E10, we combined our dataset for the *R*- and *P*-branches and the *Q*-branch of Ubachs et al. (2000). A polynomial fit is also drawn; it is linear in most cases.

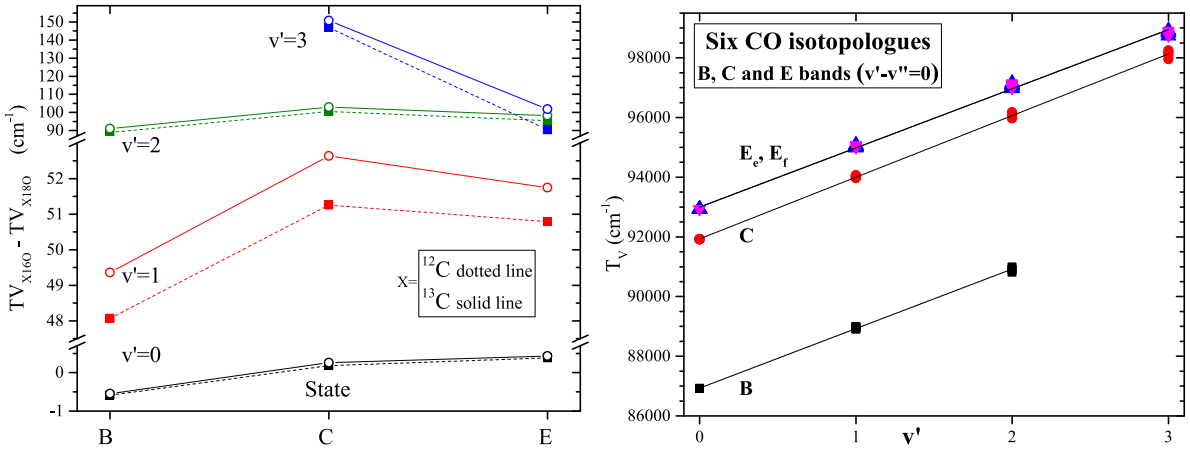

Fig. A.38. Trend comparison for the six CO isotopologues. *Left*: term value differences between ^{16}O- and ^{18}O-bearing isotopologues for ^{12}C and ^{13}C (dotted and solid lines, respectively) versus the *B*, *C*, and *E* states. *Right*: T_v versus v' for the *B*, *C*, and *E* states (each datapoint contains up to six isotopologues). For each state, a linear fit is drawn through all isotopologues.

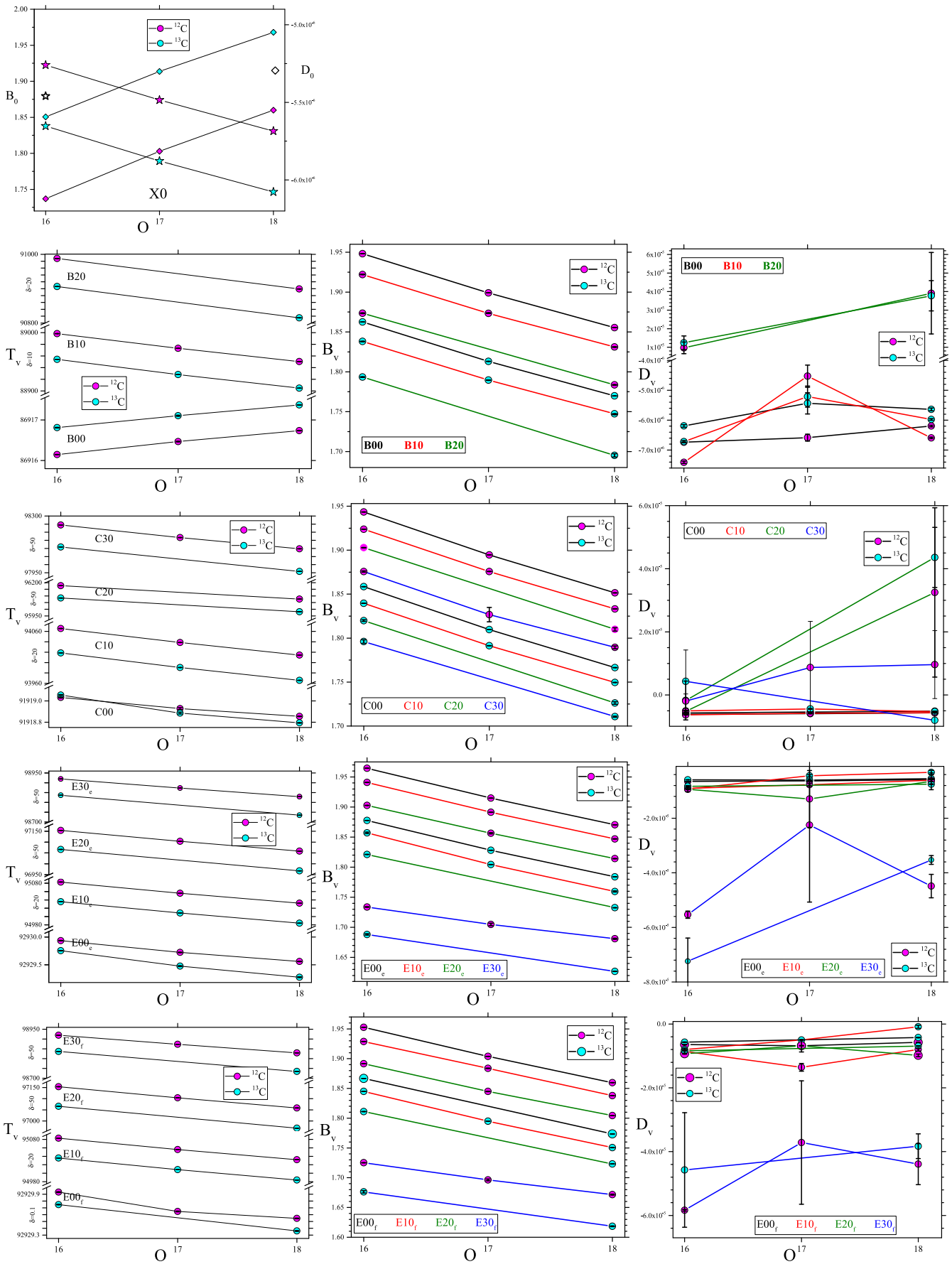

Fig. A.39. Molecular constants for the six CO isotopologues. *Top row*: B_0 and D_0 for $v'' = 0$ of the $X^1\Sigma^+$ ground state ($T_0 = 0$ for all). The standard deviation (at 2σ) is shown between two short horizontal bars. For T_V, all values are in cm^{-1}, with δ values indicating the local spacing between ticks.